HUMBOLDT-UNIVERSITÄT ZU BERLIN

Faculty of Life Sciences

Albrecht Daniel Thaer-Institute of Agricultural and Horticultural Sciences

Assessment of transgression of the planetary boundary of freshwater use, accounting for aquatic biodiversity

M.Sc. thesis in the study program: Integrated Natural Resource Management

submitted by: Wittekind, Cordula

1st Examiner (Supervisor): Prof. Dr. Gerten, Dieter

Potsdam Institute for Climate Impact Research

&

Geography Department

Division of Climatology and Plant Geography

2nd Examiner: PD Dr. Riesbeck, Frank

Albrecht Daniel Thaer-Institute

Division of Plant Nutrition and Fertilization

Berlin, 21.04.2017

Acknowledgements

First and foremost, my thanks goes to Dieter Gerten and Holger Hoff for giving me the opportunity to write my thesis at PIK. Further, I'd like to thank the whole OPEN group; Vera Heck, Jonas Jägermeyr, Sebastian Ostberg, Sibyll Schaphoff, Sarah Brauns and particularly Fabian Stenzel for sharing & discussing scripts, always being there for me and the fun times at beautiful PIK. I'm also very grateful for having friends like Hendrik Gunz, Eric Hübner & Boris Pizzeghello.

Abstract

In the light of human influence on the environment increasingly straining the resilience of the Earth System (ES), holistic frameworks to accomplish global sustainability are urgently needed. An interdisciplinary team of scientists first introduced the concept of planetary boundaries in 2009. Below the control values set for these boundaries, the ES is expected to remain stable, a prerequisite for a thriving global society. The transgression of one or more boundaries is predicted to be deleterious or even catastrophic due to the risk of triggering non-linear, abrupt environmental change with unknown consequences for the ES and our as well as other species' well-being. One of the nine proposed boundaries is global freshwater use. As the hydrological cycle and freshwater use are characterized by strong regional operating scales and non-linear eco-hydrological relationships, the global quantification of this boundary is complex. Consumptive runoff or blue water use is used as the control variable and proxy for capturing the full complexity of global freshwater thresholds. The boundary that, once transgressed, would significantly increase the risk of approaching green and blue water-induced thresholds was set at ~4,000km^3/yr of consumptive blue water use (with a zone of uncertainty of 4,000-6,000km^3/yr). Using the Lund-Potsdam-Jena managed Land dynamic global vegetation and water balance model (LPJmL), this estimate was later refined and the boundary was reassessed in a bottom-up approach including environmental flow requirements (EFRs) as an integral part of calculations. The resulting planetary boundary was hence estimated to lie at ~2,800km^3/yr.

This study analyzed patterns of EFR transgressions based on global data from LPJmL and developed a two-criteria aggregation scheme to basin and global scale. The combination with data on aquatic biodiversity facilitated to improve the spatial resolution of global EFR transgressions and accentuates the strong relationship between the two PBs biosphere integrity and freshwater use.

While the duration of transgression (non-fulfilment of the EFRs during at least half of the year) is particularly problematic on the Indian subcontinent, Central Asia, and in the Middle East, the magnitude of EFR deficits is a more global problem - major basins showing transgressions beyond uncertainty can be found on all continents, except South America. It is furthermore shown that in major basins in India, Spain, Italy, Mexico and the USA, high levels of biodiversity coincide with and depend on severely overexploited freshwater resources.

Contents

List of Figures

List of Tables

List of Abbreviations

BW blue water

CFTs crop functional types

CRU Climate Research Unit

CS current situation

CWEI corrected weighted endemicity index

DDM drainage direction map

EF Environmental Flow

EFRs Environmental Flow Requirements

ES Earth System

GPCC Global Precipitation Climatology Centre

HIL households, industry and livestock

IWRM Integrated Water Resource Management

LPJmL Lund-Potsdam-Jena managed Land

MAF mean annual flow

MMF mean monthly flow

PB Planetary Boundary

PIK Potsdam Institute for Climate Impact Research

PFTs plant functional types

PNV potential natural vegetation

SDGs Sustainable Development Goals

STN Simulated Topological Network

VMF Variable Monthly Flow

1 Introduction

Although having undergone significant state shifts in the past, Earth has been particularly stable throughout the past ~10,000 years during the Holocene (Petit et al., 1999; Dansgaard et al., 1993). This geological epoch is characterized by temperatures, freshwater availability and biogeochemical flows remaining within a comparatively narrow range (Rockström et al., 2009c). Nevertheless, since the industrial revolution 250 years ago, the impact of humans on the Earth's biosphere, atmosphere, hydrosphere and lithosphere and therein predominantly on the dynamics of ecosystems and climate has reached such an extent, that the emergence of a new geological epoch – the Anthropocene – is undeniable (Ellis, 2011; Hughes et al., 2013; Rockström et al., 2009b).

Humans now dominate the Earth, the main global-scale forcing mechanisms, straining its resilience, are human population growth and associated resource consumption, the fragmentation and transformation of habitats, energy production and consumption as well as climate change (Steffen et al., 2011; Barnosky et al., 2012). In 10,000 BC, the global population was around 2 million, having tripled since the 1950s, it is around 7 billion today. This number is expected to increase by an additional 2 billion until 2050, leading to unprecedented pressure on natural resources (Goldewijk et al., 2010). Even worse, as a phenomenon of the second half of the 20th century, human population growth has decoupled from global economic and material consumption growth which have increased many times faster (Maddison, 2001; Steffen et al., 2011). Population size alone cannot explain the extent of anthropogenic impacts as affluence and associated consumption patterns are an exacerbating factor (Dietz et al., 2007).

In terms of habitat destruction, due to alarming numbers of extinct or endangered species, some argue that anthropogenic activities have started to induce a mass extinction defined by the loss of more than three quarters of Earth's species in a geologically short interval (Barnosky et al., 2011). Regarding energy production and consumption, humans have altered the global energy budget. More than 20 percent of global net primary production is now redirected for human use. Net primary production is the amount of biomass produced annually by green plants through photosynthesis, around 120 Gt (Haberl et al., 2007). This human appropriation disturbs biogeochemical cycles and diminishes ecosystem services (Brown et al., 2011; Haberl et al., 2007). Concerning climate change, the anthropogenic impact on the climate system is clear and recent releases of greenhouse gases are the highest in history. On a global average, land and ocean surface temperature showed a warming of 0.85°C (as calculated by a linear trend) over the period 1880 to 2012 (IPCC, 2014). As oceans represent the most important carbon sink, their acidity has increased by 26 % (CBD, 2014) and their pH has decreased by 0.1 due to the higher CO_2 levels in the atmosphere since the beginning of the industrial era (Orr et al., 2005).

The location and magnitude of terrestrial carbon sinks has not been fully determined but the net effect of growing atmospheric CO_2 concentration on the biosphere is an increase in plant growth (Amthor, 1995; House et al., 2003).

Furthermore, human activities have very likely contributed to mean global sea level rise which was in total around 195 mm between the 1870s and the 2000s. The last decade alone has seen twice the rise of the previous century (Church and White, 2006). Additionally, the anthropogenic contribution to Arctic sea-ice loss is very likely (Bates et al., 2008) and the number of extreme events like heat waves, droughts, floods and wildfires has increased and demonstrated the considerable susceptibility and exposure of some ecosystems to current unpredictability of climate (IPCC, 2014). In the light of human interference increasingly threatening the resilience of the Earth System (ES), the prevention of sudden global environmental change becomes a pressing issue. The Holocene is the only known state than can support humans and other species, its stability is therefore crucial for our continued existence (Steffen et al., 2011). Planetary Boundary (PB) concept developed by Rockström et al. (2009c) aims to identify critical processes that regulate Earth system resilience and to define boundaries of anthropogenic perturbations for these processes below which the hazard of destabilization of the ES is expected to remain low (Rockström et al., 2009c; Steffen et al., 2015). The transgression of one or more boundaries is likely to be harmful or even catastrophic because of the danger of triggering non-linear, sudden, and possibly irreversible environmental change within continental – to planetary – scale systems (Rockström et al., 2009b).

One of the nine proposed boundaries is global freshwater use. Earth's climate, ecology, and biogeochemistry are significantly dependent on the terrestrial water cycle (Vörösmarty and Sahagian, 2000). Freshwater is essential for sustainable development – water resources and the variety of services they generate, like fisheries, recreation and wildlife, poverty reduction, economic growth and environmental sustainability (WWAP, 2015). These services are estimated to be worth trillions of US dollars every year (Constanza et al., 1997). The main pressures on freshwater resources are (increasing) global water demand and land use (change) as well as pollution, additionally aggravated by anthropogenic climate change (Vörösmarty and Sahagian, 2000; L'Vovich et al., 1990). Therein, the primary drivers of water demand are population growth, urbanization, food and energy security policies and macro-economic pressures like trade globalization and shifting consumption patterns (WWAP, 2015). The state of water scarcity and pollution varies among continents and regions due to different manifestation of these drivers as well as different climates and potential climate changes. Nevertheless, water managers and planners are confronted to meet growing water needs almost everywhere (Richter et al., 2012; Vörösmarty et al., 2000b). Water security represents a major challenge of the 21st century (UN, 2015). Today still around 663 million people lack access to safe water and 2.4 billion lack access to any type of improved sanitation facility (WHO, 2015). The

World Water Forum (2015) has identified the water crisis as the greatest global risk based on impact for society. As anthropogenic water demands are increasingly straining freshwater resources, the environmental water needs, or “nature’s water demand”, has gained the attention of scientists and policy makers. The renewed UN Sustainable Development Goals (SDGs) relating to water and the environment cannot be attained without the protection of freshwater ecosystems (UN, 2015). The water needed for the provision of ecological functions and services, to support resilience through humidity of landscapes and to prevent water scarcity is of critical importance for both human and other species’ well-being and ecosystem health (Rockström et al., 2014b; Vörösmarty et al., 2005; Falkenmark and Rockström, 2004). Freshwater resources represent important habitats and around 125,000 freshwater species have so far been described. Due to increasing pressure on freshwater resources, a lot of these species are endangered or have already gone extinct, at least 10,000 different species on a global scale. Although the precise extent of endangerment is unknown, freshwater biota is almost always more endangered than their terrestrial counterparts (Sala et al., 2000; Strayer and Dudgeon, 2010).

The conflict between the protection as integrated ecosystems and the development of rivers and other freshwater ecosystems as water and energy sources is complex and its resolution significant for the long-term health of human civilizations and ecosystems (Dynesius and Nilsson, 1994; Rockström et al., 2014a). The success of integrated water management strategies depends on finding a balance between human water demands and the requirements of freshwater ecosystems (WWAP, 2015; Dudgeon et al., 2006; Postel et al., 1996). One key strategy lies in the protection of environmental flows, defined as the quantity, timing and quality of water ows required to sustain freshwater and estuarine ecosystems and the human well-being that depends on these ecosystems (10th International River Symposium, 2007). This concept has been used as a basis to sustain appropriate flow conditions and therefore the ecological health and functioning of rivers and their accompanying wetlands for human use and biodiversity (Acreman and Dunbar, 2004).

The PB of freshwater use is defined as the maximum annual amount of consumptive blue water use (Rockström et al., 2009b). Environmental Flow Requirements (EFRs) have been an integral part of its quantifications. While the first calculations by Rockström et al. (2009b) were based on rough global estimates of accessible water volumes as well as EFRs, Gerten et al. (2013) as well as Brauns (2016) applied EFRs to account for the strong regional operating scale of the freshwater boundary in a bottom-up approach. The main aim of this thesis is to assess transgressions of EFRs and to aggregate these deficits to basin and global scale to receive a global picture of the violation of the PB for freshwater that reflects its spatiotemporal heterogeneity. In this explorative approach, different ways to evaluate these transgressions are combined and extended with regard to levels of associated biodiversity.

2 The Concept of Planetary Boundaries

The concept of PBs shall serve as a framework for achieving global sustainability and for defining the so-called safe operating space for humanity (Rockström et al., 2009b; Hughes et al., 2013). Scientist led by Johan Rockström from the Stockholm Resilience Centre were the first to introduce the approach in 2009. Since then, it has become an influential concept in assessments of cooperative management of global commons and in discussions on the challenge of attaining environmental sustainability (Nordhaus et al., 2012; Hughes et al., 2013).

Nine different PBs were defined, that, once transgressed, could lead to a destabilization of the ES and to non-linear, sudden environmental change at local and global scale (Steffen et al., 2015; Rockström et al., 2009b). These nine PBs, also called biophysical key processes, are climate change, ocean acidification, stratospheric ozone, biogeochemical nitrogen and phosphorous cycle, global freshwater use, land system change, rate of biodiversity loss, chemical pollution and atmospheric aerosol loading. Due to their fundamental importance for the ES and strong interlinkages with the other boundaries, climate change and biosphere integrity were defined as "core" PBs (Steffen et al., 2015). The PBs are measured by control variables that were assigned for each of the boundaries. The aim is to supply the most comprehensive, aggregated and calculable parameter for their assessment. For the quantification of these variables, the range of variation associated with the Holocene state was used within which key biogeochemical and atmospheric parameters oscillated in a relatively small range. The environmental conditions of the Holocene hence define the "desirable planetary state" that shall be preserved (Rockström et al., 2009b). The determined boundaries for these control values shall prevent the transgression of thresholds and reaching of tipping points. While control values for boundaries are human-determined, thresholds and tipping points are a result of dynamic natural processes and their exact position remains unknown (Steffen et al., 2015). Tipping points are understood as "critical thresholds where the respective ES elements flip into a qualitatively new state and perhaps annihilation" (Schellnhuber, 2009, p.20561).

In the initial first attempt Rockström et al. (2009b) estimated control values for seven of the nine proposed PBs, leaving only aerosol loading and chemical pollution undefined. This first approach was later updated by Steffen et al. (2015)[1]. As Cornell (2012) points out, conceptual challenges arise from the different threshold behavior and scaling of PBs, making it difficult to assign precise values to control variables. Rockström et al. (2009b) acknowledged that many planetary-scale processes are spatially heterogeneous, leading to effects at local and regional scale. These subglobal dynamics have to be taken into account as they play a critical role in global dynamics, and changes in control variables

[1] See ST 1 for the overview of updated PBs and control values by Steffen et al. (2015)

at subglobal scale can lead to perturbations at the global level. Therefore, a definition of subglobal boundaries compatible with the global-level boundary definition is needed. Some argue that some ES processes, particularly land use change, biodiversity loss, nitrogen levels, freshwater use, aerosol loading and chemical pollution, do not have planetary biophysical thresholds and global tipping points at all. These ES-processes would only operate on local and regional scale and not on global level with impacts ecologically independent of effects in other regions (Nordhaus et al., 2012). Steffen et al. (2015) proposed a two-level set of control variables with explicit subglobal level units of analysis to include these cross-scale interactions. They therefore defined subglobal boundaries for five of the PB that have strong regional operating scale: biosphere integrity, biogeochemical flows, land-system change, freshwater use, and atmospheric aerosol loading.

Types of Planetary Boundaries

The uncertainty of the actual position of the threshold or tipping point is accounted for by not defining the control value (used synonymously with PB) as equivalent but rather below, at a safe distance from the biophysical threshold. The derived buffer zones shall incorporate both, this uncertainty and the time for early warning signs and appropriate reactions (Steffen et al., 2015; Rockström et al., 2009c). Figure 1 shows two conceptual descriptions for PBs taking into account the different system properties of PBs. The left one illustrates boundaries with a known global threshold effect and the other illustrates boundaries that are based on slow planetary processes that once surpassing a dangerous level do not display threshold behavior but significant interactions with other thresholds and state shifts (Barnosky et al., 2012; Rockström et al., 2009b). It is very difficult to quantify PBs and define control variables as biological states are neither constant nor in equilibrium and naturally entail variation from a median state. The exact threshold value usually is unknown beforehand and transgressions are caused by accumulation of incremental changes, its effects are thus challenging to foresee (Barnosky et al., 2012).

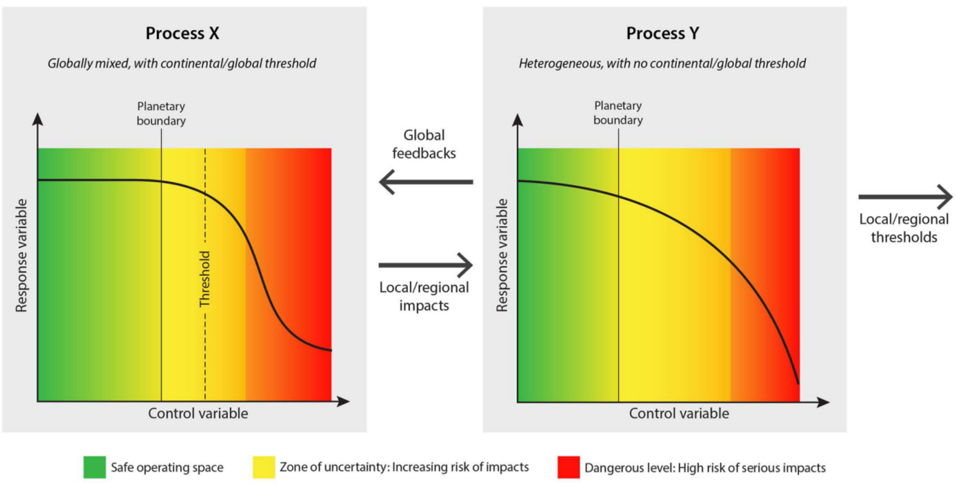

Figure 1: Types of Planetary Boundaries (Rockström et al., 2009b; Steffen et al., 2015)

As regime shifts in ecosystems are induced when major processes and their underlying organization changes, the effects of transgressing boundaries cannot be predicted and it is uncertain if human activities will lead to transgression of tipping points and regime shifts in the near future (Hughes et al., 2013; Scheffer et al., 2001). Furthermore, due to many slow progressing regional and planetary scale processes and their complex interplay, it is unlikely that the transgression of global tipping will manifest as sudden and synchronous collapses worldwide. While regime shifts often appear to be due to a recent short-term event, the resilience of the system has often slowly been eroded over a longer time period beforehand (Hughes et al., 2013; Minckley et al., 2012).

Hughes et al. (2013) identified climate change, land-use change and harvesting, direct manipulation of biogeochemical cycles, release of toxins, and invasive species as the main regional and global drivers of ecological regime shifts today as well as in the foreseeable future. While some of these drivers like climate change and biogeochemical cycles act on a global scale, others like invasive species, land use and harvesting take effect more locally with globally prevalent consequences.

2.1 Current Status of the Planetary Boundaries

Concerning the current situation of the ES with regard to PBs, it was estimated that four boundaries have already been transgressed by humanity as they surpass the proposed PB (as shown in Figure 2). These PBs are climate change, change in biosphere integrity (formerly biodiversity loss), biogeochemical flows and land-system change (Steffen et al., 2015).

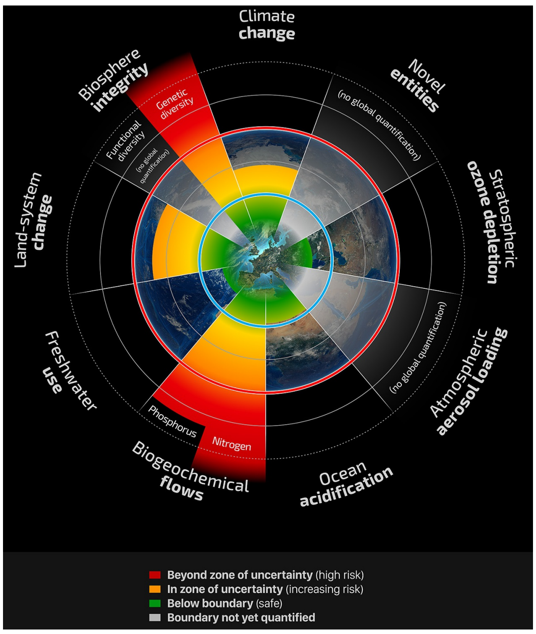

Figure 2: Current Status of the Planetary Boundaries (Steffen et al., 2015)

2.2 The Planetary Boundary for Human Freshwater Use

The PB for freshwater use is defined as the maximum allowed amount of blue water (BW) consumption and is expressed in km^3/yr. When examining and quantifying the planetary boundary for global freshwater use, the high complexity of the hydrological cycle represents the main challenge. Only around three percent of the Earth's water is freshwater and most of it is stored as ice and snow and in underground aquifers, leaving only around one percent of the global water volume as accessible freshwater (Wallace and Batchelor, 1997). The terrestrial water cycle is regulated by local to global interplay between land, ocean and atmosphere. Subglobal dynamics (e.g. monsoon system) at local or regional scale, play a crucial role for planetary level thresholds as transgression of subglobal boundaries and accumulation of subsystem impacts may influence the ES at the global level (Steffen et al., 2015; Rockström et al., 2009b).

The residual of precipitation after evapotranspiration and infiltration is terrestrial runoff which is called BW and forms surface and subsurface freshwater resources (Bogardi et al., 2013). Trenberth et al. (2007) estimated precipitation over land to be 113.000 km^3/yr of which 73.000 km^3/yr is evaporated back to the atmosphere, while they estimated current runoff (BW) to be 40.000 km^3/yr. Haddeland et al. (2011) estimated terrestrial evapotranspiration to range between 60,000 and 85,000km^3/yr and runoff to be between 42,000 and 66.000 km^3/yr. As a specific boundary for water available in soils has not yet been set, the boundary of BW consumption as defined by Rockström et al. (2009b) serves as a proxy for PB-Water (subsequently freshwater use refers to BW use). The amount of BW present in river basins "reflects the complex processes of precipitation partitioning into green water/soil moisture, BW and flow dynamics in the landscape" (Gerten et al., 2013, p.551). Thus, the major aim in setting this PB for freshwater resources is to balance both, sufficient moisture feedback to regenerate precipitation and prevent the loss of soil moisture resources (green water) as well as to protect sufficient BW for human water supply and aquatic ecosystems (Falkenmark, 2013). The transgression of this BW boundary implies the risk of approaching both green and BW induced thresholds (Gerten et al., 2013).

2.3 Calculation of the Planetary Boundary for Freshwater Use

The calculations for the PB are based on total renewable BW resources. From this volume, the accessible BW resource is derived by subtracting flows that are inaccessible due to their location or due to their timing. The first refers to flows that are not (yet) accessed by humans because they are occurring in sparsely populated and remote locations like the Amazon region and Northern latitudes. The second refers to flows that are inaccessible as they represent floodwater that is hard to capture. Further components that play a role are the freshwater volumes currently stored in reservoirs and impounded by dams. These constructions, to a certain extent, facilitate to capture floodwater, therefore change temporal accessibility and have to be integrated in their assessment. The derived "total accessible runoff" is reduced by the amount required to cover physical water stress (Gerten et al., 2013; Rockström et al., 2009b). Physical water stress is reached when withdrawals of water exceed 60% of the utilizable resource (de Fraiture et al., 2001). The hence obtained volume represents the usable water. The PB is set at the lower end of an uncertainty zone.[1] The calculations by Rockström et al. (2009b) were derived from estimations of the limit of accessible global BW resources by Postel et al. (1996) and de Fraiture et al. (2001). Using their upper limit that was estimated at around 12,500 – 15,000km^3/yr and the assumptions by Vörösmarty et al. (2000b), de Fraiture et al. (2001) and SEI (1997) that withdrawals of more than 5,000 – 6,000km^3/yr lead to physical water scarcity, the PB was set at the lower limit of an uncertainty range of 4,000 – 6,000km^3/yr at ~4,000km^3/yr.

This rough first approach involved high uncertainties and neglected the significant regional operating scale of freshwater. Many components of this PB calculation left room for refinement to gain more accurate results. In their refinement and reassessment of the planetary boundary for freshwater use, Gerten et al. (2013) point out, that these estimations were based on very broad global determinants of PB-water that do not sufficiently incorporate spatiotemporal dynamics. Furthermore, the water requirements for habitats of aquatic flora and fauna were not spatially explicit but treated as a global average.

The most prominent approach to account for spatiotemporal heterogeneity in the calculation of the PB of freshwater use, is the concept of EFRs. EFRs were suggested as they allow to incorporate local water availabilities and constraints in a spatially and temporally explicit manner (Gerten et al., 2013; Steffen et al., 2015). Though no uniform method for calculating EFRs across all river basins or for upscaling exists, the classification of rivers per their flow regime and associated EFRs facilitates the definition of local tolerance levels of water use and their transgression, that can either be expressed at cell or at basin level. The received estimates of local water boundary values are then summed up to receive an explicit planetary boundary value (Gerten et al., 2013). This procedure still only provides a single value estimate but its calculation is more exact and it can be disaggregated to obtain spatial distribution of both EFRs and subsequent transgression of EFRs. Gerten et al. (2013) used the Lund-Potsdam-Jena managed Land (LPJmL) modelling framework to determine PB-Water based on EFRs on a 0.5°x 0.5° grid. The received spatially improved estimates of local water boundaries were then globally aggregated. The resulting planetary boundary was calculated to lie between 1,100km^3/yr and 4,500km^3/yr depending on the strictness of the assumption of EFR, the average therefore being 2,800 km3/yr. Further studies on PB-Water were done by Steffen et al. (2015) and Brauns (2016). The latter reassessed temporal inaccessibility (high flows) and developed an adapted approach

[1] See subsection S 1.2, subsection S 1.4 and subsection S 1.3 for a detailed description and an overview of the calculation of the PB for human freshwater use

for the calculation of EFRs coupled with water stress and new estimates for spatial inaccessibility. As Brauns (2016) also calculated basin values, this allows for defining a basin based boundary, which amounts to 5,205km^3/yr if the strictest EFR calculation is considered for each catchment.

As mentioned above, the planetary boundary of freshwater use is characterized by strong regional operating scales (Steffen et al., 2015). The significance of a single boundary estimate for water has been subject of debate - the effect of transgressing boundaries might be ecologically independent from one region to another. It is furthermore problematic due to the many temporal and spatial dimensions, nonlinear relations and interactions with other ES processes that characterize the hydrological cycle and freshwater use (Bogardi et al., 2013; Hughes et al., 2013; Nordhaus et al., 2012).

EFRs represent an integral component of the assessment of the PB-Water and its transgression on different scales. They not only facilitate to integrate and reflect the spatiotemporal heterogeneity of freshwater but also allow to emphasize the connection to other boundaries.

3 Environmental Flow Requirements

In the Brisbane Declaration, the 10th International River Symposium (2007) defined environmental flows as the "quantity, quality and timing of water flows required to sustain freshwater and estuarine ecosystems and the human livelihoods and well-being that depend on these ecosystems". EFRs represent the minimum amount of blue water that has to remain within a river basin to preserve ecosystem processes and resilience of depending landscapes (Steffen et al., 2015). Like households, industry, agriculture and power generation, maintaining EFRs adds a further competitor for water and therefore effectively also constitute a sector – this sector representing the 'environmental demand' (Smakhtin, 2008). EFRs in global water resources assessment allow to develop environmentally relevant policy options with improved water concepts at country, basin or other levels (Smakhtin et al., 2004b).

Rivers and depending ecosystems like floodplains represent complex interactions and their health and ecological integrity depend on many different processes (Poff et al., 1997). The maintenance of flow variability has been recognized as the major criterion for the determination of EFRs as it is the main driver involved in sustaining a river's good ecological status and it is now widely recognized that all elements of a flow regime are important for the health of aquatic and riparian ecosystems (Poff et al., 1997; Bunn and Arthington, 2002). The first approaches for determining EFRs mainly focused on keeping the flow above a critical level to only prevent low flows. The importance of high flows, e.g. for channel maintenance, bird breeding, wetland flooding and sustaining riparian vegetation, as well as moderate flows, for fish migration and cycling of organic matter from river banks, is reflected and incorporated in most methods used today (Poff et al., 1997; Junk et al., 1989; Smakhtin, 2008).

Five basic components have been identified to regulate ecological processes in river ecosystems and determine river flow: magnitude, frequency, duration, timing and rate of change of hydrological conditions (Poff et al., 1997). The environmental flow should reflect the natural flow regime as close as possible to sustain the health of river ecosystems, but flows' natural variability makes it complex to determine EFR in a one-fits-all approach. Calculations have to be as specific with regard to spatial eco-hydrological conditions as possible (King and Louw, 1998; Acreman and Dunbar, 2004). The sum of environmental flows represents the water volume that could be allocated to environmental purposes. Depending on the objective of environmental water management or the aspired conservation status (natural, good, fair or poor), the volumes allocated to EFRs can vary. Common EFR calculation methods are designed to attain a fair ecological status that can entail disturbed dynamics of the biota, loss or reduction of some sensitive species and the occurrence of alien species (Smakhtin et al., 2004a). A description of the flow elements' importance for aquatic ecosystems can be found in the following subsection 3.1.

More than 200 methods for the calculation of EFRs have been developed (Tharme, 2003). Most methods have in common that the natural variability of river flow is reflected by allocating different flow components to high and to baseflow. This is usually done by calculating EFRs based on mean monthly flow (MMF) (Steffen et al., 2015; Smakhtin et al., 2004b). EFR methods can be classified into four types:

1. Hydrological rating methods are usually based on annual minimum flow thresholds. They offer simple and fast methods and can easily be applied on global scale depending on data availability.

2. Hydraulic methods are only applied at local scale when river cross-section measurements are available

3. Habitat simulation methods are based on eco-hydrological relationships like flow velocity and certain freshwater species.

4. and holistic methods combine components of the other three methods and include assessment of the whole ecosystem and all aspects of the hydrological regime as well as water quality (Pastor et al., 2014; Acreman and Dunbar, 2004).

Global scale environmental water demand is largely unknown today as it has not been considered sufficiently in past water management approaches, is very case-specific and often data-intensive and complex to determine accurately (Smakhtin, 2008). As this thesis represents a global assessment, it is based on hydrological calculation methods for EFRs, the Variable Monthly Flow (VMF) method, the Tessmann method and the method developed by Smakhtin et al. (2004b). They are calculated based on undisturbed monthly river flow in pristine conditions and allocate percentages of flows. These "percent of flow" approaches are well employable at large scales and, when implemented, facilitate a high degree of protection of natural flow variability (Richter et al., 2012).

The Variable Monthly Flow Method

The VMF method was developed by Pastor et al. (2014). It takes into consideration the need to sustain natural variable flow regimes while it can also be aggregated and validated at basin and global scale. It defines EFRs on a monthly basis and adjusts them according to flow season. This is done by classification of the flow regime into high, intermediate and low-flow months. EFRs are then allocated as a percentage of MMF, following the natural variability of river flow. VMF considers inter-annual variability by comparing MMF with mean annual flow (MAF). Specifically, it allocates 30% of MMF as EFR during high flow seasons (when MMF is $>$ 80% of MAF), 45% of MMF during intermediate-flow seasons (when MMF is 40–80% of MAF), and 60% of MMF during low-flow seasons (when MMF $\leq 40\%$ of MAF). In extremely dry conditions (MMF < 1 ms) there is no EFR allocation (Pastor et al., 2014).

Tessmann's Method

Both Tessmann (1980) and VMF distinguish between high-, intermediate- and low-flow months to incorporate intra-annual variability. Tessmann, like VMF, defines low-flow seasons as MMF $\leq 40\%$ of MAF, but while the VMF method allocates only 60% of the mean monthly flow to low-flow months, the Tessmann method allocates all of the MMF to EFRs during low-flow months. Therefore, it is not allowed to withdraw water during low-flow seasons. Tessmann allocates 40% of MMF as EFR during high flow season (when MMF $>$ 0.4*MAF and when at the same time 0.4*MMF $>$ 0.4*MAF), and 40% of MAF during intermediate season (when MMF $> 40\%$ of MAF and when at the same time 40% MMF $\leq$ 40%MAF). The relatively high EFRs allocated to low-flow seasons in both the VMF and in Tessmann's method are applied due to the assumption that the retention of water during low-flow season is more important for the environment. The aim is to prevent seasonal droughts that could otherwise negatively impact freshwater ecosystems (Bond et al., 2008; Pastor et al., 2014).

Smakhtin's Method

Unlike Tessmann and the VMF method, Smakhtin et al. (2004a) don't distinguish intermediate, low and high flow months but assume stable EFRs throughout the year that consist of a minimum baseflow Q_{90} and a percentage of MAF that depends on the river flow variability. Q_{90} is the monthly flow that is on average exceeded in 90% of the time throughout a year. Four different cases of distribution, which are based on these two values, are distinguished. For basins with highly variable flow regimes where most of the flow appears as flood ($Q_{90} < 10\%$ MAF), the EFR is Q_{90} and additionally 20% of MAF. For rivers where 10% MAF $\leq Q_{90} <$ 20% MAF, EFR is Q_{90} plus 15% of MAF and if 20% MAF $\leq Q_{90} <$ 30% MAF then the flow requirement is Q_{90} plus 7% MAF. For very stable flow regimes with high base flows ($Q_{90} \geq 30\%$ MAF) the flow requirement is Q_{90} (Smakhtin et al., 2004a). Since this approach of defining EFRs allocates seasonally constant EFRs, in some cases these EFRs are higher than the pristine flow during that month, this has to be corrected in calculations by defining EFR as MMF (Jägermeyr et al., 2016b). Other notable hydrological methods that have been used to assess EFRs are Tennant's method and the Q_{90}_Q_{50} method. Both were used in PB calculations (Gerten et al., 2013) and calculations of inaccessible high flows (Brauns, 2016). Pastor et al. (2014), who developed the VMF and Q_{90}_Q_{50} method tested them together with the ones by Tessmann (1980), Tennant (1976) and Smakhtin et al. (2004a), compared the results with eleven case studies of locally assessed EFRs. VMF and Tessmann showed the highest correlation with the locally calculated EFRs with an R^2 value of 0.91. These two methods are best to fit many different flow regimes. Their advantage is their ability to capture the intra-annual variability and allocation of peak ows during the high-ow season in the case studies. Moreover, the transition between high and low-flow seasons is smoother due to the introduction of intermediate-flow seasons. On average the Smakhtin method resulted in the lowest EFR with 26% of MAF and Q_{90}_Q_{50} resulted in the highest EFRs with 48% of MAF, Tennant allocated on average 30% of MAF, VMF on average 33% and Tessmann 43% (Pastor et al., 2014).

The calculations of this thesis are based on VMF, Tessmann and Smakhtin like described above and implemented in LPJmL by Jägermeyr et al. (2016b). By including several methods an uncertainty range reflecting methodological differences is incorporated. EFRs are based on values for river flow (MMF,MAF,Q_{90}) derived from simulation runs of today's global water cycle. The global scale requires methodological simplifications such as the exclusion of channel and habitat maintenance floods but allows for the process-based quantification of EFRs and their transgression in the dynamic simulation environment provided by LPJmL (Jägermeyr et al., 2016b).

3.1 EFRs and Aquatic Biodiversity

The EFR concept aims at the protection of freshwater habitats. Though occupying less than 1% of the Earth's surface, the importance of these habitats as biodiversity hotspots is remarkable, supporting ~10 % of all known species as well as ~1/3 of vertebrate species (Strayer and Dudgeon, 2010). These freshwater habitats comprise lakes, reservoirs, rivers and floodplain marshes, swamps and wetlands, in total around 8-9% of the Earth's continental surface (Lehner and Döll, 2004). Most freshwater species occupy only small geographic ranges as freshwater habitats are often insular in nature. This fragmentation decreases the ability to migrate and reestablish local populations. This leads to biota with high endemism, species richness and species turnover between basins and a particularly high sensitivity to anthropogenic disturbances of habitats (Strayer and Dudgeon, 2010; Dudgeon et al., 2006). Aquatic systems are particularly vulnerable due to high human population density near lakes, rivers and estuaries, where many of the world's cities were built (Janse et al., 2015; Strayer, 2006) . Due to increasing human pressure on freshwater resources, a lot of species have already gone extinct or are endangered (Strayer and Dudgeon, 2010; Sala et al., 2000). The "Living Planet Report 2016" by the WWF found that the abundance of the monitored freshwater populations has declined by 81% between 1970 and 2012. Consequently, freshwater resources are hotspots of both – endangerment and biodiversity (Strayer and Dudgeon, 2010; Strayer, 2006; WWF, 2016).

Natural Flow and Aquatic Biodiversity

The health of freshwater ecosystems and associated habitats and biodiversity is determined by various interlinked factors. Apart from the discharge/flow regime, the physical structure of the channel and of the riparian zone, the water quality, channel management, the level of exploitation, habitat structure and the connectivity are crucial determinants (Acreman and Dunbar, 2004; Norris and Thoms, 1999).

The natural flow regime, that EFRs are trying to mimic affects biodiversity via several interrelated mechanisms operating over different spatial and temporal scales. While mainly large events play a role in determining the physical nature of the aquatic habitat as they determine channel form and shape, droughts and low-flow events are also seen as significant factors for aquatic biodiversity as they can limit overall habitat availability. Aquatic species have developed and progressed in direct response to flow regimes. Therein, particularly the seasonality and predictability of the overall pattern and the timing of particular flow events is of central importance (Bunn and Arthington, 2002). General habitat availability is regulated by droughts and low-flow events, while the distribution of riffle and pool habitats as well as the stability of the substrate is determined by the interaction between flow regime and local geology and landform (Cobb et al., 1992; Bunn and Arthington, 2002).

Another important aspect of the health of aquatic ecosystems is the access to otherwise disconnected floodplain habitats (Ward et al., 1999). Floodplains provide habitats with high spatiotemporal heterogeneity and depend on the hydrological connectivity between river channel, floodplain and groundwater. Flooding leads to the lateral expansion of oodplain habitats and generates important laying, nursery and foraging areas for many sh species and a wide range of other vertebrates. The longitudinal dispersal of migratory aquatic organisms is crucial as the viability of populations of many species of fully aquatic organisms depends on their ability to move freely through the stream network (Junk et al., 1989; Strayer and Dudgeon, 2010).

The modification of their river basins and hydrological disturbance through water withdrawals and regulation of water flows (e.g. through dams), pollution and invasive aquatic species are the main direct drivers contributing to the decline of aquatic biodiversity at the global scale (Janse et al., 2015; WWF, 2016).

The reduction of habitat size and availability as well as the alteration of habitat structure (habitat loss and degradation) have been identified as the most common threat to populations by the Janse et al. (2015). Safeguarding EFRs and therein locally adapted water quantity and timing to guarantee a natural flow regime can be a measure to prevent these. Unfortunately, due to the complexity of the relationship between natural flow regime and aquatic biodiversity, it is impossible to determine the "best" flow regime regarding conservation management. Aquatic science is not able to sufficiently predict and quantify biotic response to anthropogenic changes in natural flow. Moreover, holistic approaches for the determination and evaluation of ecosystem response to specific flow characteristics are only possible for local applications as every river has its own characteristic flow regime and associated biotic community (Richter et al., 1997; Bunn and Arthington, 2002; Naiman et al., 2002).

Coupling of EFR deficits and aquatic biodiversity

Due to this knowledge gap the fraction of EFRs that is necessary to maintain freshwater requirements of aquatic biodiversity cannot be determined specifically. Nevertheless, it can be assumed that a violation of EFRs and the involved changes concerning the magnitude, frequency, duration, timing and rate-of-change of flow negatively affects all aquatic biota and the entire associated ecosystems' health. EFRs based on natural flows represent a reasonable approach in the assessment of the extent of exploitation of freshwater resources on a global scale. In the evaluation of EFR deficits and their aggregation, data on biodiversity can facilitate the improvement of the spatial resolution of these transgressions and reflect possible consequences in terms of degradation of aquatic biodiversity. This thesis represents a revised assessment of transgression of PB water use based on EFRs including different variants on how local-scale transgressions can be aggregated globally. In a first exploratory and integrated approach this assessment is combined with biodiversity data to accentuate the strong relationship between the two PBs – biosphere integrity and freshwater use. It is an extension to recent studies on PB components (Brauns, 2016; Gerten et al., 2013) and interactions with global food production (Jägermeyr et al., 2016b). In areas with severe overexploitation of water resources and high biodiversity, regional boundaries for both - freshwater use and biodiversity - are strained.

3.2 Global Freshwater Resources and Transgression of the Planetary Boundary

In this section the most important human interventions in the terrestrial water cycle and their large scale effects are described. Water is an essential good for society, economy and nature. It is sufficiently available on a global scale, nevertheless it is scarce in wide regions of the world (Wallace and Batchelor, 1997). This is due to the heterogeneous natural distribution of physical water (simulated availability map shown in Figure 3). While it is abundant in tropical regions and at high latitudes like in wide parts of South America, Southeast Asia and tropical Africa, it is scarce in arid and semi-arid regions like in northern parts of Africa, the Middle East, Central Asia and Central America as well as Western Australia (Postel et al., 1996; UNEP, 2008). Water scarcity in terms of availability per capita on the other hand doesn't necessarily develop in arid or semi-arid areas, but mainly in regions with dense populations like Central Europe and India. Consequently, countries like Australia with few resources but low population are not affected as much (Gerten et al., 2011).

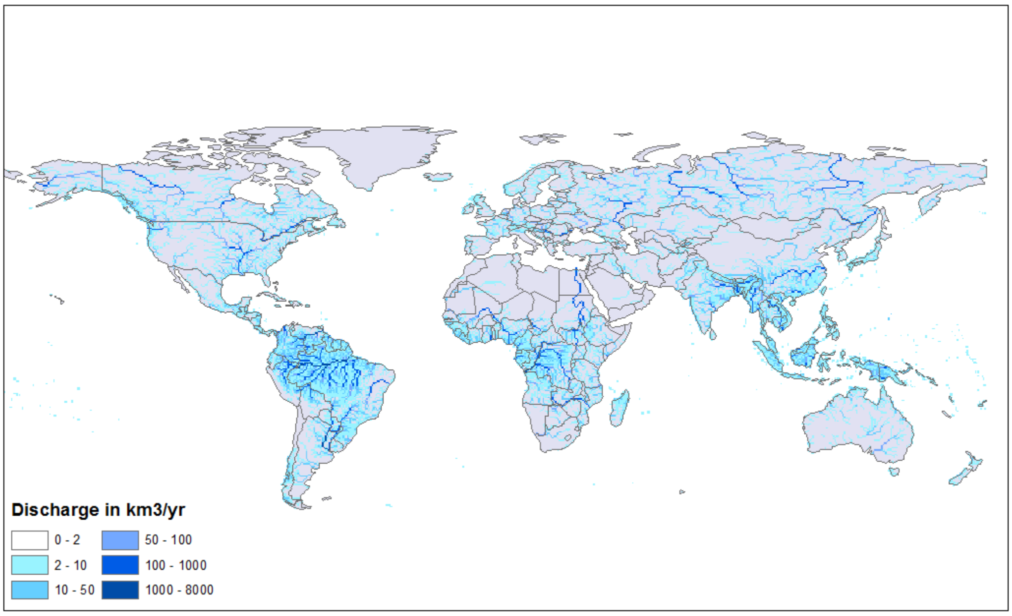

Figure 3: Mean annual discharge in km^3/yr averaged over the years 1980 to 2009, simulated by LPJmL

The mean annual EFRs as allocated by the scenario assigning the strictest requirement of the three basis methods (VMF, Tessmann and Smakhtin) in each month and each cell are shown in Figure 4[1]. Even today, society is strongly dependent on and often limited

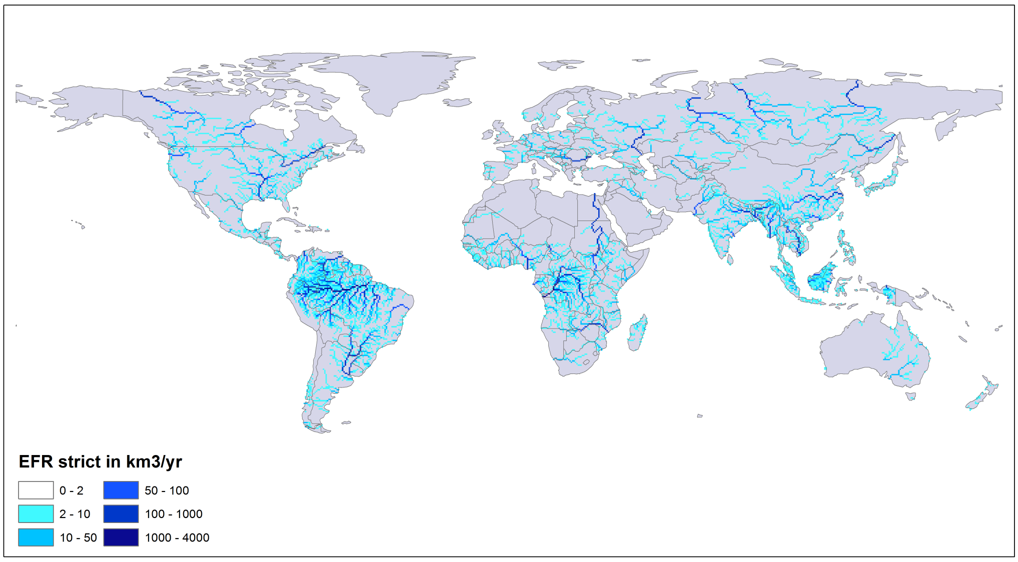

Figure 4: Environmental Flow Requirements for the strict scenario in km^3/yr averaged over the years 1980 to 2009, simulated by LPJmL

by the terrestrial water cycle. Human populations have adapted and developed numerous measures to improve the use of available water. Notably the construction of reservoirs and dams (to restrict blue water variability), irrigation of cropland (to reduce green water deficits) and groundwater abstraction are important today. These measures shall shortly be

[1] See Figure SF 9 for the other four scenarios

described. Another important measure not discussed here is international trade (transport of virtual water) which has become an important system to alleviate water scarcity in many regions of the world as it allows to extent the access to water beyond the boundaries of the individual basin (Siebert and Döll, 2010; Kummu et al., 2010).

Over half of the world's global river systems are regulated by dams (Nilsson and Renofalt, 2008). Figure 5 shows their global distribution. Displaying a high spatial variability, the total cumulative storage capacity of dams is around 20% of global annual runoff (Vörösmarty et al., 1997). In 2000, the total storage capacity of large dams was around 8,300km^3 (Chao et al., 2008). Particularly in the USA, Europe, Eastern China, Japan, India and Southern Africa river basins are influenced by the operation of dams and reservoirs.

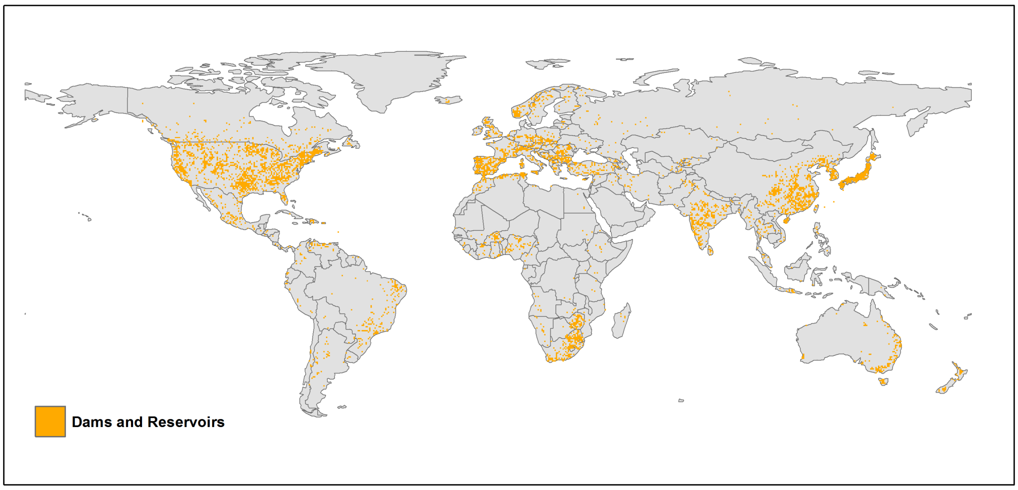

Figure 5: Distribution of dams and reservoirs with significant capacities, after Biemans et al. (2011) and Billing (2016)

Withdrawal for Irrigation, Household, Industry and Livestock

Closely linked to reservoir operation is irrigation in agriculture. Only around 20% of global cropland is irrigated. Nevertheless, irrigated food production represents the largest global freshwater user, accounting for over 70% of human water withdrawals and for over 90% of total consumptive blue water use (Siebert and Döll, 2010; Rost et al., 2008). Here, anthropogenic water consumption is understood as total water withdrawal minus return flow to the river. This consumption can be divided into productive water use – productive transpiration from plants and non-agriculture consumptive water use – and unproductive water use which includes evaporative conveyance losses, unproductive evaporation from soils, water bodies and vegetation and interception losses (Jägermeyr et al., 2016a; Rost et al., 2008). Irrigation leads to an increase of net evapotranspiration and decrease in river discharge. Biemans et al. (2011) showed that the total global discharge is decreased by 1 to 2% per month through irrigation extraction, the effect of reservoirs and irrigation combined resulting in a mean annual decrease in global discharge of 2.1% or~930km^3. While agriculture accounts for 85-90% of all withdrawals in Asia, the Middle East, North Africa and sub-Saharan Africa, it is proportionally lower in Russia and the OECD states where the other sectors are stronger (Vörösmarty et al., 2005). Estimates for global irrigation volumes for the year 2000 range from 1,900km^3/yr to around 3,800km^3/yr (Rost et al., 2008; Vörösmarty et al., 2005; Wisser et al., 2008). This study is based on 2,409.3km^3/yr withdrawal for irrigation.

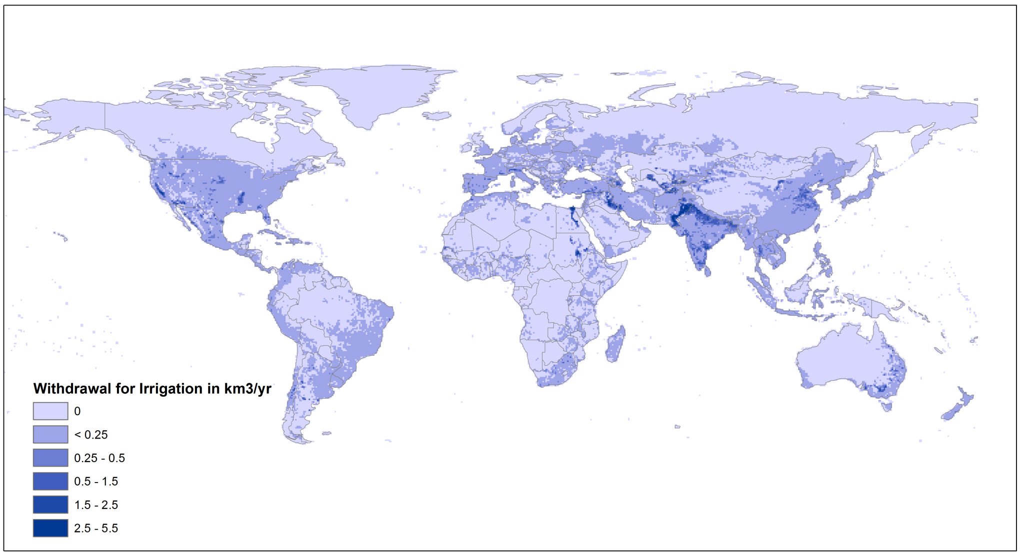

Figure 6: Mean annual water withdrawal for irrigation, averaged over 1980 – 2009, in km^3/yr

Industry's share in total withdrawal is around 20%, while it is around 10% for municipalities. Estimates for global withdrawal volumes for households, industry and livestock (HIL) range around 1,100km^3/yr (Molden, 2007; Vörösmarty et al., 2005). The value used in this study is 1070.5km^3/yr for HIL combined. Figure 6 and Figure 7 show the distribution of irrigation withdrawal and withdrawal for HIL. It can be seen, that irrigation is particularly extensive in North America, along the Nile, in the MENA region, on the Indian subcontinent and in Eastern China. Withdrawals for HIL play a more important role in Europe, India, Western China and North America than in less industrialized Africa and Eastern China. An important point to keep in mind is that water consumption differs from water withdrawal as discussed in Figure 4.2.

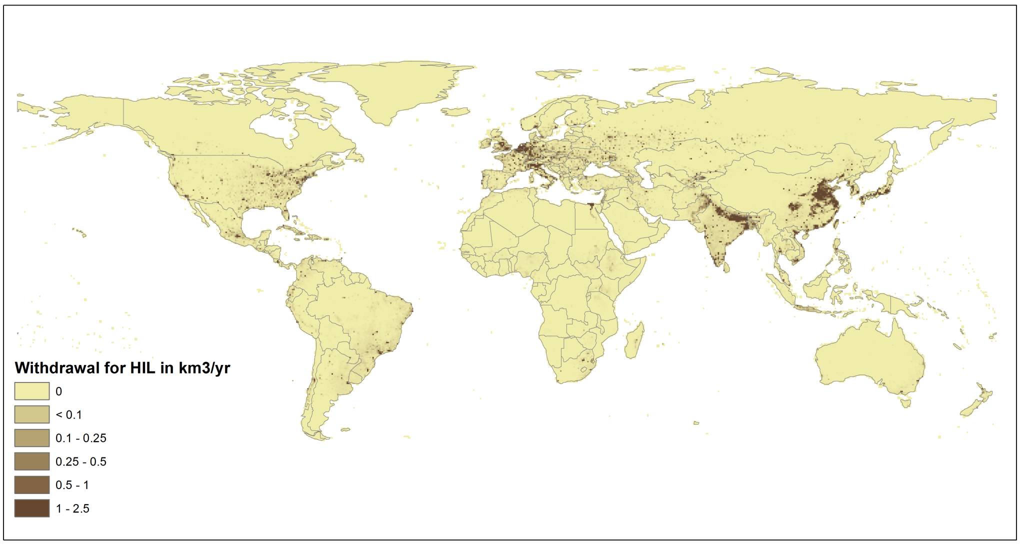

Figure 7: Mean annual water withdrawal for households, industry and livestock, averaged over 1980 – 2009, in km^3/yr

Another important source of water is mined (fossil) groundwater which is often the main water resource in regions with large aquifer systems. Water recharge rates to these aquifers are very low, especially since this water is mostly used for irrigation (Vörösmarty and Sahagian, 2000). Wada et al. (2010) estimated that global groundwater abstraction was 734 $(\pm 82) km^3/yr$. In many world regions irrigation water demand can only partially be met by locally available blue water and it can be assumed that a considerable part of additional water demand is met by groundwater abstraction (Vörösmarty et al., 2005). Particularly in Europe, North-East China, the United States, Iran, India and Pakistan abstraction rates are high and around 1.5 billion people depend on groundwater as drinking water (Wada et al., 2010; UNEP, 2008).

Global impacts

Vörösmarty and Sahagian (2000) identified changes in water storage and sea level rise, distortion of continental runoff and aging of continental runoff as the main (environmental) effects of human control of the water cycle. The distortion of continental runoff is caused by large reservoir systems, consumptive water use and inter-basin transfers. Alterations to natural river flow regime manifests in changes in long-term net runoff, in different timing and magnitude, frequency, duration and rate of change. The impacts of large reservoirs are strongest in Asia, Europe and Africa where discharge into the ocean is decreased by up to 10% in some months (Biemans et al., 2011). Although not the focus of this thesis, groundwater depletion and aquifer degradation represent a major challenge with regard to the overexploitation of the global water cycle. Overexploitation or persistent groundwater depletion occurs when abstraction rates exceed recharge rates for extensive areas and long times (Wada et al., 2010). Continuous decline in water tables leads to a reduction of discharge to the aquatic environment as well as to severe irreversible side effects like the intrusion of sea water (Foster and Chilton, 2003).

The overexploitation of freshwater resources through withdrawals for irrigation and HIL and implicitly the hydrological alterations of rivers through dams and reservoirs (the model applied here takes these into account in its simulation of discharge) are the main focus of this thesis. In particular, irrigation for food production strongly relies on water that would actually be needed to sustain riverine ecosystems, the EFRs (Jägermeyr et al., 2016b).

3.3 Objectives of this Study

This thesis pursues the following research question:

To what extent can the PB for human freshwater use be regarded as transgressed based on local transgressions of EFRs and where is global aquatic biodiversity most endangered by these transgressions.

The following analysis steps were undertaken:

- for five different EFR scenarios, mean annual EFR deficits (1980-2009) were calculated and analyzed based on LPJmL outputs of discharge and EFRs
- a two-criteria set was developed to aggregate local scale EFR transgressions to basin scale, one criterion incorporates the magnitude and uncertainty of EFR deficits and the other reflects the temporal dimension of EFR deficits
- three basin classes were defined: one for transgressed basins, one for basins at risk of transgression and one for basins that are not transgressed
- on basin scale, data on aquatic amphibian species richness and endemicity by Tisseuil et al. (2013) was incorporated to receive four spatially refined subclasses for each basin class. For this purpose, high biodiversity basins were distinguished from low biodiversity basins based on a threshold value for both biodiversity descriptors
- twelve classes of basins distinguished by state of EFR transgression and associated biodiversity, allow to depict what share of global water resources and total land area can be regarded as transgressed and where and to what extent global amphibian biodiversity is most affected by this

4 Methods and Data

As discussed in subsection 2.2, for all boundaries displaying strong regional operating scales, we lack understanding of how regime shifts through excessive transgression of local and regional freshwater thresholds spread across scales and whether global implications exist (Hughes et al., 2013). The aggregation scheme from local to global scale, concerning the state of EFRs, developed here, aims at as little information loss regarding spatial and temporal variability as possible. Further, it is important to sufficiently consider uncertainty in the calculation and evaluation methods used, and to depict their ranges. Another challenge was the compatibility of the data on discharge and EFR with the data on biodiversity.

The uncertainty in the calculation approach stems from the various EFR calculation methods available. There are several combinations of EFR methods that can be employed when evaluating their transgression. Three different methods were considered (Smakhtin et al., Tessmann, VMF) and two combinations of the three. One scenario assigning the mean of the three methods to each cell for each month (EFR_mean) and another scenario assigning the strictest/highest EFR of the methods in each month (EFR_strict) are included. Therefore a range of methodological differences is depicted and these could also be interpreted as the outcome of different environmental policies (Jägermeyr et al., 2016b). There is a wide range of possible criteria available that can be applied to examine transgression of EFRs and their propagation on different scales. This thesis is based upon two main criteria, one for the spatial and one for the temporal distribution. The first criterion is called the “transgression-to-uncertainty-ratio” and the second “duration of transgression”. In the following, first the LPJmL as well as the model specification applied in this thesis are described in detail. Afterwards, in subsection 4.2, the calculation procedure is explained.

4.1 The Lund-Potsdam-Jena managed Land dynamic global vegetation and water balance model (LPJmL)

LPJmL is a process-based, dynamic global vegetation and hydrological model that simulates the connected terrestrial carbon and water cycles. First described by Sitch et al. (2003), it was developed by scientists from Lund University, Max-Planck-Institute in Jena andPotsdam Institute for Climate Impact Research (PIK) and it was updated hydrologically in 2004. The consolidated version of LPJmL incorporated additional processes such as interception and soil evaporation and stochastic distribution of precipitation. When LPJmL was developed, the aim was to receive a broad range of potential applications to global questions while including major processes of vegetation dynamics and working with a computationally efficient representation of processes using the widest possible range of data sets from atmospheric and ecosystem science (Sitch et al., 2003; Rost et al., 2008). Key ecosystem processes that LPJmL can simulate are photosynthesis, evapotranspiration, autotrophic and heterotrophic respiration as well as allocation of assimilated carbon (Rost et al., 2008). While the original model mainly simulated changing patterns of potential natural vegetation based on soil properties and climate (Sitch et al., 2003; Gerten et al., 2004), LPJmL includes a dynamic representation of crop- and grazing land and can simulate plant growth, production and management regime (Bondeau et al., 2007; Fader et al., 2010). To be able to calculate daily transitional discharge volumes in each grid cell, the model has been enhanced with a river routing and irrigation module (Rost et al., 2008). Furthermore, a dam and reservoir module has been implemented to account for the significant impacts these structures have on natural discharge patterns (Biemans et al., 2011). Biemans et al. (2009) validated the model against discharge observations in 300 different river basins and Rost et al. (2008) validated is against global water use and consumption. To account for different types of natural vegetation, nine different plant functional types (PFTs) representing natural vegetation at the level of biomes were defined to include the functioning and variety of structure among plants (Gerten et al., 2011; Sitch et al., 2003; Smith, 1997). Moreover, 12 crop functional types (CFTs) representing the world's major food crops are distinguished according to Bondeau et al. (2007). The model simulates growth, production, and phenology of these nine PFTs, of grazing land and of the 12 CFTs. While PFTs' composition and distribution are simulated by the model, CFTs' coverage of the grid cells is specified beforehand. Unlike previous global vegetation models, LPJmL incorporates explicit representations of vegetation structure, dynamics, and competition between PFT populations as well as soil biogeochemistry.

Spinup Years and required Input Data

When running LPJmL, a spinup period is required. The effect of the spinup is to reach an equilibrium for carbon pools and PFT distribution. During the spinup, randomly shuffled data from the first 30 years of climate input data is applied (Jägermeyr et al., 2016a).

Input data for LPJmL include climate data, data on soil properties, CO_2 concentration, human land use and river flow direction. The model runs on daily time steps for 67,420 grid cells covering the globe's land surface at a spatial resolution of 0.5° longitude by 0.5° latitude (Gerten et al., 2004; Sitch et al., 2003). To be able to run at daily time steps, input values have to be adjusted by interpolation as they are only available in larger time units (Gerten et al., 2004). The runs used in this thesis were forced with the Climate Research Unit (CRU)'s TS 3.10.01 monthly climatology for temperature data and for cloudiness (Harris et al., 2014) and with the Global Precipitation Climatology Centre (GPCC) Full Data Reanalysis precipitation data version 6 (Rudolf et al., 2010; Schneider et al., 2014). To receive the number of monthly rainy days, data from CRU and GPCC was combined as described by Heinke et al. (2013).

Discharge and EFR Modelling in LPJmL

As previously discussed, green water is an important part of the global hydrological cycle. Several studies have proven LPJ's/LPJmL's capabilities to assess global green and blue water fluxes as well as their inter-annual variations. Furthermore, soil moisture, runoff and evapotranspiration are reproduced well (Gerten et al., 2011; Rost et al., 2008; Fader et al., 2010). To compute the daily transitional discharge volume in each grid cell (the blue water stocks and flows) and river discharge Q, a river routing module was implemented (von Bloh et al., 2010). The transport directions in rivers simulated in LPJ are based on the global 0.5° drainage direction map (DDM) Simulated Topological Network (STN) 30 by Vörösmarty et al. (2000a). STN organizes the land area into drainage basins and specifies the river network topology. This DDM assumes that cells either drain into one of their eight neighboring cells or into none if the cell is an inland sink or if it is a basin outlet to the ocean. As dams and reservoirs play a big role in global hydrological cycle, the implemented dam and reservoir module contains information on 6,862 different dams and associated reservoirs based on the Global Reservoir and Dam database by Lehner et al. (2011) and allows for the improved simulation of discharge in impacted basins (Biemans et al., 2011).

The model incorporates irrigation by assigning distribution of irrigation systems for each grid cell and CFT. Different scenarios can be run distinguishing water availability, efficiency and type of irrigation system (Jägermeyr et al., 2015). The model divides precipitation water and irrigation water, into soil moisture , transpiration, soil evaporation, interception and runoff. Interception loss together with evaporation from soil, lakes and canals make up unproductive water consumption, which in turn depends on potential evapotranspiration. To calculate the productive water consumption for each CFT and PFT, the lesser of either soil water supply or atmospheric demand is determined for each. These fluxes are calculated and differentiated by the share of green and blue water for different rainfed and irrigated CFTs and for PFTs (Rost et al., 2008).

Currently, LPJmL has 158 different outputs defined. The format of LPJ's output data is plain binary and represents either annual, monthly or daily outputs depending on the variable. This study is based on model outputs of discharge and EFRs, LPJmL computes both in cubic hectometers per day (hm^3/d).

LPJmL model specifications

The time period of simulation was 1950-2009. The MIRCA2000 land-use dataset by Portmann et al. (2010) was used to specify global cropland extent and the extent of irrigated land was taken from Siebert et al. (2015). Human water use includes irrigation as well as HIL's water use and is constrained by local availability of renewable freshwater, while contributions from fossil groundwater are not implicitly presumed in LPJmL (Jägermeyr et al., 2016a). HIL represents an input parameter, both withdrawal and consumption is specified beforehand like defined by Flörke et al. (2013), while irrigation water use is simulated by the model (Jägermeyr et al., 2016b; Rost et al., 2008).

The calculations in this thesis are based on five different LPJmL runs. One to simulate the current situation (CS) with water use for both HIL and irrigation, one to simulate potential natural vegetation (PNV) and no anthropogenic water use, no land use and no reservoir and dam operation and three individual runs for the three EFR methods. In these "respect EFR" simulations a temporal restriction for total water withdrawal is applied if these withdrawals would tap EFRs (Jägermeyr et al., 2016b). EFRs in LPJmL were calculated like described in section 3.

Table 1 shows the different runs and the respective values for discharge, water use and water consumption. In the three simulations respecting EFRs, withdrawals for HIL and irrigation were restricted if these would tap the prescribed EFRs in the respective cells which therefore also reflects in the global total of discharge in these runs.

Table 1: Global sums of annual discharge, water abstraction and consumption for HIL and irrigation for the different LPJmL runs (in km^3/yr)

Run	**Global annual discharge**	**Irrigation withdrawal**	**Irrigation consumption**	**HIL withdrawal**	**HIL consumption**
Current situation	54601.9	2409.3	1254.7	1070.5	192.8
Potential natural vegetation	55514.73	0.0	0.0	0.0	0.0
VMF	54951.5	1574.0	894.9	909.4	165.1
Tessmann	55001.8	1542.6	863.9	843.9	142.7
Smakhtin et al.	54953.9	1592.5	898.4	779.7	158.8

The aim of using different model runs was to include and reproduce the accumulated impacts of human water appropriation on naturalized flow regimes, including downstream effects (Steffen et al., 2015). As EFRs were calculated based on natural water conditions, the run omitting human water use (PNV) represents these natural conditions and together with the CS run allowed for a calculation of transgression of EFRs as well as a comparison between current/actual and optimum conditions. Average monthly values of the last thirty years (1980-2009) were the basis of calculations. The EFRs as computed by LPJmL were averaged over the same period. If not specified differently, results are given in

km^3/yr. Calculations were performed with the programming language R, while plots and visualizations were done using the geographical information systems ArcGIS and QGIS.

Adjustment of considered Area

Some areas had to be excluded from calculation to account for volumes that humans cannot access. Moreover, areas where the amount of discharge is very low and therefore no environmental flows are allocated were omitted. By doing so it is assured that transgressions of EFRs are caused by anthropogenic withdrawals and are not artifacts in the model. The world's total land area is 146,376,945 km^2, of which 110,675,112km^2 (=75.61%) were regarded as affected by humans in the following calculations. Furthermore, there were no EFRs assigned to months where discharge in PNV was less than $1m^2/s$. Therefore, cells where this is the case twelve months a year were not considered when area shares are calculated. This is the case when aggregating transgression from cell to basin scale. The annual sum of discharge in these areas is $3.96km^3/yr$[1].

4.2 Calculation Procedure

The calculation procedure is depicted in Figure 8 After examining the sums of global EFR deficits/transgressions for the five scenarios, its spatial patterns were assessed and then the two criteria were evaluated on cell scale. Afterwards, these criteria were used for the aggregation to basin scale. As these two main criteria were applied over all five EFR methods, 10 different setups were received varying in terms of calculation method and focus upon assessment of transgression. Nevertheless, to reduce the number of setups that had to be considered, after an assessment of transgressions on basin scale, the criteria were combined. It was therefore possible to assess the transgression status on cell and basin scale and distinguish areas that are transgressed due to duration or severity or both, but afterwards this was not possible anymore. The five setups were combined with the data on aquatic biodiversity for a spatial refinement and finally, these results were used to evaluate current state of freshwater use concerning the approach of the planetary boundary with specific focus on aquatic biodiversity.

[1] see section S 2 for details

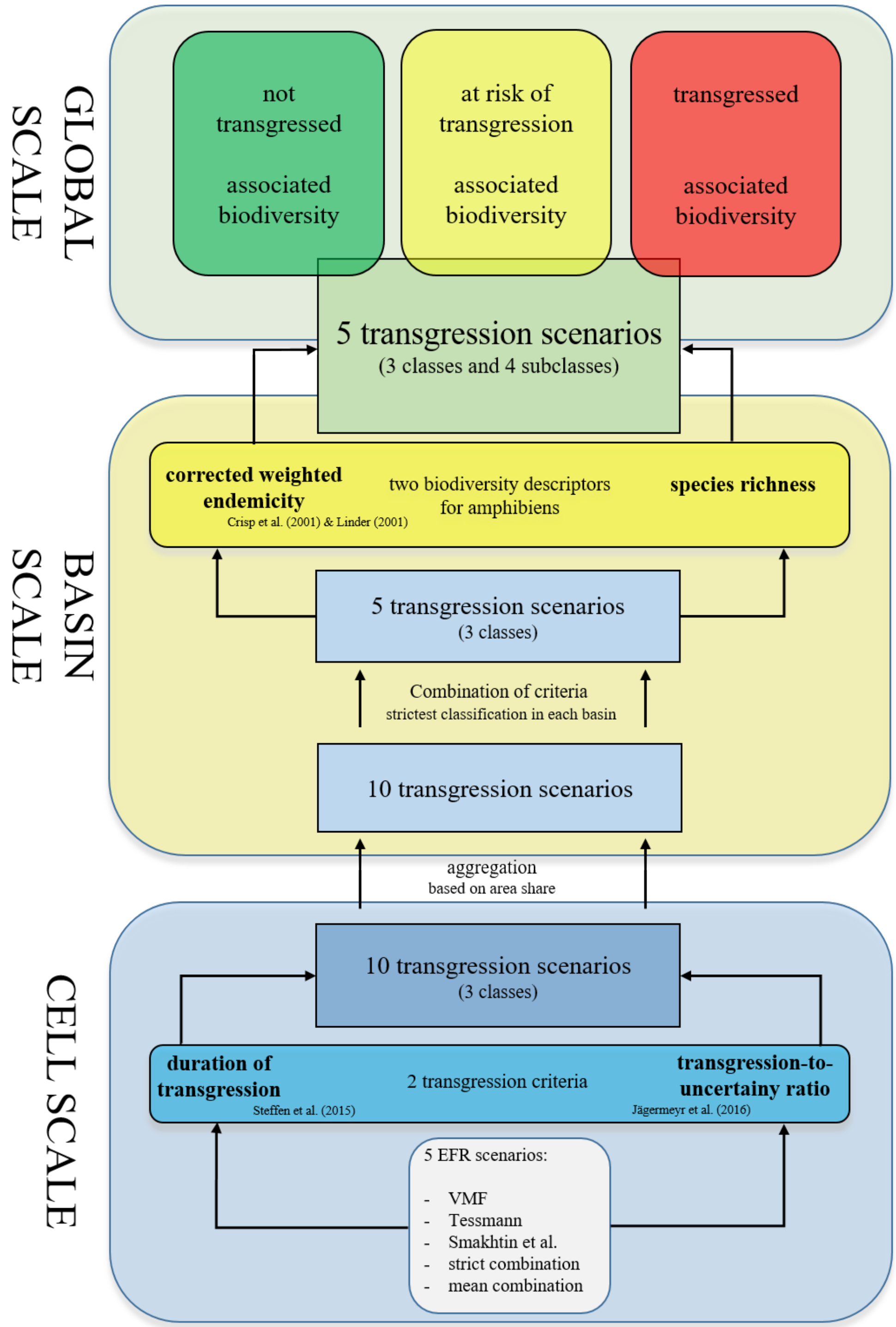

Figure 8: Calculation Procedure

Calculation of Transgression

The transgression of EFRs was calculated from the difference between EFRs and the discharge in the scenario including land use (disCS) as simulated by LPJmL. As shown in Figure 9, the difference between the discharge in the scenario with potential natural vegetation (disPNV) and the one with human water use (disCS) is assumed to equal the total anthropogenic consumptive water use. By using the discharge as a calculation basis instead of withdrawal data, all anthropogenic effects on water volumes were included and return flows were accounted for, as described in subsection 3.2. Nevertheless, this approach entails the disadvantage that spatial information on the distribution of water overexploitation is lost to some extent, as only the consumptive water use component and its downstream effects are assessed. Here, the return flow was regarded as a quantity that can be reused over and over again in the basin while in reality this water is missing at the place and time of extraction with effects on the ecosystems located there (Falkenmark and Lannerstad, 2005). Figure 9 shows the transgression of EFRs on the left (a), while the case where EFRs are not tapped is shown on the right (b). Note that, concerning the gross effect of human activities on the global water cycle, precipitation increase, land use and land cover conversion's consequences counterbalance and cancel out the effects of irrigation and HIL withdrawals (see section 6). Globally, discharge has increased and evaporation has decreased between 1901 and 2002 (Gerten et al., 2008; Rost et al., 2008).

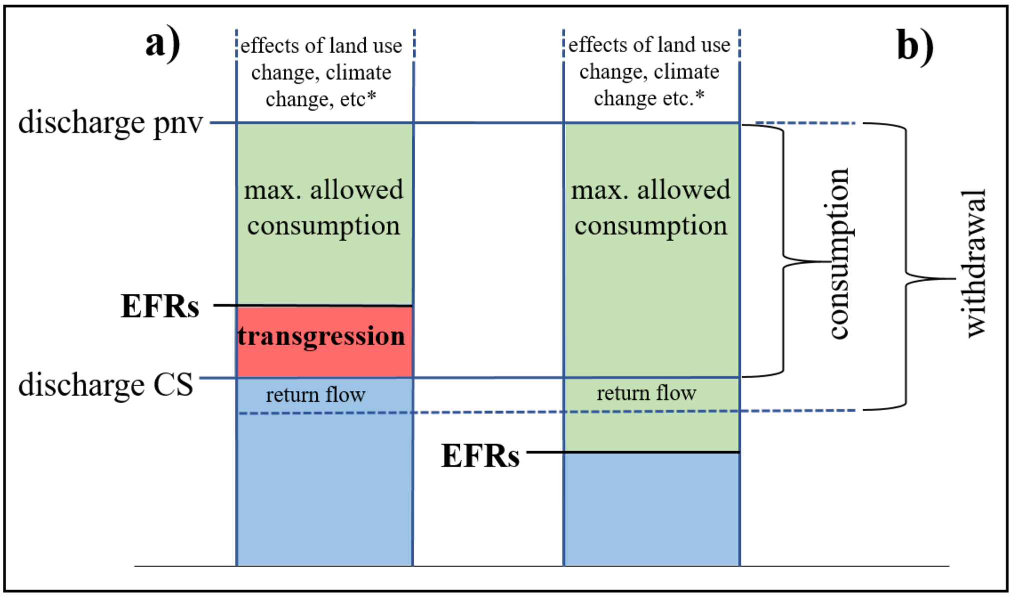

Figure 9: Schematic representation of transgression (a) and fulfillment (b) of EFRs as well as total anthropogenic water consumption

∗not considered in this analysis, the proportion of these water volumes is considerably higher in reality, see discussion and (Gerten et al., 2008)

It can happen that the different methods assign higher EFR volumes than actually present in the scenario without human land use. Therefore, transgressions were corrected by subtracting the difference between respective EFRs and corresponding values of dis pnv if necessary[1]. In addition, transgressions were set to zero for all transgression smaller than 1 m^3/s, this value was chosen arbitrarily to account for uncertainties regarding EFR calculations and discharge modelling, this is stricter than the threshold set by Jägermeyr et al. (2016b) who chose 0.1 hm^3/d (=1.157407m^3/s). Also, transgressions were set to

[1]This is the case if (EFR − dis PNV) > 0

zero for every month in every cell where the discharge in the scenario without human land use (dis pnv) is smaller than $1 m^3/s$. This was done to account for the mobility of small rivers and diversion of many streams in discharge CS.

4.3 Criteria

To evaluate the transgression of EFRs, a classification system facilitated to distinguish cells according to the severity of transgression. Each of the two criteria applied was divided into three ranges, distinctions were drawn based on the severity of possible harm that may arise from the transgression and as suggested by Jägermeyr et al. (2016b) and Steffen et al. (2015). The highest category of each criterion defines cells that are transgressed.

First Criterion: Transgression-to-uncertainty ratio

To account for both the height of transgression as well as methodological uncertainty concerning the EFR calculation, the "transgression-to-uncertainty ratio" (in the following called uncertainty ratio) was used, which distinguishes three levels of uncertainty to categorize results regarding their reliability. It is the proportion of the transgression (EFR deficit) and the span of the EFRs, the span represents the difference between the strictest and the most tolerant of the three EFR methods. This indicator combines both height of transgression with the range of EFR. It is calculated as

$$\text{Transgression-to-uncertainty ratio} = \text{EFR deficit}/\Delta\ \text{EFR}$$

It accounts for both, the insecurities/differences in EFR calculation methods and height of transgression. The ratio:

- is high for cells where EFR values are similar over all methods (their range therefore small) and transgression is high,
- is small for "uncertain" EFR values and small transgression.

The case discrimination follows the classification of uncertainty by Jägermeyr et al. (2016b). If the transgressions' share in the range of EFRs is $>100\%$, the area is regarded as beyond the uncertainty range. Freshwater resources in these cells are classified as transgressed. If the ratio is between $\geq 5\%$ and $\leq 100\%$ EFR deficits are regarded as within uncertainty and if it is $< 5\%$ it is below the uncertainty range. The uncertainty ratio was calculated for all cells the EFR range as EFR transgression in the respective scenario were larger than $1\ m^3/s$. Further, cells where this ratio was less than 1% were not included. This was done for every month and grid cell and then averaged over the year.

Second criterion: Duration of Transgression

The duration of transgression criterion was applied to incorporate the temporal dimension. Mean values of EFR transgressions such as average monthly values are difficult to evaluate as there might be a considerable temporal variability not visible in these mean values. Annual values/sums of EFRs/transgression on the other hand don't reflect the allocation over the year either. Therefore, this criterion is used to distinguish cases regardless of the height of transgression solely based on the duration of transgression. Transgressions of less than 3 months were regarded as safe, while transgressions of 3 to 5 months were assumed to show increasing risk of transgression and more than 5 months high risk/-transgressed. This case discrimination follows the classification used by Steffen et al. (2015)[1], the only difference is that 6 months of transgression were regarded as high risk while Steffen et al. were less strict and classified these cells as increasing risk.

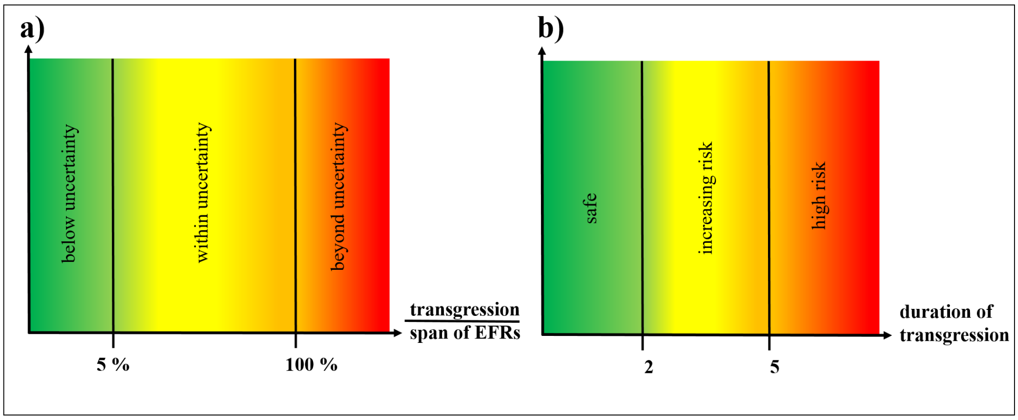

Figure 10: Classification system for the two criteria, transgression-to-uncertainty ratio (a) & duration of transgression (b)

Definition and Classification of Transgression of EFRs

Green cells signify transgressions classified as below uncertainty (1st criterion) or safe (2nd criterion). These cells' areas and freshwater resources were considered as not transgressed. Transgressions that are within uncertainty (1st criterion) or displaying increasing risk (2nd criterion) are marked as yellow cells. These water resources were considered as already strained and endangered to be transgressed by human activities. EFR deficits that were characterized as beyond uncertainty or showing high risk define red cells. The EFRs in these cells were considered as definitely transgressed.

Basin Scale Evaluation

Unfortunately, literature for the classification and evaluation of basins with regard to aggregation of local boundaries and the status of local EFRs is lacking as discussed before. Several possibilities for upscaling exist, particularly classifications based on share in discharge, but due to the aggregation of discharge along the river basin to the basin mouth

[1]In their Supplementary Materials, p.21

this is complex and afflicted with uncertainties. Therefore, the area share of cells falling into the respective ranges was applied to determine the basins' classification. The concept behind this is that if the transgressed or severely strained share of area in a basin increases, the accessible places of refuge for aquatic biodiversity decrease, there are less compensating flows within the basin to mitigate the effects of overexploitation, and due to the hydrological connections within a basin, transgressions are amplified.

In this explorative approach, the values for the classification of basins were chosen arbitrarily but based on reasonable and cautious assumptions to appropriately depict severity and distribution of transgressions. For this purpose, histograms and maps of the distribution of different shares and their global frequency were evaluated[1] the classification in Table 2 was chosen.[2]

Table 2: Thresholds for the classification of basins based on cell area

Basin classification	**Share of cell area**
Transgressed - red	$\geq$ 10% of area in a basin is transgressed
Risk of transgression - yellow	$\geq$ 30% of area in a basin either transgressed or strained (while less than 10% are transgressed)
Not transgressed - green	$>$ 70% of area show no transgression or transgression is classed as safe/below uncertainty

4.4 Incorporation of the Data on aquatic Biodiversity

As a next step, the data on biodiversity was incorporated into the assessment. The aim was a refinement of basin classification to distinguish basins with high biodiversity from basins with lower levels of biodiversity. Many hotspots of high species richness and endemism have been identified by conservationists. Nevertheless, substantial global data summaries are still rare and vary in choice of parameter. The data incorporated in the quantification of biodiversity endangerement used in this thesis is derived from a recent approach Tisseuil et al. (2013). Their analysis of freshwater species diversity is based on two parameters – species richness and the corrected weighted endemicity index (CWEI). While species richness simply represents the total number of native species found in a drainage basin, the CWEI is a measure of proportion of endemics in a drainage basin. This index was first introduced by Crisp et al. (2001) and Linder (2001), it is "calculated as the sum of species present in a drainage basin weighted by the inverse of the number

[1] those maps and histograms can be found in subsection S 3.5 and subsection S 4.1

[2] Another classification with the threshold shares at 30% for red and 50% for yellow is examined in subsection S 4.2

of drainage basins where the species occurs divided by the total number of species in the drainage basin" (Tisseuil et al., 2013, p.366). This measure of restricted range diversity reduces the correlation of endemicity and species richness usually characterized by a roughly similar log-normal distribution of species-range sizes (Gaston et al., 1998; Linder, 2001). The index calculated by Tisseuil et al. (2013) hence displays only moderate correlation with species richness unlike other indicators like simple endemicity indices. While species richness does not correlate among basins, the CWEI does. As data availability was limited to a coarse grain, the datasets are compiled at river basin scale. Of course, many species do not inhabit the entire basin, therefore limiting the significance particularly in larger basins.

In 819 examined river basins the data comprises 13,413 freshwater species among five taxonomic groups: crayfish, aquatic amphibians, freshwater fishes, aquatic birds and aquatic mammals. As the usage approval by the authors is limited to one dataset, the amphibian dataset was chosen. Tisseuil et al. found that this taxon displayed the highest congruency with the other taxa for the two diversity descriptors, [1] therefore representing a good surrogate for global freshwater assessment. This dataset comprises 3,263 species. Figure 11 and Figure 12 show the global distribution of total native species richness and endemicity for amphibians.[2] Note that the classification of values was chosen based on natural breaks in the data values for a better demonstration of differences between basins.

Four taxonomic groups show highest values for both descriptors in tropical and subtropical drainage basins. Only crayfish diversity is concentrated elsewhere, in North America, Southeast Australia and to some extent Europe. South America, Eastern Africa and South-East Asia display the highest species richness as can be seen in Figure RR. Amphibians´ species richness is seldom more than 7 species per catchment in the northern latitudes, while the Amazon basin is home to almost 498 different species, in the neighboring La Plata and Orinoco basins 320 and 221 species were found, 225 in the Congo Basin and 182 different species in the Yangtze Basin. In terms of endemicity, it is generally highest in northern South America, Central Africa and South-East Asia, only the endemicity of crayfish is highest in the Mississippi basin. Figure 12 shows that the centers of endemicity for amphibians lie in the Amazon basin (CWEI = 0.648), the Yangtze basin (0.742) and the Ganges-Brahmaputra basin (0.601).

[1] Congruency was tested by assessing the effect of each environmental predictor and taxon on the two diversity descriptors. Pairwise comparison was done using a simultaneous autoregressive model excluding the predictor of interest. Amphibians correlation is highest with birds (p = 0.82), followed by fish (p = 0.69) and mammals (p = 0.59) and it is lowest with crayfish (p = 0.21). For details see Tisseuil et al. (2013)

[2] See section S 6 for the datasets for fishes, crayfish, aquatic mammals and birds

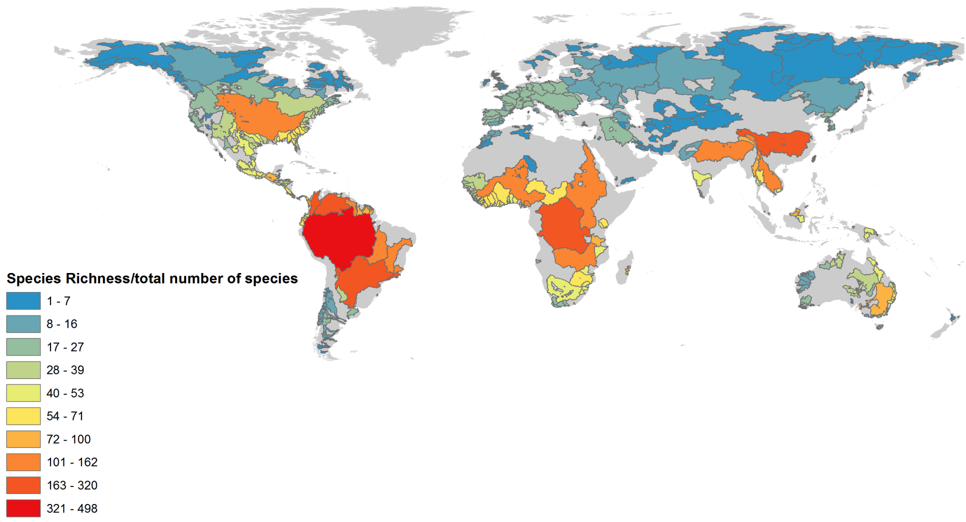

Figure 11: Global distribution of amphibians, total native species richness (Tisseuil et al., 2013)

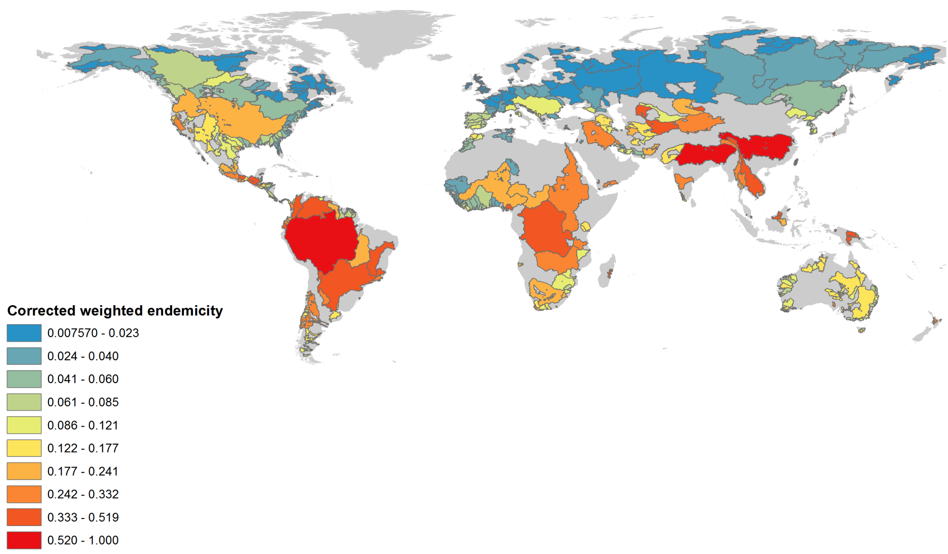

Figure 12: Global distribution of amphibians, corrected weighted endemicity index (Tisseuil et al., 2013)

As an analysis with a better spatial resolution was not possible, data integration was done indirectly by downscaling from basin scale. Basins for which only data for either - water or biodiversity – were available were left out of the assessment. The area covered by the dataset by Tisseuil et al. (2013) is smaller than the area EFR (transgressions) are simulated for by LPJmL. Unlike in LPJmL, the delineation of river basins for these datasets was done using the HydroSHEDS database like described by Lehner and Grill (2013). Therefore, the data by Tisseuil et al. (2013) is rasterized based on the LPJmL grid. Further calculations are then performed on cell and basin scale as delineated by STN.

Choice of biodiversity thresholds

The main challenge in the combination of the datasets was the prevention of information loss particularly due to the different basin delineation[1]. In the evaluation of EFR transgression and associated levels of biodiversity, biodiversity data was considered for basins that were at least 50% overlapping.[2] The two criteria –the uncertainty ratio and duration of transgression – were combined to reduce the number of setups. A basin fell into the red category if either of the two assigned it to the red category. This differentiation was excluded in the assessment of biodiversity to reduce the number of setups that had to be evaluated. The basin classes were assessed separately and nine subclasses were introduced, three for each basin class. The new subclasses were defined by the height of the biodiversity descriptors in the respective basins. The first subclass was defined by particularly high biodiversity according to both biodiversity descriptors and the other two subclasses by particularly high biodiversity according to one of the descriptors. Therefore, the red, yellow and green classes were divided into four classes, one with no particularly high biodiversity.

The main challenge that had to be met was to find a suitable definition of "particularly high" biodiversity. In the assessment of global pattern of biodiversity, the differences in spatial scale are important. For example variation in latitude, longitude, altitude, depth, aridity and topography (Gaston, 2000). As a separate analysis of biodiversity along these gradients was beyond the scope of this study, a simple global threshold was chosen. Above the 50^{th} percentile/median biodiversity was considered as high. This corresponds to a CWEI of at least 0.075435 and/or species richness of at least 18. The resulting classification allowed to distinguish where high endemism, high species richness or both occurs in transgressed or from transgression endangered basins. Furthermore, the biodiversity in basins that are not transgressed (green) was shortly assessed. For the assessment of the transgression of EFRs on a global scale, instead of using an aggregation scheme, shares in area and discharge were assessed. By looking at the different classes of basins and their combined share in total global land surface as well as discharge, a distinction of global water resources in terms of their transgression status is possible. Further, the share of these areas coinciding with high biodiversity can be distinguished.

[1] see Figure SF 4 for a map of HydroSHED superimposed on the basin delineation used in LPJmL
[2] consult subsection S 4.3 for a comparison of the datasets with 50% and 30% overlapping

5 Results

5.1 EFRs and EFR deficits

First the global sums of EFRs and of EFR transgressions/deficits through withdrawal by irrigation and HIL are analyzed, then the results of the two criteria are examined on local scale. Depending on the respective scenario, the simulated sum of global EFRs ranges between 11,932km^3/yr and 18,156km^3/yr in the period of 1980 – 2009 (as shown in autoreftab:UI). In this assessment, the sums of transgression (i.e. water withdrawals tapping EFRs) range between 117 and 207km^3/yr. 148km^3/yr is the result for the scenario using the mean EFR in each months and cell. The sum of annual EFR deficits/transgressions represents the global sum of anthropogenic freshwater overexploitation per year averaged over 1980-2009. This overexploitation is tapping EFRs and missing to sustain river ecosystem health and functions depending on it. Although the requirement totals are lower, sustaining EFRs using the Tessmann method implies more transgression than the VMF method does. The main difference in their algorithms is the allocation of EFRs to low-flow season, VMF allocates 60% of MMF and Tessmann 100%. This means that withdrawals during low flow season in the Tessmann scenario always represent transgression, while VMF allows the withdrawal of 40% of MMF. Pastor et al. (2014) reasoned that low flow seasons usually show the highest demand of the irrigation sector, a complete ban, as the Tessmann method implies, might therefore be too strict.

Table 3: Annual global sum of EFRs and EFR deficits (in km^3/yr)

Scenario	**strict**	**mean**	**vmf**	**Tessmann**	**Smakhtin et al.**
Sum of EFRs	18 156	12 408	13 538	11 932	14 419
Sum of EFR deficits	207	148	117	152	153

The annual amount of EFR deficits can be illustrated by assigning the value of the sum of the annual transgression that is occurring to the respective cell. Figure 13 shows the sum of annual transgression for the three basis scenarios in absolute terms.[1]

[1] for visibility reasons, only basis scenarios are depicted here, see subsection S 3.2 for strict and mean scenarios of global sums and both water criteria results

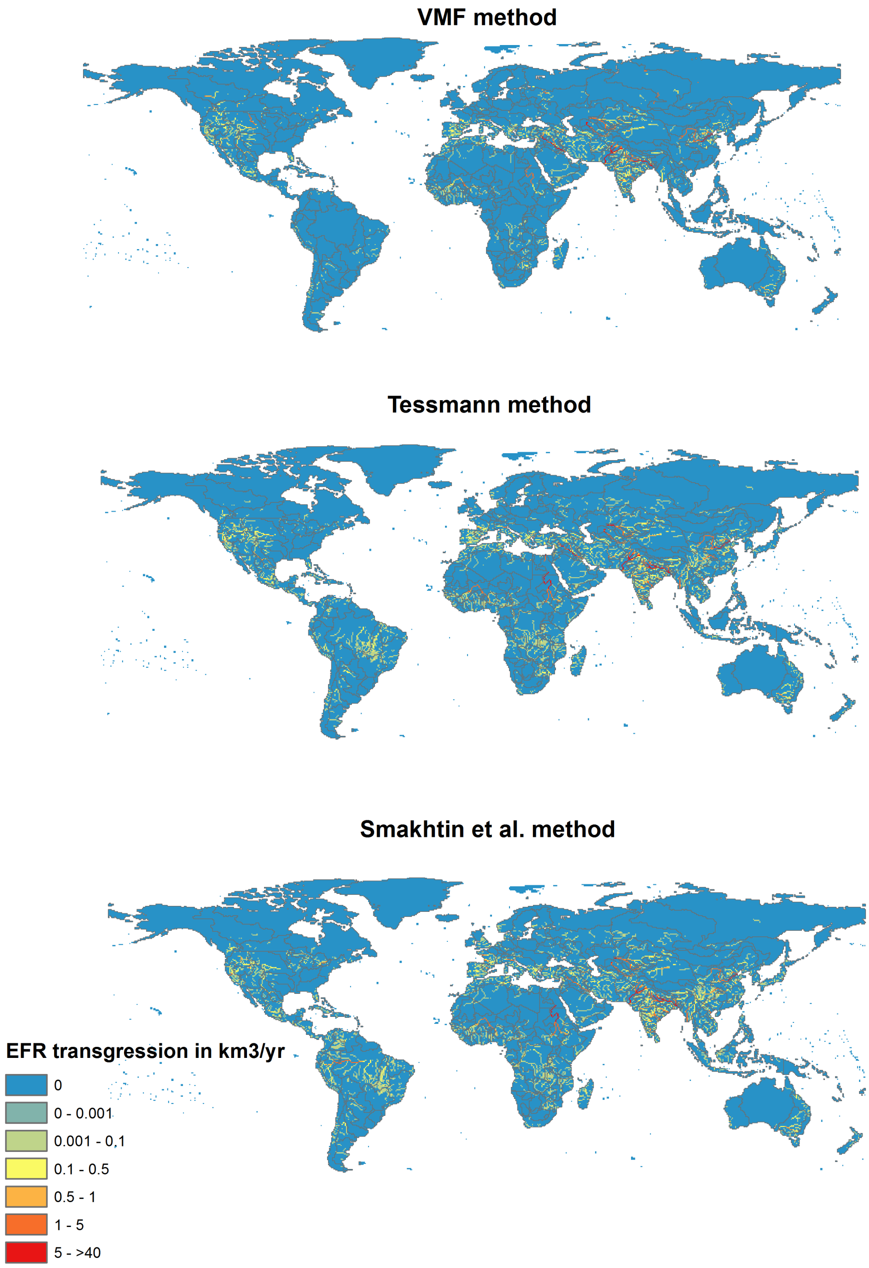

Figure 13: Sum of annual transgression of EFR on cell scale (1980-2009, 0.5° resolution) in km^3/yr, for the three basis methods, major river basins delineated

Severe annual deficits are especially observed in the river basins of the Indus in Pakistan, the Amu Darya in Uzbekistan, the Chu-Talas in Kazakhstan, the Ganges in India, the Nile in Egypt/Sudan, the Euphrates River in Iraq/Syria, and the Yellow River in China. The Indus and the Ganges rivers display transgressions to such an extreme extent that its combined share in total global transgression is larger than 35% regardless of the EFR method applied. The VMF even assigns a share of 42% in total deficit to the Indus River alone, while only 5% to the Ganges. Combined with the Yellow River, the Amu Darya River and Chu-Talas, the share of total deficit amounts to around 50% in these Asian basins alone, again regardless of EFR scenario.[1] Furthermore, in the Indus Basin, the annual transgressions' share of remaining discharge exceeds 300%, this means that discharge would have to increase more than three times for EFRs to be fulfilled.[2] The differences concerning the spatial distribution between the basis EFR methods can not only be seen in the Ganges, but also in other regions. In the Nile basin, VMF leads to substantially lower transgressions than the Smakthin et al. and Tessmann methods. Either of the latter two suggests widespread transgressions in Central Asia and extensive but low transgressions in South America, while the VMF scenario implies more intensive transgressions in fewer basins.

5.2 Local Scale Results

First criterion – transgression-to-uncertainty ratio

The results of the cell classification according to the first analysis criterion are shown in Figure 14: green areas lie below, yellow areas within and red areas beyond the uncertainty range. Areas excluded for reasons of small discharge are colored in grey, those excluded for being outside of anthropogenic influence in green-grey. Severe degradation – an EFR deficit beyond uncertainty – can be found in West, Central and South Asia, in the Mediterranean, in Western North America, and the North China Plain. While the aforementioned river basins show high volumes of transgression in the global comparison, the first criterion assigns substantial transgressions beyond uncertainty to the Murray-Darling River in Australia, the Midwestern and Western River Basins in the USA, the Mediterranean River basins in Italy, Spain, Turkey, Greece, Tunisia, Algeria, Libya and Morocco and to the Wadi Zabib basin in Yemen. The Nile is not classed beyond uncertainty as the VMF assigns substantially smaller EFR volumes to this basin than the other methods do. The uncertainty ratio is based on the span of EFRs which is large for the Nile, the resulting ratio therefore smaller.[3]

[1] See subsection S 4.5 for a detailed breakdown of river basins' share in total global transgression
[2] See subsection S 4.6 for details
[3] see subsection S 3.3 for details on the categories of uncertainties

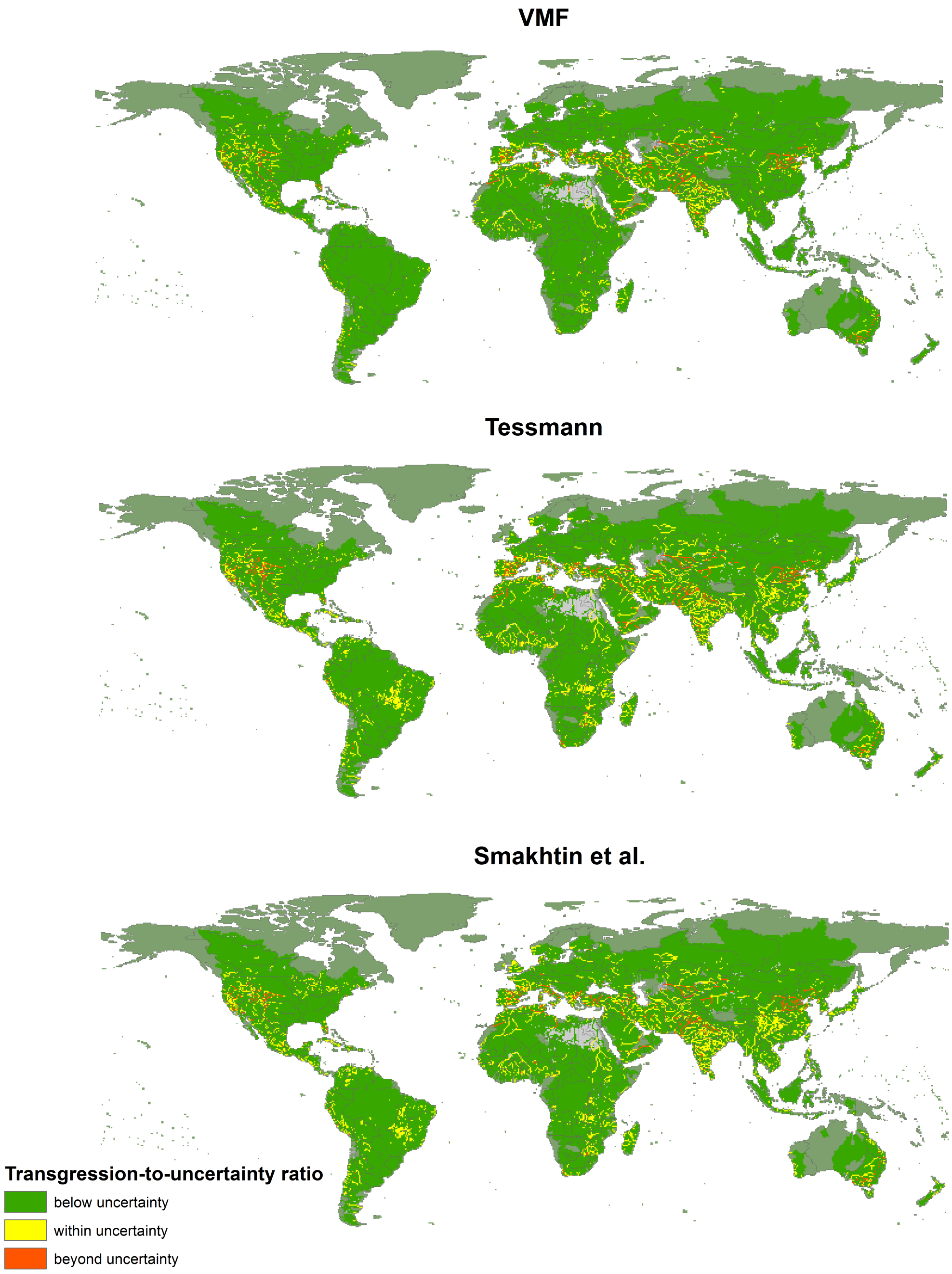

Figure 14: Current status of transgression of environmental flow requirements on cell scale (1980-2009, 0.5° resolution), expressed as the transgression-to-uncertainty ratio (>5% "within uncertainty" and > 100% "beyond uncertainty"), for the three basis methods, major river basins delineated

Second criterion – duration of transgression

As a next step, the second criterion, the temporal dimension, is examined on cell scale. An overview of the temporal distribution of EFR transgressions is given in Figure 15. It shows the number of months with transgressions for every cell regardless of the respective magnitude. Wide areas especially in India and Central and Western Asia, in the Western USA and the Middle East but also the Segura River in Spain, the Murray Darling basin in

Australia and the Abay Basin in Ethiopia show transgressions of EFRs that Steffen et al. (2015) characterized as (basins) at high risk.[1] In these areas, EFRs are not fulfilled during half of the year or longer. The intermediate category is less frequently assigned than in the first criterion, partly due to the quite narrow range of only three months.

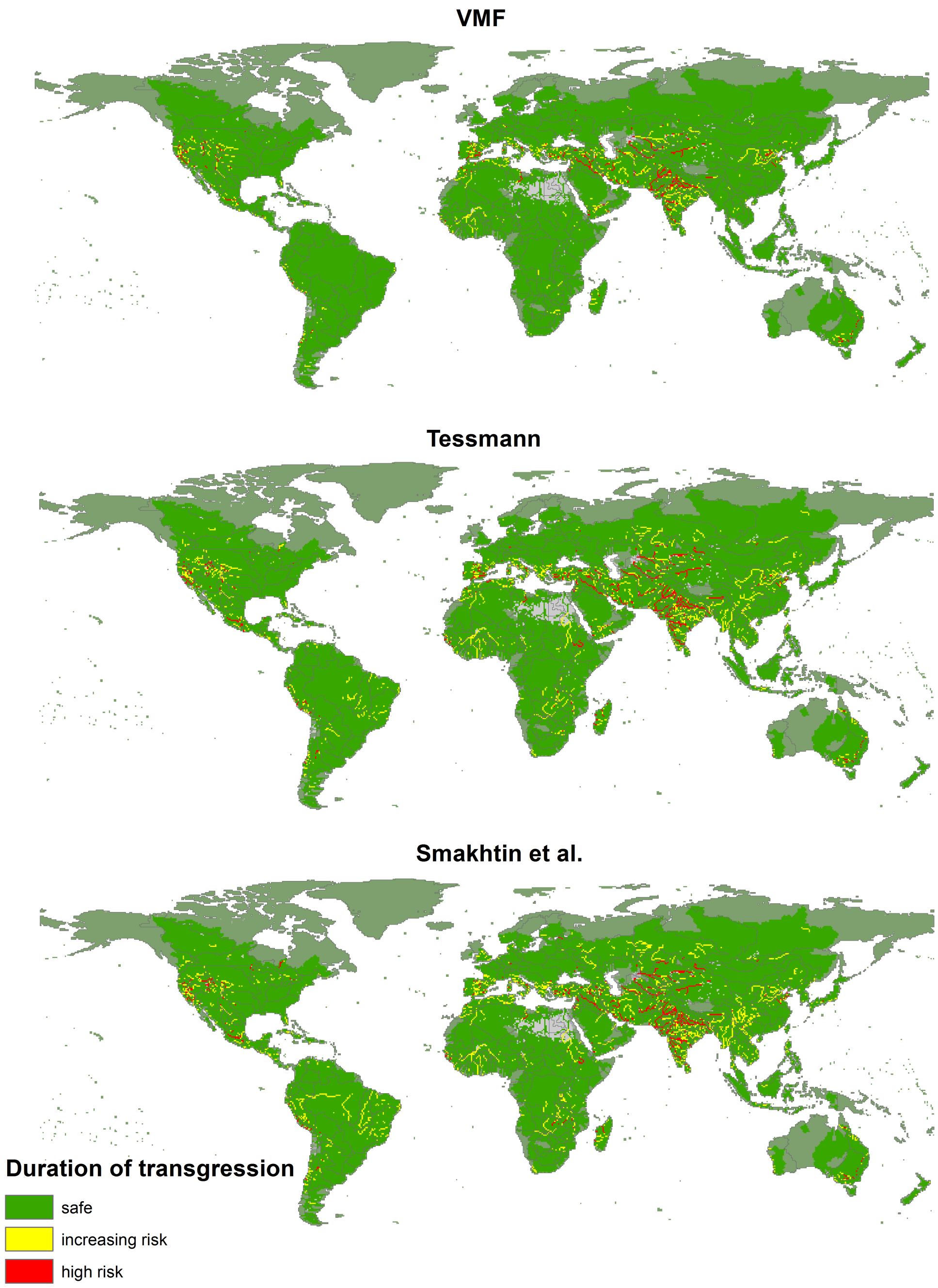

Figure 15: Current status of transgression of environmental flow requirements on cell scale (1980-2009, 0.5° resolution), expressed as the duration of transgression (0 – 2 months “safe”, 3 – 5 months “increasing risk”, 6 – 12 months “high risk”), three basis scenarios

[1] with the exception of 6 months of transgressions, these are here classified as at high risk, while Steffen et al. assigned them to the increasing risk category

5.3 Basin Scale Results & Refinement with associated Biodiversity

First criterion – transgression-to-uncertainty ratio

As two criteria were evaluated for five different EFR methods, 10 different setups were obtained. The first criterion – the uncertainty ratio (depicted in Figure 16) shows fewest basins in the red category for the VMF scenario (93). Smakhtin's method leads to most transgressed basins (103). Regardless of the underlying EFR method, major overexploitation of EFRs is particularly found for basins in the Northern midlatitudes, in Pakistan, India and China but also in Europe and North America. As their share in total sum of transgression is considerable, the red (high risk) classification of the Indus, Yellow and adjacent basins is not surprising.

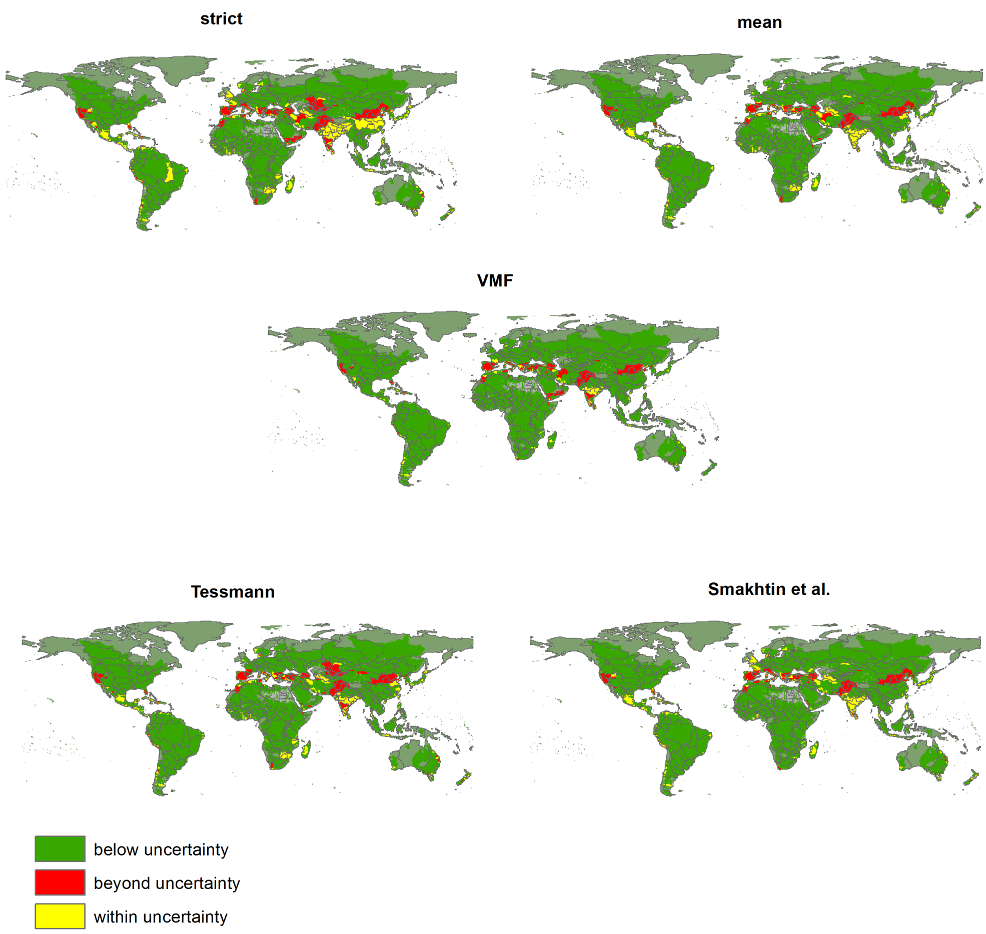

Figure 16: Transgression-to-uncertainty ratio, aggregated to basin scale

Nevertheless, the Ganges is not classified as transgressed beyond uncertainty but as below in all three basis methods, only the strictest scenario classes this basin as transgressed within uncertainty. This is due to the fact, that the VMF method is assigning substantially lower EFRs to this basin than the other two methods, the span of EFRs is therefore considerably high, decreasing the value of the uncertainty ratio. Further overexploitation is predominantly visible in Central Asia, Europe, the Western USA and Central America. South America as well as Africa show few strained basins according to the first criterion. Similar to the case of the Ganges, the Nile is not classified as transgressed beyond or within in either of the methods. This is also due to the VMF method requiring substantially lower flows than the other methods.

Second criterion – Duration of transgression

In the basin scale classification employing the second criterion (shown in Figure 17) for the VMF method, 47 basins fall in the high-risk category. Tessmann and Smakhtin again show similar results with 82 and 78 basins in this category respectively.

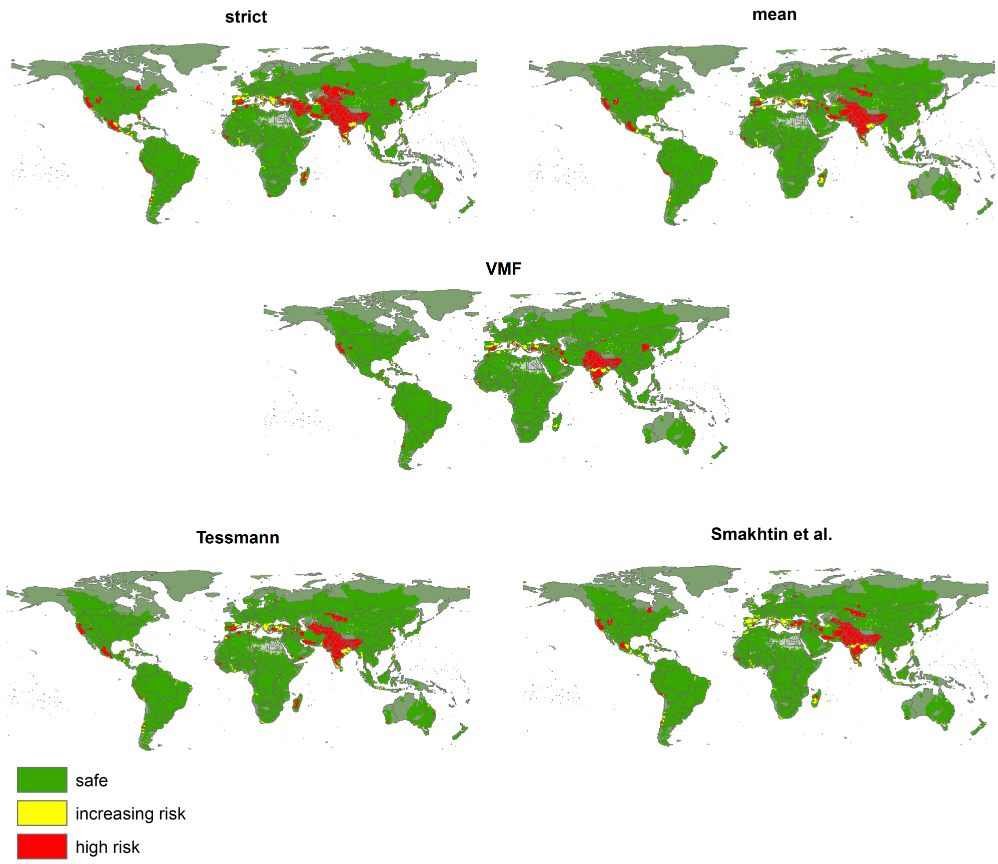

Figure 17: Duration of transgression, aggregated to basin scale

The duration of transgression of EFRs over at least half of the year notably seems to be problem in the Middle East, the Indian Subcontinent and Western Central Asia as well as in four major basins of North America, whereas only few African basins (in Madagascar-2 methods & in Guinea–2 methods) are transgressed due to the duration of non-fulfillment of EFRs.

Comparison of the criteria

The overexploitation of EFRs is characterized by major spatial differences. The main differences between the two criteria are depicted in Figure 18 which shows basins that are defined as transgressed and at risk of transgression by both criteria and those that are defined as transgressed in only one of the two criteria exemplified by the strict scenario.

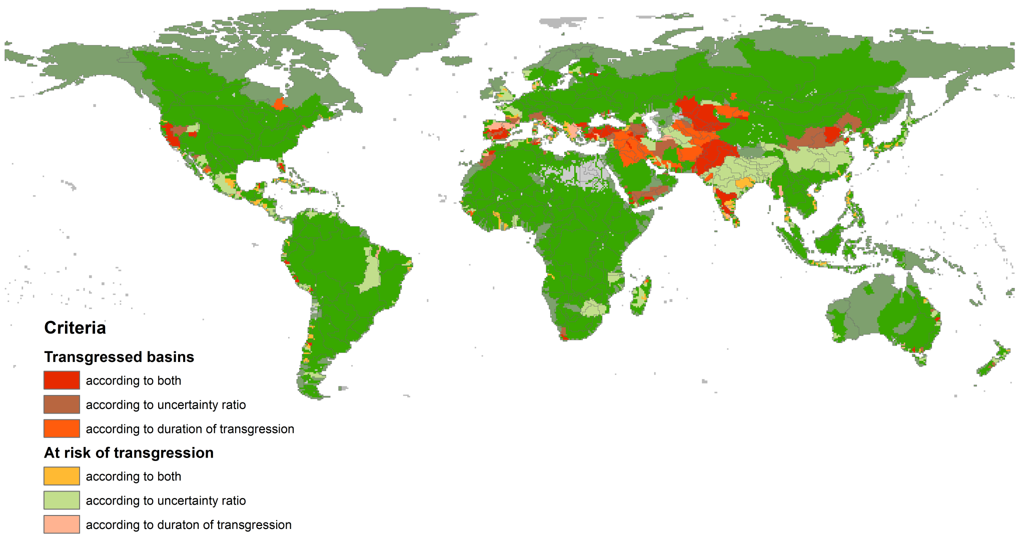

Figure 18: Transgressed basins and basins at risk of transgression and differentiation of criteria

The general frequency and distribution of basins in the intermediate category is the first main difference between the two criteria. A maximum number of 334 basins (strictest method) falls in this category when the first criterion is employed, while the second criterion only ranks a maximum number of 160 (Smakhtin et al.) as endangered with transgression. This was already apparent on cell scale and is partly due to the very narrow range that defines this second category. Concerning differences in distribution, particularly in China, different results are obtained. While the first criterion (depicting height and uncertainty of the EFRs) defines the North China Plain as severely exploited beyond uncertainty and the South of China as within uncertainty, concerning the duration of transgression only the VMF lists one major river basin in China – the Haihe Basin – in the high risk category. Whereas the duration of transgression is predominantly affecting Indian, Middle Eastern, Central Asian and to some extent Northwestern American water resources, the height of EFR deficits is a more global problem, though predominantly the middle latitudes are affected. Major basins classified as transgressed (red) or at risk of transgression (yellow) according to the first criterion are found in Europe, Western Asia, South East Africa and North West and Central America.

Combination of the two criteria

To reduce the number of setups and classes that have to be considered separately when incorporating data on biodiversity, the two criteria are combined (as shown in Table 4 and in subsection S 4.8). In the combined classification, a basin is classed in the strictest category either of the two criteria assign it to. This means that a basin is transgressed if at least one of the two criteria define it as transgressed. The cautionary principle applied regarding the basin classification also reflects in the considerable increase of basins classed as transgressed or at risk of transgression in the combined classification compared to the individual criteria classifications.

Table 4: Details on the basin classification

		strict	**mean**	**vmf**	**Tessmann**	**Smakhtin et al.**
Transgressed	**in combination**	202	145	111	162	149
	Uncertainty range	141	89	93	116	103
	Duration of transgression	119	85	47	82	78
At risk of transgression	**in combination**	294	242	118	245	282
	Uncertainty range	334	274	125	273	307
	Duration of transgression	155	129	60	124	160

Refinement with associated biodiversity

The associated biodiversity of the three basin classes was assessed separately. In this context, a look on the general relationship between the biodiversity descriptors and the corresponding classification of EFR transgressions is interesting. In basins at risk of transgression species richness is generally highest, while it is lowest in basins classified as transgressed. Endemicity shows a more even distribution over the basin classes than species richness does (as shown in Figure 19). The threshold chosen to distinguish “high biodiversity” (=global biodiversity median) implies that more than 75% of cells lying in basins defined as transgressed show high biodiversity in terms of CWEI and almost 50% show high biodiversity in their native species richness. Further, more than 75% of cells in basins at risk of transgression show high biodiversity according to both descriptors.

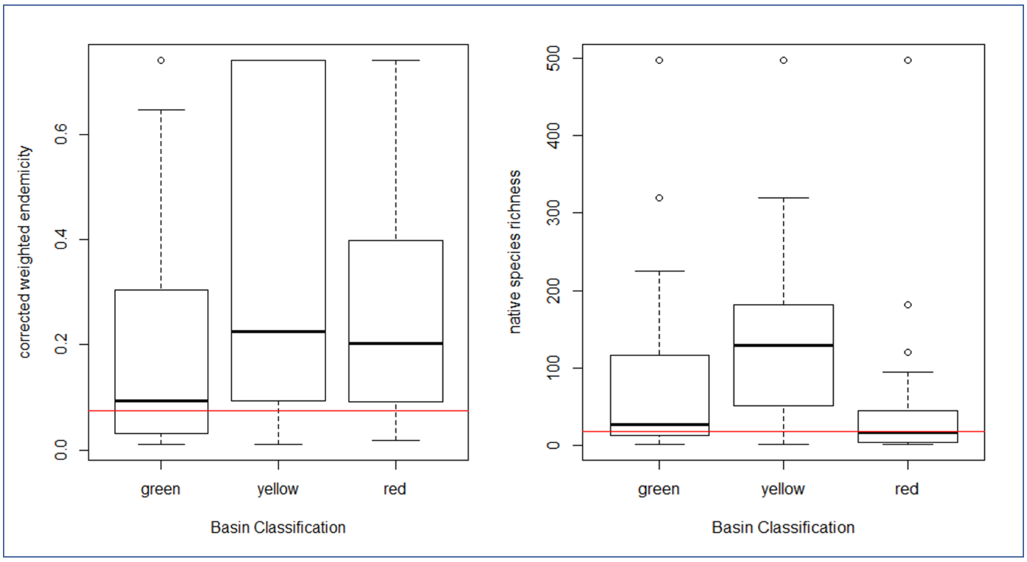

Figure 19: Boxplots of CWEI and total native species richness over basin classification on cell scale, strictest scenario, thresholdS in red (species richness =18, CWEI = 0.075435)

Biodiversity in basins that are not transgressed

Areas characterized by low levels of water exploitation and/or low extent of anthropogenic influence on freshwater resources show high biodiversity in major river basins (Figure 20). Most tropical and subtropical basins in China, Africa, North America and Australia do so. Unsurprisingly, the Amazon Basin but also all other major South American river basins display high endemicity as well as species richness. Only one of them, the Tocantins Basin, is classified as endangered of transgression in the strict scenario. Species richness is observed in north Western Africa, Central Europe and North as well as Eastern North America. High endemicity without high species richness is rarer.

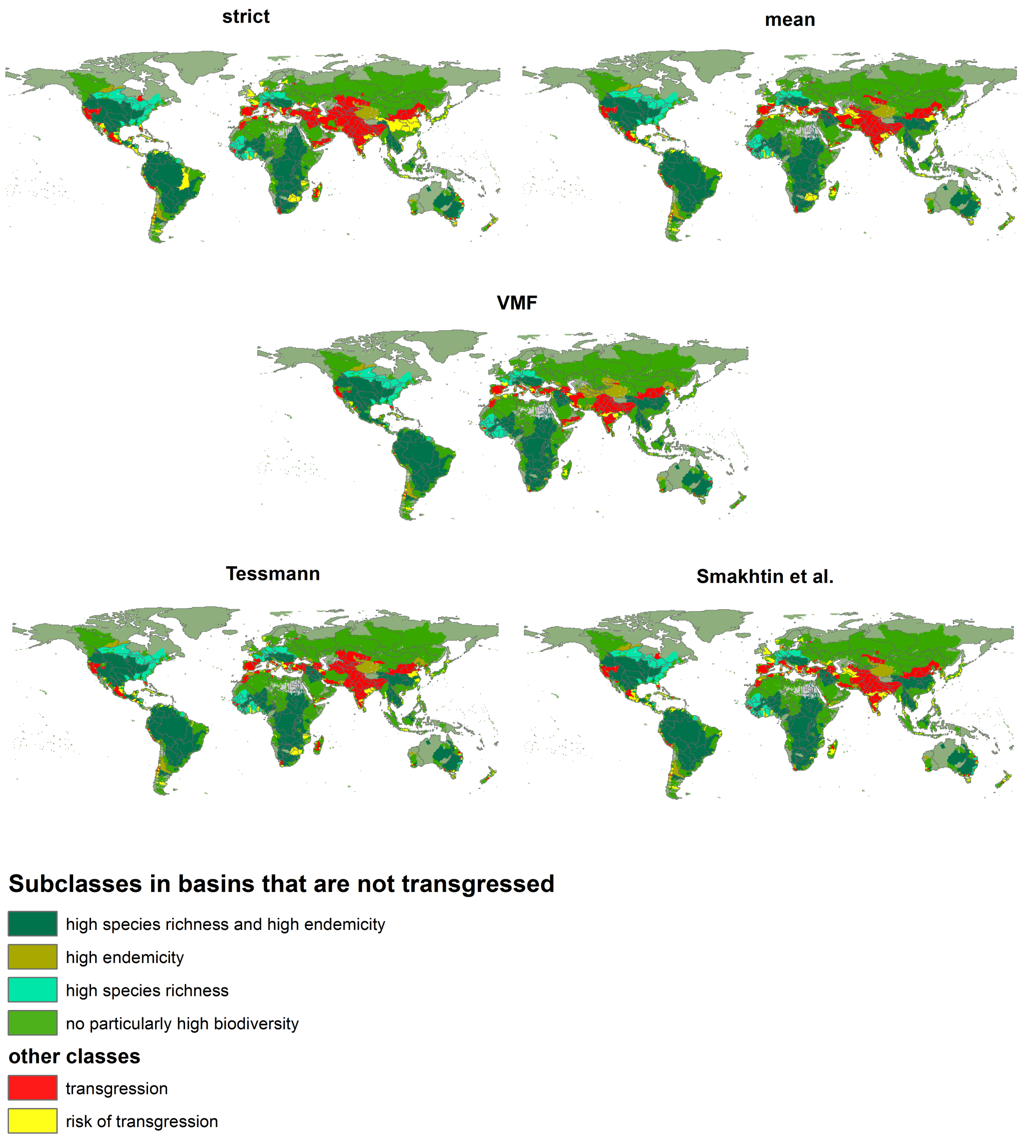

Figure 20: Basins that are not transgressed and subclasses for endemicity and species richness

The aquatic biodiversity in basins that display risk of transgression (shown in Figure 21) depends on water habitats that were characterized by medium exploitation. Though not defined as transgressed in the classification chosen here, EFR deficits are threatening high biodiversity in Central America, some small basins on the Australian east coast, East Africa and China.

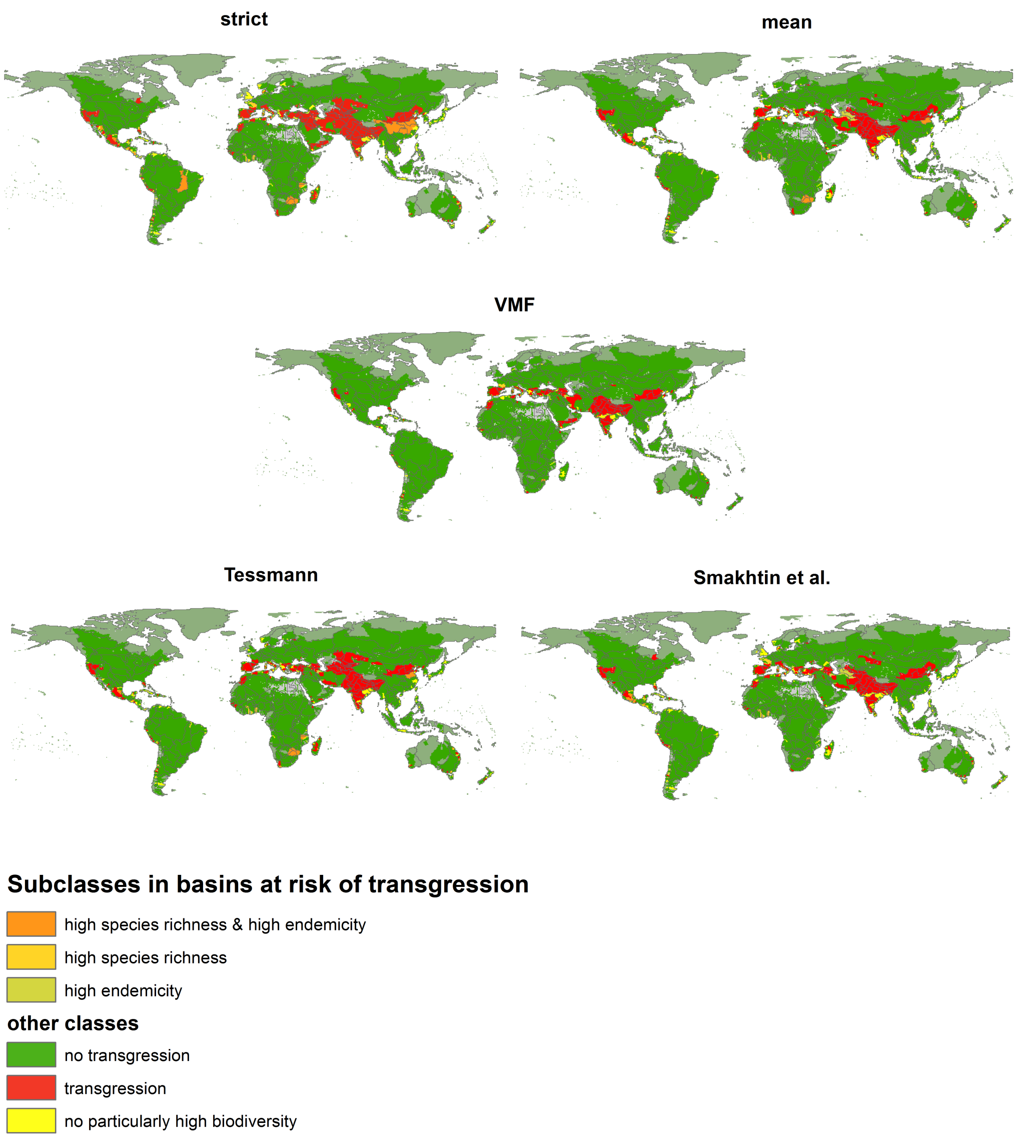

Figure 21: Basins at risk of transgression and subclasses for endemicity and species richness

Biodiversity in transgressed basins

High rates of amphibian biodiversity often coincide with high rates of overexploitation (shown in Figure 22). Regardless of EFR method, this is the case for major river basins such as the Ganges and Krishna Basins in India, the Douro and Tagus Basins in Northern Spain and the San Joaquin-Sacramento Basin in California. Tessmann as well as Smakhtin et al. further group the Guzman Basin in Northern Mexico in this category. Smakhtin et al. further assign the Po Basin to this subclass. High species richness coinding with transgressed freshwater resources and no high endemicity is only observed in one major river basin according to all methods, the Ebro Basin in Spain. Tessmann as well as Smakhtin et al. further assign this category to the Garonne River Basin in France. High endemicity on the other hand coincides with in all scenarios transgressed basins in the Kura Araks Basin in the Middle East, the Mahi Basin in India and the Guadiana and Guadalquivir Basins in Southern Spain. Tessmann as well as Smakhtin et al. further classify the Ili River Basin, the Chu Talas Basin and the East Caspian Sea Basin in this category. Smakhtin further assigns this category to the Liahohe Basin in Eastern China while Tessmann puts the Amu Darya Basin in this category.

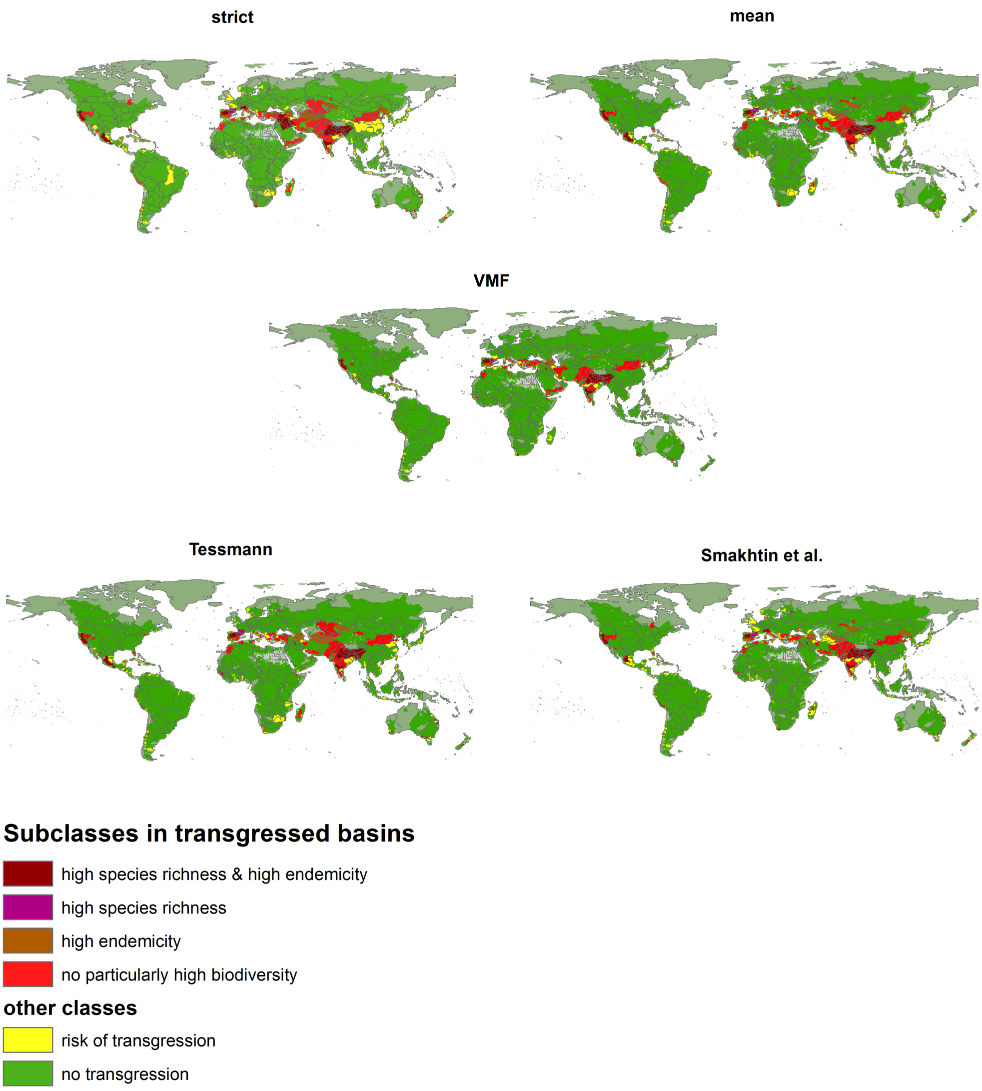

Figure 22: Transgressed basins and subclasses for endemicity and species richness

Nevertheless, there are also areas that are characterized by high overexploitation and naturally low or already diminished biodiversity. Regarding only major river basins, this is the case in the Yellow River in China, the Indus in Pakistan, the transgressed basins in Northern Africa as well as the Mediterranean. Comparing the biodiversity descriptors and their occurrence in the different basin classifications, it particularly stands out that there is around a third more transgressed basins that display high endemicity than high species richness.[1] In basins in the safe category, it is the other way around, species richness is

[1]See subsection S 4.7 for a detailed overview of biodiversity descriptors occurrence in the different basin classes

more often high in these basins than endemicity, while in the intermediate category the frequency is about the same. It can be concluded that the introduction of data on biodiversity facilitates the refinement of EFR transgressions' spatial resolution as it highlights that biodiversity is endangered by overexploitation in major basins in various world region. Particularly endemic species are often found in basins with severe transgressions, if hydrological alterations destroy their habitats these species will be irretrievably lost.

5.4 Global Scale Results

For water resources of 5.7-10.4% of the Earth's surface area (shown in Figure 23) EFRs are classified as transgressed. This corresponds to 3.4 to 4.9% of global discharge, depending on EFR scenario (Figure 24). In terms of area classification, Tessmann is the strictest of the three basis methods, denoting 8.2% of area as transgressed and 2.7% as at risk of transgression, so in total around 11% of the total land area as transgressed or at risk of transgressing local boundaries. This corresponds to 7.6 and 1.8% of the area under anthropogenic influence . This means that if EFRs were to be allocated according to the Tessmann method, already 8.2% of the total world area are severely overexploited. The Smakhtin method leads to similar results. It classes groups 10.5% in these two categories. This corresponds to 10.8% of area that is regarded as influenced by anthropogenic interference with freshwater resources. In terms of discharge, Tessmann again shows slightly worse results than Smakhtin with 4.3% of discharge classified as transgressed and additional 3.6% at risk of transgression. A further 1.4 to 5.1% of area display as endangered of transgression corresponding to 1.5 to 7.0% of global discharge. This means that between 7.1 and 15.5% of total area and between 4.9 and 11.9% of global discharge were classified as either transgressed or at risk of transgression.

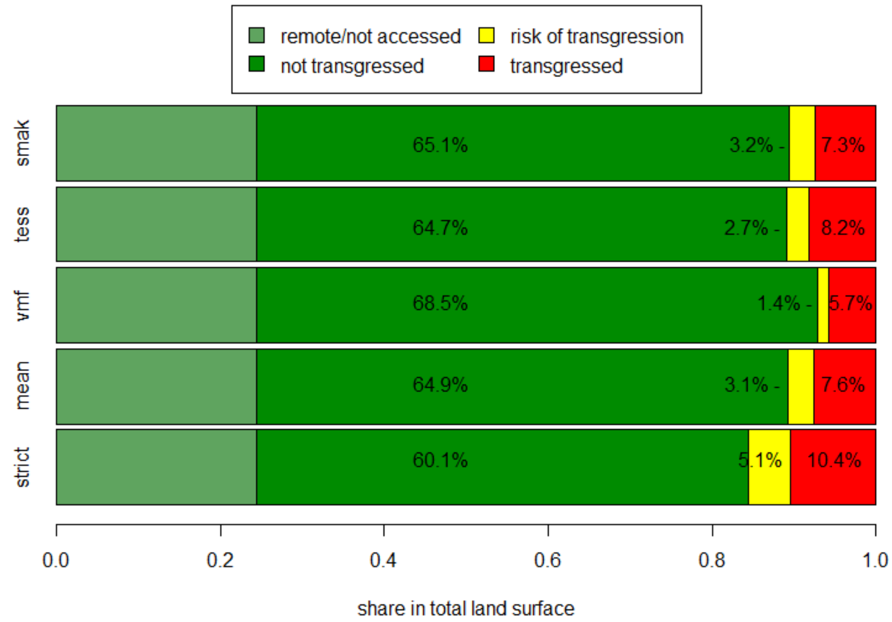

Figure 23: Share of transgressed area in total land surface area

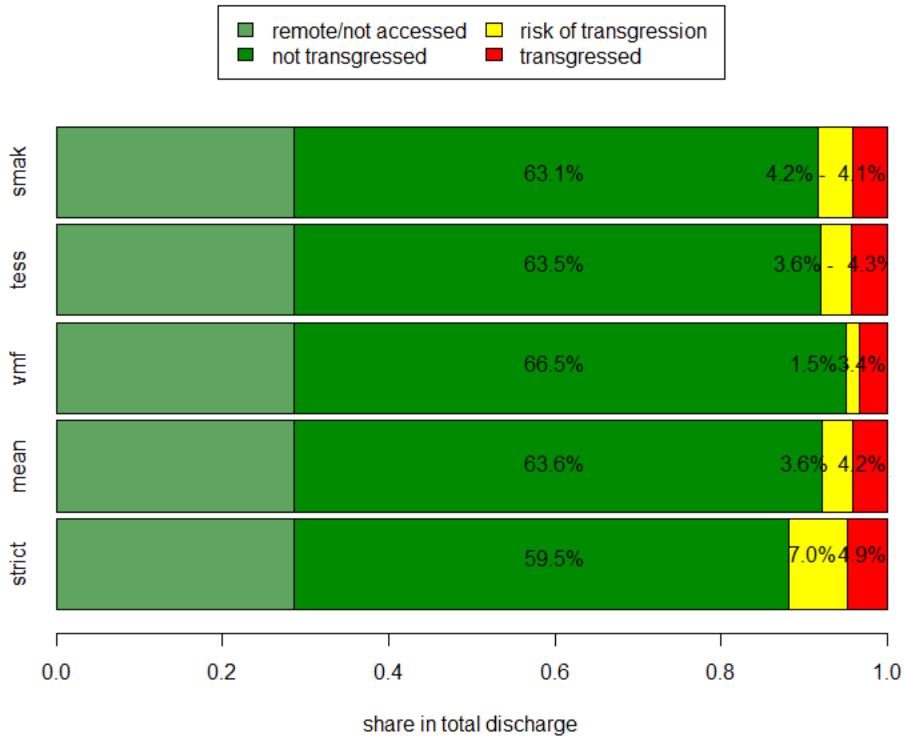

Figure 24: Share of transgressed discharge in total global discharge

Transgressed area and associated biodiversity

The biodiversity in areas with transgressed EFRs displays as particularly high on 2.2 to 4.5% of total land area. 18 major river of more than 50,000km^3/yr basins fall into this subclass. According to both descriptors it presents as high on 1.6 to 2.6% of land area (shown in Figure 25) which concerns 7 major river basins, and on further 0.6 to 1.9% of area according to either endemicity or species richness. In total, between 38 and 45% of the area denoted as transgressed, show high biodiversity levels.

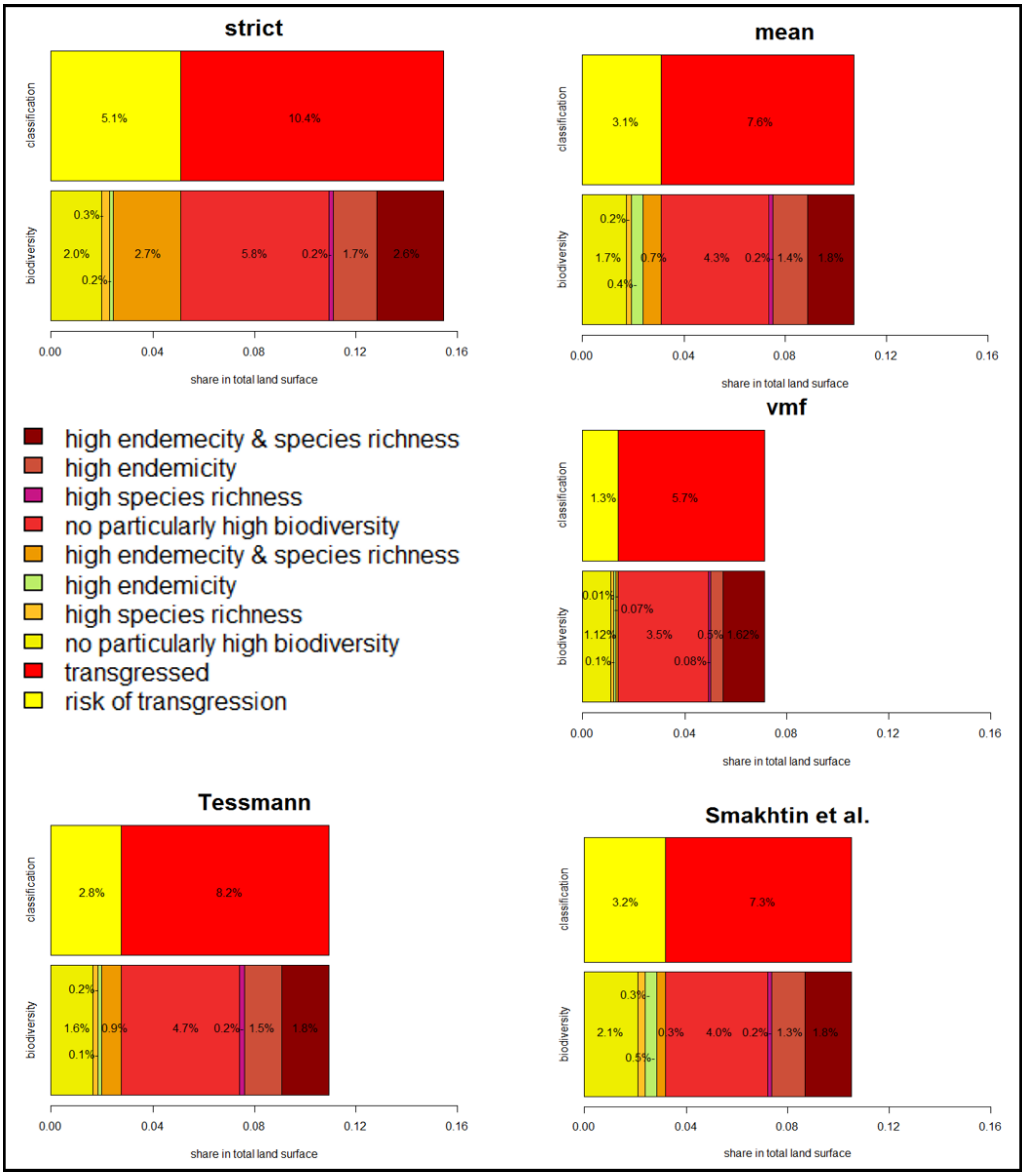

Figure 25: Biodiversity associated to transgressed basins and share in total land area

Biodiversity in world areas with water resources that are classified as not transgressed, show high biodiversity according to both descriptors on 25 to 28% of total area. A further 6.3 to 7.8% of total area show high biodiversity according to either of the biodiversity descriptors.

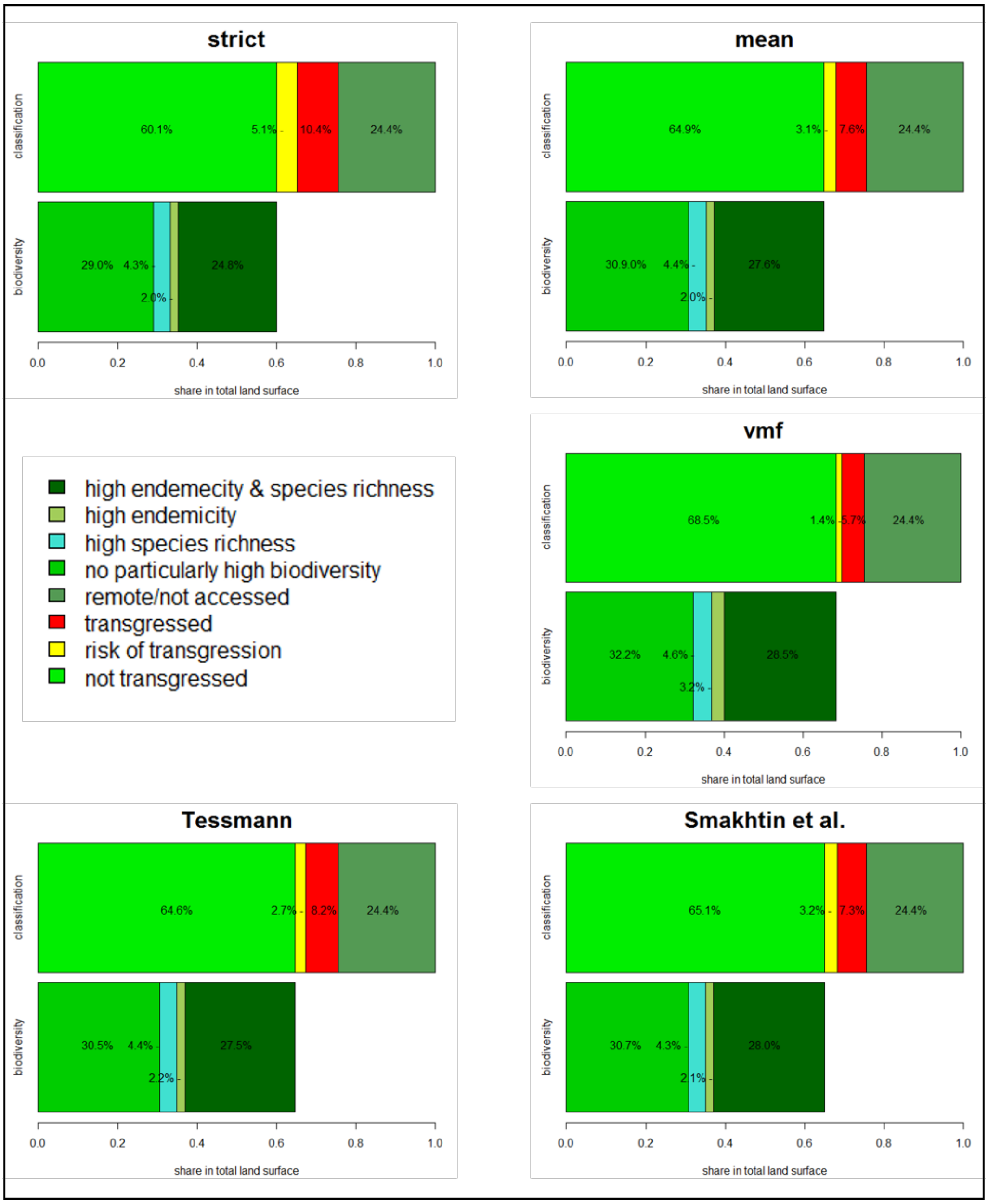

Figure 26: Biodiversity associated to basins classified as not transgressed and share in total land area

The major river basins classified as transgressed according to at least one of the basis methods are given in Table 5 (only showing basins with an area of at least 50,000km^2, “high” biodiversity levels with sufficient overlap are given on a grey background). Some of these basins like the Po basin in Italy and the Amu Darya basin in Uzbekistan show quite different annual EFR deficits depending on the respective method. Most of the affected basins can be found in South and Central Asia (12 basins) and the Middle East (4 basins). Many are adjacent like the Chu Talas and Amu Darya basins in Central Asia. It can further be seen where the basis methods differ in their classification. If EFRs according to VMF were to be preserved, less basins would be defined as transgressed than according to the other two methods. With regard to the annual EFR deficits, it can again be seen that the biggest share of global transgressions concentrates in a few large basins (details given in subsection S 4.5). However, many additional basins are classed as transgressed due to the wide spatial extent and/or sheer duration of deficits. Concerning associated biodiversity is can furthermore it is shown that if the thresholds is set as the median of the global biodiversity distribution, 18 of the 24 major world river basins show high biodiversity in at least one of the descriptors and 7 in both (see also map in Figure 22). Nevertheless, as shown in grey, although high biodiversity is present, some basins like the Indus and Yellow basin where not classified in the high biodiversity category, as the area share in these basins displaying as high was not large enough (less than 50% overlapping).

Table 5: Major river basins, their location, area, range of EFR deficit, transgression status and max. level of biodiversity in basin cells

River Basin	**Countries**	**Continent World Region**	**Area in** km^2	**Range of annual EFR def. in** km^3/yr	**Classification**			**Biodiversity (max.value in basin))**	
					green	yellow	red	CWEI	species richness
Ganges	India	Asia	1 634 008	5.7–22.4			all	0.6069	120
Indus	Pakistan	Asia	1 151 447	33.1–49.4			all	0.6069	120
Krishna	India	Asia	254 642	0.17–0.77			all	0.2953	44
Mahi	India	Asia	131 195	0.17–0.28			all	0.6069	120
Yellow	China	Asia	895 996	5.9–8.2			all	0.7422	182
Haihe	China	Asia	252 676	1.7			all	–	–
Liahohe	China	Asia	274 035	0.19–0.22				0.0984	17
Northern Inland	China	Asia	310 571	0.28–0.41			all	0.35	12
Ili	Kazakhsthan China	Asia	310 571	0.27–0.41	vmf		tess smak	0.35	12
Kura Araks	Azerbaijan Armenia Georgia Turkey&Iran	Asia	218 892	1.5–2.1			all	0.2853	18
Amu Darya	Uzbekistan	Asia	628 052	4.2–7.9	vmf		smak tess	0.3981	5
Chu Talas	Kazakhstan Kyrgyzstan	Asia	1 072 316	4.8–6.1	vmf smak		tess	0.3981	12

Table 5 continued

East Caspian	Azerbaijan Armenia Georgia Iran	Asia Middle East	449 418	0.52–0.88	vmf	smak	tess	0.2437 / 0.3981	7/4
North Yemen	Yemen S.Arabia	Asia Middle East	417 368	0.03–0.04	smak tess		vmf	0.2722	3
Sakarya Kizilirmak	Turkey	Asia Middle East	175 992 (combined)	0.17-0.34			all	– / 0.2853	– / 18
Great Kavir	Iran	Asia Middle East	332 890	0.15–0.21	smak	tess	vmf	0.2853	18
Guzman	USA/Mexico	N.America	194 757	1.2–1.9	vmf		smak tess	0.2330	48
San Joaquin Sacramento	USA	N.America	194 995	1.12–1.72			all	0.2604	27
Western Cape	South Africa	Africa	50 064	0.02–0.03	vmf smak		tess	0.1671	17
Douro Tagus	Spain	Europe	170 461 (combined)	0.66–0.79			all	0.0859	21/20
Ebro	Spain	Europe	82 835	0.81–1.29			all	0.0754	21
Guadal-quivir	Spain	Europe	53 718	0.44–0.61			all	0.0889	17
Guadiana	Spain	Europe	65 017	0.09–0.13			all	0.0889	20
Garonne	France	Europe	66 814	0.54– 1.25		vmf	tess smak	0.0397	22
Po	Italy	Europe	108 818	1.42–4.42	tess vmf		smak	0.0872	22

6 Discussion

This revised assessment of the transgression of the PB for freshwater use based on EFRs has shown that overexploitation of global water resources is characterized by major spatial differences. Although blue water consumption lies below the suggested boundaries of ~2,800km^3/yr estimated by Gerten et al. (2013), ~4,000 by Steffen et al. (2015) and ~5,205 estimated by Brauns (2016), there are considerable transgressions of EFRs on local as well as aggregated regional scale. Mainly freshwater resources of the Indian subcontinent, Pakistan, the Middle East, Central Asia and the Mediterranean display as severely altered from their natural state. Major basins in these regions can be regarded as transgressed. Concerning the duration of EFR transgression particularly India and Central Asia stand out, but basins in Northwest and Central America and East Africa are also affected. The magnitude of transgressions represents as a more global problem affecting major basins of all continents apart from South America - particularly basins of the Northern midlatitudes often present as severely transgressed.

This study was the first to assess global patterns of EFR transgressions in conjunction with associated aquatic biodiversity and hence combined the assessment of the transgression of the PB for water use with an analysis of transgressions in the sphere of the PB for biosphere integrity. It was shown that a considerable share of the most severely overexploited basins constitutes a habitat for amphibians of high biodiversity. Also in basins which are endangered of transgression, biodiversity is often high.

Every river has its own characteristic flow regime and associated biotic community (Richter et al., 1997; Bunn and Arthington, 2002). The incorporation of data on biodiversity has facilitated to add further meaning to EFR transgressions, because it has highlighted where most biodiversity is endangered by overexploitation of freshwater resources. Particularly in basins in India, Central Asia, Spain, and some more isolated basins, high rates of amphibian biodiversity coincide with high rates of overexploitation. The here chosen thresholds and aggregation scheme imply that on 2.2 to 4.5% of total land area and in 18 large river basins of at least 50,000km^3/yr, high amphibian biodiversity coincides with severe transgressions of EFRs. Particularly endemicity displays as high in these transgressed basins.

6.1 Model Limitations

As real systems are too complex, the aim of modelling natural systems is to represent them in a simplified way. Though it is unique and well established, like all other models, LPJmL relies on assumptions and simplifications. Arnell (1999) argued that the accuracy of modelled water budgets is considerably dependent on the quality and spatial resolution of climate input data. Uncertainties in precipitation data are directly transferred to uncertainties in discharge estimations at similar or even greater magnitudes (Fekete et al., 2002).

As described in subsection 4.1, model runs used in this thesis are forced with GPCC's Full Data Reanalysis precipitation data version 6. Biemans et al. (2009) compared an older version of GPCC to six other precipitation datasets covering time periods of at last 20 years using LPJmL. The results confirmed the significant impact of precipitation uncertainty on discharge simulations. The GPCC dataset's total annual precipitation lies in the middle of the other datasets' range, though the total precipitation of the new version used in this thesis is smaller. To estimate the uncertainty of discharge simulations at least two precipitation datasets should be used.

Gerten et al. (2004) reinforced the hypothesis by Fekete et al. (2002) and Arnell (1999) and showed that LPJmL significantly under- or overestimated runoff in certain regions compared to observations. While annual means are within other estimates' range, runoff is frequently underestimated in subarctic regions and overestimated in semi-arid and arid regions, particularly in northern Africa, India and to some parts South America. Although flow requirements are simulated based on discharge simulations and are therefore probably biased in the same direction, this implies that the overexploitation in India could in reality be even worse than indicated in this thesis and that South America and northern Africa might have been underestimated.

A further inaccuracy in timing and amount of discharge is introduced through the reservoir module applied in LPJmL. Instead of local information on the management of individual reservoirs, it is based on general assumptions of their operation schedule. This module improves the simulation of discharge in most areas. But as the simulation of outflow follows irrigation water demand, it is not able to improve discharge simulations in some regions, such as China and India. In these countries irrigation water demands are particularly high and currently the accuracy of simulated growing season is insufficient(Biemans et al., 2011). Another uncertainty arises due to the land mask used in LPJmL. The differences between the discharge volume between this studies and the one by Brauns (2016) and Gerten et al. (2013) are partly due to the different size of mask applied. While Antarctica is excluded from the terrestrial surface basis used in the simulations for this thesis, Greenland and many small islands are still included and the current land mask with 67,420 cells leads to numerous transgressions of EFRs that are due to artefacts inherent in the model. They occur in areas not influenced by human doing. The adjustments described in subsection 4.1 partly cover this aspect. About 24.4% of total land cover were disregarded in all calculations. Nevertheless, to receive improved estimates of discharge and EFRs, areas without water storage capacity in the form of vegetation cover or due to soil characteristics should additionally be excluded as their contribution to the global water cycle is negligible.

Currently LPJmL is not able to evaluate fossil groundwater availability and extraction rates although this is an important water source in many countries (see subsection 3.2). Groundwater contributions are indirectly assumed over irrigation demand. If a grid cell's water volume is insufficient to fulfil the crops' demand, implicit contributions from fossil groundwater as well as river diversions or large scale water transport is assumed (Kummu et al., 2010; Rost et al., 2008). Only groundwater abstraction which doesn't exceed natural recharge rates is sustainable. The groundwater resources of major basins found to be transgressed due to overexploitation of EFRs (e.g. in the North China Plain, Mexico, northwest India, Middle East) are already depleted to a large extent (Wada et al., 2010; Foster and Chilton, 2003; Chen et al., 2016). An integration of groundwater simulations into the model to accurately account for its contribution to irrigation and HIL would increase the simulated volume of discharge and the accuracy of results. Nevertheless, it is unlikely that there are major implications for the conclusions drawn here. Although groundwater can serve as a strategic water reserve, particularly in times of prolonged drought, it should not be used to fulfil EFRs. As surface and groundwater are strongly interlinked they should be managed conjunctively (McNutt, 2014). Like in the protection of EFRs (see below), groundwater preservation can be attained through improvements in agriculture efficiency (Famiglietti, 2014).

A new version of LPJmL 4.0, including, among other improvements, an upgraded representation of sowing dates to enhance the accuracy of simulated growing seasons and a newly introduced representation of multi cropping systems is expected to be released in 2017.

6.2 Basic Assumptions

The discharge values (MMF, MAF, Q_{90}) underlying the EFR runs used here are based on a simulation of the global water cycle of today (CS). Another possibility would be to calculate EFRs based on PNV runs. The resulting requirements as well as EFR transgressions would be lower as global discharge today is higher than under the assumptions of PNV, in particular due to climate change and deforestation (Gerten et al., 2008). Hence, the here chosen assumptions are more cautious and depict the challenges of anthropogenic pressure on freshwater ecosystems in the 21st century in a more realistic way. If the implications of climate change and land use change on freshwater resources were to be examined, the application of runs with other assumptions, like for example PNV, would be sensible.

EFRs provide a simple method to assess the spatio-temporal patterns of transgressions of the planetary boundary for human freshwater use and combine the regional with the global operating scale of freshwater use (Gerten et al., 2013; Steffen et al., 2015). Nevertheless, the global quantification of EFRs is difficult and subject to many uncertainties (Poff et al., 2010; Smakhtin, 2008). The main problem with the EFRs calculation approach used in this analysis, is that due to the global application, which requires EFRs to be flexibly applicable over all world regions, methodological simplifications such as the exclusion of channel and habitat maintenance floods are inevitable (discussed in section 3 and by Jägermeyr et al. (2016b)). Using three different basis methods and two scenarios combining these three methods, this analysis well depicts methodological uncertainty and the results reflect the wide range of possible outcomes of policies, differing in their strictness (Jägermeyr et al., 2016b). Pastor et al. (2014) showed that the methods applied here performed well in different regions of the world depending on the variability of flow regime. VMF and Tessmann displayed the best results on a global scale. Nevertheless, these estimates lack local validation. Holistic approaches that are able to sufficiently include the ecosystem requirements and particularities in terms of flow regime are only possible on local scale, though under constraints as well (Bunn and Arthington, 2002). As there is little scientific basis on how to scale up EFRs and their transgressions, the approach chosen here is very cautious in its assumptions (Steffen et al., 2015). The choice of thresholds for transgressions to be considered was set at 1m3/s and rivers with average discharge less than 1m3/s were left out. This is quite strict as compared to other approaches that only included considerable big streams and transgressions like Jägermeyr et al. (2016b).

As the share of different areas in total global transgression shows, most overexploitation in terms of volume take place in only few major basins, the majority of which in Asia. Here, the focus lies on the analysis of spatio-temporal pattern of EFR transgression and, though outweighed in terms of volume on a global perspective, the chosen thresholds have facilitated to show the global distribution of transgressions in terms of duration and magnitude. The main challenge therein was to appropriately reflect the temporal and geographical dimensions of the tapping of EFRs, to account for uncertainties concerning the calculation method for EFRs, and to apply an appropriate method for the upscaling of these transgression.

The two-criteria analysis using duration and the transgression-to-uncertainty ratio, allows to evaluate and classify transgressions in a clear and simple way. As the exact effects of EFR deficits in terms of duration and severity are unknown and vary widely on the global scale, the approach of the criteria evaluation presented here applies the precautionary principle by applying low thresholds. As these criteria are combined on basin scale assigning basins the strictest category of the two, this cautiousness is transferred across scales and reinforces. The evaluation of transgressions was done individually for each of the criteria, while an integrated assessment of both would facilitate to depict interdependencies between the temporal dimension and the height of transgression. If, for example, high transgressions concentrate in only one or few months the effects for aquatic ecosystems can be devastating. These cases are not well represented in the evaluation of criteria chosen here.

Appropriate water quality in terms of concentration of different constituents in the water as well as its temperature and state, is an integral part of EFRs (Nilsson and Renofalt, 2008). Both good water quality and adequate quantity are necessary for achieving the Sustainable Development Goals for food and water security as well as health (UNEP, 2016). As the focus of this assessment lies on flow volumes/quantities it is not explicitly considered. Nevertheless, water quality plays an integral role in water resources protection and the fulfilment of EFRs in terms of quantity and timing, as assessed here, is insufficient to sustain freshwater ecosystems if water quality is poor. The characteristics and functioning of riverine ecosystems is jointly determined by both, water quality and quantity (Nilsson and Renofalt, 2008; Arthington et al., 2010). Already one third of river stretches in Africa, Latin America and Asia are affected by severe pathogen pollution and one seventh by severe organic pollution. Moderate to severe salinity pollution is a affecting around one tenth of African, Asian and Latin American river stretches (UNEP, 2016). As many aspects of water quality and quantity are closely interlinked, quality can vary in importance depending on dilution rate and actual water quantity (Chen et al., 2013).

6.3 Biodiversity Data Limitations & disregarded Boundary Interactions

The main challenge underlying this analyses is the coarse resolution of the biodiversity data and the limited compatibility of the datasets. This inevitably implies information loss associated with rasterization and limited overlap. While data on EFRs is calculated at a spatial resolution of 0.5° x 0.5°, the data by Tisseuil et al. (2013) represents an assessment on basin scale only. When analyzing the importance of EFR(s) (transgressions), an integration of data on cell scale is much more sensible due to the wide variation of water availability and biodiversity within basins and the direct dependence of aquatic biodiversity on local freshwater availability. Also for conservation planning efforts the river basin scale is too broad (Tisseuil et al., 2013). The criterion that only biodiversity of datasets that are 50% overlapping is considered, is relatively strict but to a certain extent it facilitated to maintain accuracy.

Furthermore, although a good surrogate dataset, as only amphibian biodiversity was included into the assessment, it remains a rough estimate and cannot replace differentiated local analyses of biodiversity levels for different taxa. Additionally, global comparisons of biodiversity patterns are difficult due to the influence of diverse factors such as latitudinal gradients or species-energy relationships (Gaston, 2000). Unfortunately beyond the scope of this thesis, a detailed classification of river basins according to habitat categories would allow for better evaluation of biodiversity levels. Comparisons should then be done among similar habitats (Abell et al., 2008). The here chosen median thresholds systematically underestimate biodiversity levels, particularly at high latitudes (another, lower threshold is examined in subsection S 4.4). However this is partially compensated, as large parts of the excluded areas are at high latitudes in Eurasia and America. Further, it is not clear to what extent biodiversity levels, particularly those in basin that have gone severe hydrological alterations, have already been compromised. The here examined levels might already represent an impaired state, particularly in basins classed as transgressed with rather low biodiversity. Concerning the effects of resources use for aquatic biodiversity, modified flow is only one threat and often the presence of multiple stressors makes a definite separation of impacts impossible (Bunn and Arthington, 2002). Important stressors not included in this assessment are the intrusion of exotic species, declining water quality and the extensive effects of climate change such as increases in water temperatures and declines in summer flow (WWF, 2016; van Vliet et al., 2011; Naiman et al., 2002). This study has to be taken as a first, broad analysis that cannot replace holistic approaches (explicitly considering the link between biodiversity, habitat conditions and discharge) with local scale validation (Acreman and Dunbar, 2004; Pastor et al., 2014).

Boundary Interactions

When scientifically examining PBs and when they shall be applied in management options and policy frameworks, it is crucial to observe and assess processes of boundary interactions (Steffen et al., 2015).

This thesis represents a first assessment to combine the analysis of transgression of the PB for water use with the sphere of the PB for biosphere integrity. As described in subsection 3.1, the human appropriation of water leads to disturbances in river, wetland and lake ecosystems and deterioration of ecosystem services. The focus lies on the effects of water withdrawals for HIL and irrigation on discharge and depending biosphere integrity. It is shown that in major basins in India, Spain, Italy, Mexico and the USA, high levels of biodiversity coincide with and depend on severely overexploited resources.

Nevertheless, particularly the core boundary climate change has to be considered. It presents a severe threat for the health of freshwater resources and dependent ecosystems (Kundzewicz et al., 2008; Gerten et al., 2013; Bates et al., 2008). River flow regimes for around 90% of the global land surface area are significantly affected by it (Döll and Zhang, 2010). The fulfillment of EFRs and the protection of dependent ecosystems is thereby mostly threatened by changes in precipitation. Though it is difficult to establish trends due to the spatio-temporal variability of precipitation, particularly wet areas in northern latitudes are expected to get wetter and drier areas are expected to get even drier (Vörösmarty et al., 2000b; Hagemann et al., 2013; Allan et al., 2010). The transgressed basins in the Middle East and Southern Europe are projected to be particularly affected, as runoff is expected to decrease by 10–30% (Milly et al., 2005). In areas with a projected increase in precipitation like in the severely transgressed basins of Central and southeast Asia, variability in runoff will temper the beneficial effects for EFRs and aquatic habitats (Milly et al., 2005; Kundzewicz et al., 2008). Additionally, climate change not only alters river flow regimes, it further leads to increasing water temperatures and changes in water quality (Ficke et al., 2007).

Next to climate change particularly land system change, biogeochemical flows and atmospheric aerosol loading display close interactions with freshwater use as discussed in section Planetary boundaries (Rockström et al., 2009b). The strong effect of land use change and land cover conversion on freshwater resources is due to lower transpiration from agricultural areas compared to natural vegetation, in particular from forests. This is because of shallower rooting depths, lower interception losses and shorter growing seasons of crops as compared to natural vegetation (Rost et al., 2008; Gerten et al., 2008). Although changes in precipitation are dominant in their effect on global discharge, there are strong regional differences and pronounced effects of land use, $CO_(2)$, temperature, and irrigation as indicated here. While discharge in North and West Africa, Central Europe, East Europe and parts of South Asia has decreased since the beginning of the 20^{th} century, it has increased in Western Asia and parts of North America (Gerten et al., 2008). In an approach to distinguish the joint and individual influences of land use change and climate change on discharge volumes, Rost et al. (2008) found that between 1971 and 2000, land cover conversion and increasing precipitation lead to an increase in total global discharge, cancelling out the decreasing effect of withdrawals for irrigation. In total there was an increase of around 7.7% in global discharge since 1901 (Gerten et al., 2008). Conversely, freshwater use can increase the effects of climate change as it leads to a reduction of growth in natural ecosystems, diminishing their function as carbon sink. Furthermore, irrigation induces raising CH4 emissions and reduces carbon transport from land to ocean as river flows decrease (Steffen et al., 2015). Regional climate patterns like monsoon behavior could be disturbed (Rockström et al., 2009b). When applying and extending the results of this study, the interconnections with the other boundaries have to be accounted for and above all the effects of climate change have to be considered.

6.4 Measures of Mitigation & Scientific perspectives

One way to operationalize the PB for freshwater use is the introduction of strict EFRs in the form of maximum extraction rates (Rockström et al., 2014a; Pastor et al., 2014). From an ecological point of view, their enforcement is of highest importance in transgressed basins that show high biodiversity, particularly in those where this is the case for all EFR scenarios, such as in the Indian Ganges and Krishna basins and the Spanish Ebro and Douro-Tagus basins. On the other hand, if biodiversity levels are low and other demands, particularly food production aggravate the enforcement of EFRs in these regions, their fulfilment is not as important from an ecological point of view as in the first cases. Further extension of hydrological alteration is also a threat to high biodiversity levels in basins at risk of transgression, e.g. in France and East China.

Water Policy

This thesis has given an overview of local to global scale EFR transgressions. Unfortunately, there is very little research on global scale governance issues and implementation of EFRs is a demanding task (FC-GWSP, 2005; Le Quesne et al., 2010). Many open questions have yet to be answered like on the feasibility of water management on the global scale and how greater resilience is to be achieved, either by applying a worldwide uniform approach in water governance or by a diversity of regional agendas (Alcamo et al., 2008). In hot spot regions facing increasingly severe water degradation, adequate technical and economic capacity is often insufficient and has to be fostered (Rockström et al., 2014a). For the purpose of maximum withdrawal rates, national capacities in environmental ow assessment have to be developed, policy support should be strengthened and appropriate infrastructure supporting environmental EFRs has to be planned (Acreman et al., 2014). Solutions should be found in bottom-up processes and include ecohydrological management of landscapes as well as adapted governance arrangements across scales (Rockström et al., 2014a). Furthermore, the successful introduction of EFRs into river basin management on a global scale requires scientists to stress and transparently illustrate their economic benefits (Smakhtin, 2008; Moore, 2004).

EFRs should be a basic requirement in Integrated Water Resource Management (IWRM), as for example outlined in the EU Water Framework Directive (EU, 2015). Water resources management schemes like demanded by the SDG framework have to be extended to attain efficient water allocation between human needs and EFRs (UN, 2015). Agriculture and thereby IWRM and the protection of freshwater ecosystems are central to attaining the renewed SDGs, however conflicts with other goals, particularly food production, are possible (Jägermeyr et al., 2016b; Griggs et al., 2013). To solve this set of complex challenges, no uniform approach but locally adapted arrangements have to be found (FC-GWSP, 2005; Le Quesne et al., 2010). Priority should be given to policy and management responses that tackle threats at their source instead of expensively fight the symptoms (Vörösmarty et al., 2010).

The role of agriculture

Agricultural expansion and intensification are the main contributors to freshwater degradation. “Agriculture is a major force driving the environment beyond the planetary boundaries" (Foley et al., 2011, p.337). To attain environmental sustainability while at the same time achieving food security, requires the transformation of agricultural systems (Power, 2010; Foley et al., 2011; Tilman et al., 2002).

Although globally there is sufficient water available for future agricultural requirements (see subsection 3.2), there is considerable scope for water use improvements, particularly in arid and semi-arid areas (Wallace and Batchelor, 1997). Scientists agree that in this context, agricultural land expansion is no longer a viable option (Steffen et al., 2015; Foley et al., 2011). Water management in agriculture is the major strategy to achieve both, prevent further hydrological alterations through the improvement of fulfilment of EFRs while at the same time contributing to higher agricultural productivity to feed growing populations (Gordon et al., 2010; Molden, 2007).

In this study, basins in Pakistan, India and the Middle East display as most overexploited. In wide areas of these basins surface irrigation systems still prevail. Irrigation efficiencies are therefore considerably lower than in Europe, Northern China and North America (Jägermeyr et al., 2015). A transition from traditional surface (furrow or flood irrigation) to more water efficient systems like sprinkler or drip systems can increase productivity as water is applied more accurately and water use decreased (Gleick, 2003; Molden, 2007).

Hoff et al. (2010) emphasize that the whole spectrum of water management options needs to be applied to close the growing water gap in food production. Particularly green water based solutions are crucial as it accounts for about 90% of agricultural water consumption (Rost et al., 2008; Hoekstra and Mekonnen, 2012; Liu et al., 2009). While having reached blue water shortages, many countries have not yet unlocked their whole green water potential (Falkenmark et al., 2009; Rockström et al., 2009a). The possibilities are an improvement of water conservation, or more precisely water-use efficiency and water productivity enhancements (Gleick, 2003; Rockström et al., 2009a). An increase in efficiency is increased when green water losses are reduced through an increase of water transpired productively instead of evaporating unproductively from soils, canals or lakes or as interception loss (white water) (Falkenmark and Lannerstad, 2005; Rost et al., 2008).

Green water based solutions include techniques like rainwater harvesting/supplemental irrigation (Oweis and Hachum, 2006), water recycling and reuse of agricultural drainage water (Allam et al., 2016), land leveling (Gleick, 2003), careful water accounting and scheduling of irrigation (Perea et al., 2016; Villalobos et al., 2016), as well as direct seeding, mulching and low tillage (soil and nutrient management) (Foley et al., 2011; Bhushan et al., 2007). In water-scarce regions affected by climate change, an increase of irrigation is often still seen as the sole mitigation strategy thus preventing urgently needed green water based innovations (Wittekind et al., 2016).

An essential factor in global water resources assessment today and expected to become even more important in the future, is virtual water trade. It allows to improve global water productivity and can help to save water resources and associated habitats when production is transferred to other regions with less susceptible water resources (Hoff et al., 2010; Hoekstra, 2011). On the other hand, some important international water dependencies might be overlooked and have to be considered (Wichelns, 2001; Allan, 2003; Rockström et al., 2014a).

Certainly, virtual water trade supports the notion of a broad global scale approach in water resources assessments like undertaken here.

Outlook - Possible future Studies building on this Thesis

Regarding the set of PBs on the global scale, it is beyond doubt that the resilience of the ES is strained to an unprecedented extent. Nevertheless, it is unknown when it is destroyed (Rockström et al., 2009c). The implications of the here assessed widespread transgressions in often adjacent basins have unknown consequences for the global water cycle and for depending sub processes like the functioning of aquatic habitats.

It can be concluded that there is considerable room for refinement of this first explorative assessment of the transgression of the PB of human freshwater use with consideration of freshwater biodiversity. Above all, a refined assessment of EFR deficits requires local validation of the underlying EFRs and scientific assessments of the effects of transgressions and of their propagation across scales.

Future assessments should further focus on the identification of hot spots of competition for water between food production and EFRs as well as biodiversity against the background of climate change. Vulnerabilities have to be assessed not only on local but also on global scale as has been done with focus on climate change as well as food production (Vörösmarty et al., 2000b; Alcamo et al., 2008). Integrative analyses of changes in streamflow and interactions with biodiversity and climate change's influences, such as alteration of thermal habitat characteristics, have to be undertaken (Milly et al., 2005; van Vliet et al., 2013). This can serve to develop the "truly global evidence base, with much greater integration among issues" demanded by (Steffen et al., 2015, p.9). The data coupling should therein be done on the finest grain possible. Furthermore, ecological risks associated with further impacts on freshwater resources due to growing populations have to become an integral part of water assessments (Vörösmarty et al., 2000b).

These assessments have rarely been done on a global scale. EFRs have to be globally compared to anthropogenic water requirements for goods and services (Alcamo et al., 2008). By further integrating the complex interactions between freshwater, climate change and aquatic biodiversity in the assessment of anthropogenic effects on environmental processes, holistic sustainable management solutions can be advanced. Finally, possible threats to the stability of the ES can be examined.

The strengthening of the scientific knowledge base on the state and development of freshwater availability and scarcity and the effects on EFRs in the future, while integrating climate change and socioeconomic changes in these projections, is of major importance for adapted decision making in sustainable management of water resources (Bates et al., 2008; Molden, 2007).

7 Conclusion

As the most essential natural resource, water represents the very core of sustainable development as it is crucial to the survival of people and the planet. Considerable levels of global biodiversity are dependent on the health and functioning of freshwater ecosystem. Overexploitation of freshwater resources is a dynamic process with severe impacts on the Earth System and strong interlinkages with other processes such as climate change and functioning of the biosphere. Therefore, it needs to be represented adequately in holistic frameworks for sustainable management like the highly influential concept of planetary boundaries.

This two-criteria analysis of transgressions of EFRs and coinciding biodiversity accomplishes to provide an elaborate representation of the extent of exploitation of freshwater resources and their spatio-temporal distribution. While the duration of transgression (non-fulfillment of the EFRs during at least half of the year) is particularly problematic on the Indian subcontinent, Central Asia, and in the Middle East, the magnitude of EFR deficits is a more global problem - major basins showing transgressions beyond uncertainty can be found on all continents, except South America. Furthermore, the high number of species, many of them endemic that depend on in some areas severely strained freshwater resources were integrated into the assessment. The aim was to improve the spatial resolution of global EFR transgressions with regard to levels of aquatic biodiversity. Major Indian, Spanish, Italian, Mexican and US-American basins with severely overexploited freshwater resources support high levels of amphibian biodiversity. The introduction and enforcement of strict EFRs (e.g. in the form of maximum extraction rates) is crucial in these basins to protect these valuable habitats.

To attain the SDGs it is indispensable to protect freshwater ecosystem, though conflict with other goals like food security is possible. Integrated water resources management schemes like demanded in the SDG framework have to be extended to efficiently allocate water to both human and environmental requirements. This entails locally adapted arrangements and fast action while prioritizing policy and management responses that are able to block threats at their source instead of through expensive elimination of symptoms. To achieve global water security for both humans and freshwater biodiversity against the background of climate change and environmental degradation, while staying within the safe operating space of the Earth system as delineated by the PBs, remains a major challenge of today's society.

References

10th International River Symposium
2007. The brisbane declaration - environmental flows are essential for freshwater ecosystem health and human well-being. *3rd - 6th September 2007 Brisbane (Australia).*

Abell, R., M. L. Thieme, C. Revenga, M. Bryer, M. Kottelat, N. Bogutskaya, B. Coad, N. Mandrak, S. C. Balderas, W. Bussing, M. L. J. Stiassny, P. Skelton, G. R. Allen, P. Unmack, A. Naseka, R. Ng, N. Sindorf, J. Robertson, E. Armijo, J. V. Higgins, T. J. Heibel, E. Wikramanayake, D. Olson, H. L. Lopez, R. E. Reis, J. G. Lundberg, M. H. S. Perez, and P. Petry
2008. Freshwater ecoregions of the world: A new map of biogeographic units for freshwater biodiversity conservation. *Bioscience*, 58(5):403–414.

Acreman, M. and M. J. Dunbar
2004. Defining environmental river flow requirements - a review. *Hydrology and Earth System Sciences*, 8(5):861–876.

Acreman, M. C., I. C. Overton, J. King, P. J. Wood, I. G. Cowx, M. J. Dunbar, E. Kendy, and W. J. Young
2014. The changing role of ecohydrological science in guiding environmental flows. *Hydrological Sciences Journal-Journal Des Sciences Hydrologiques*, 59(3-4):433–450.

Alcamo, J. M., C. J. Vörösmarty, R. J. Naiman, D. P. Lettenmaier, and C. Pahl-Wostl
2008. A grand challenge for freshwater research: understanding the global water system. *Environmental Research Letters*, 3(1):010202.

Allam, A., A. Tawfik, C. Yoshimura, and A. Fleifle
2016. Simulation-based optimization framework for reuse of agricultural drainage water in irrigation. *Journal of Environmental Management*, 172:82–96.

Allan, J. A.
2003. Virtual water - the water, food, and trade nexus useful concept or misleading metaphor? *Water International*, 28(1):106–113.

Allan, R. P., B. J. Soden, V. O. John, W. Ingram, and P. Good
2010. Current changes in tropical precipitation. *Environmental Research Letters*, 5(2).

Amthor, J. S.
1995. Terrestrial higher-plant response to increasing atmospheric [co2] in relation to the global carbon-cycle. *Global Change Biology*, 1(4):243–274.

Arnell, N. W.
1999. A simple water balance model for the simulation of streamflow over a large geographic domain. *Journal of Hydrology*, 217(3-4):314–335.

Arthington, A. H., R. J. Naiman, M. E. McClain, and C. Nilsson
2010. Preserving the biodiversity and ecological services of rivers: new challenges and research opportunities. *Freshwater Biology*, 55(1):1–16.

Barnosky, A. D., E. A. Hadly, J. Bascompte, E. L. Berlow, J. H. Brown, M. Fortelius, W. M. Getz, J. Harte, A. Hastings, P. A. Marquet, N. D. Martinez, A. Mooers, P. Roop-

narine, G. Vermeij, J. W. Williams, R. Gillespie, J. Kitzes, C. Marshall, N. Matzke, D. P. Mindell, E. Revilla, and A. B. Smith
2012. Approaching a state shift in earth's biosphere. *Nature*, 486(7401):52–58.

Barnosky, A. D., N. Matzke, S. Tomiya, G. O. U. Wogan, B. Swartz, T. B. Quental, C. Marshall, J. L. McGuire, E. L. Lindsey, K. C. Maguire, B. Mersey, and E. A. Ferrer
2011. Has the earth's sixth mass extinction already arrived? *Nature*, 471(7336):51–57.

Bates, B., Z. W. Kundzewicz, S. Wu, and J. E. Palutikof
2008. Climate change and water, technical paper of the intergovernmental panel on climate change. Report, IPCC Working Group II.

Bhushan, L., J. K. Ladha, R. K. Gupta, S. Singh, A. Tirol-Padre, Y. Saharawat, M. Gathala, and H. Pathak
2007. Saving of water and labor in a rice-wheat system with no-tillage and direct seeding technologies. *Agronomy Journal*, 99(5):1288–1296.

Biemans, H., I. Haddeland, P. Kabat, F. Ludwig, R. W. A. Hutjes, J. Heinke, W. von Bloh, and D. Gerten
2011. Impact of reservoirs on river discharge and irrigation water supply during the 20th century. *Water Resources Research*, 47(3).

Biemans, H., R. W. A. Hutjes, P. Kabat, B. J. Strengers, D. Gerten, and S. Rost
2009. Effects of precipitation uncertainty on discharge calculations for main river basins. *Journal of Hydrometeorology*, 10(4):1011–1025.

Billing, M.
2016. *Recalculation of global, inaccessible blue water using a global dynamic hydrology and vegetation model (LPJmL).* Internship report.

Bogardi, J. J., B. M. Fekete, and C. J. Vorosmarty
2013. Planetary boundaries revisited: a view through the 'water lens'. *Current Opinion in Environmental Sustainability*, 5(6):581–589.

Bond, N. R., P. S. Lake, and A. H. Arthington
2008. The impacts of drought on freshwater ecosystems: an australian perspective. *Hydrobiologia*, 600:3–16.

Bondeau, A., P. C. Smith, S. Zaehle, S. Schaphoff, W. Lucht, W. Cramer, D. Gerten, H. Lotze-Campen, C. Muller, M. Reichstein, and B. Smith
2007. Modelling the role of agriculture for the 20th century global terrestrial carbon balance. *Global Change Biology*, 13(3):679–706.

Brauns, S.
2016. *Improved Quantification of the Planetary Boundary for Freshwater Use*. Thesis.

Brown, J. H., W. R. Burnside, A. D. Davidson, J. P. DeLong, W. C. Dunn, M. J. Hamilton, N. Mercado-Silva, J. C. Nekola, J. G. Okie, W. H. Woodruff, and W. Y. Zuo
2011. Energetic limits to economic growth. *Bioscience*, 61(1):19–26.

Bunn, S. E. and A. H. Arthington
2002. Basic principles and ecological consequences of altered flow regimes for aquatic biodiversity. *Environmental Management*, 30(4):492–507.

CBD
2014. An updated synthesis of the impacts of ocean acidification on marine biodiversity. Report, Secretariat of the Convention on Biological Diversity.

Chao, B. F., Y. H. Wu, and Y. S. Li
2008. Impact of artificial reservoir water impoundment on global sea level. *Science*, 320(5873):212–214.

Chen, H., L. K. A. Ma, W. Guo, Y. Yang, T. Guo, and C. Feng
2013. Linking water quality and quantity in environmental flow assessment in deteriorated ecosystems: A food web view. *Plos One*, 8(7).

Chen, J. L., J. S. Famiglietti, B. R. Scanlon, and M. Rodell
2016. Groundwater storage changes: Present status from grace observations (vol 37, pg 397, 2016). *Surveys in Geophysics*, 37(3):701–701.

Church, J. A. and N. J. White
2006. A 20th century acceleration in global sea-level rise. *Geophysical Research Letters*, 33(1).

Cobb, D. G., T. D. Galloway, and J. F. Flannagan
1992. Effects of discharge and substrate stability on density and species composition of stream insects. *Canadian Journal of Fisheries and Aquatic Sciences*, 49(9):1788–1795.

Constanza, R., R. D'Arge, R. de Groot, S. Farber, M. Grasso, B. Hannon, K. Limburg, S. Naeem, R. V. O'Neill, J. Paruelo, R. G. Raskin, P. Sutton, and M. van den Belt
1997. The value of the world's ecosystem services and natural capital. *Nature*, 387:253–260.

Cornell, S.
2012. On the system properties of the planetary boundaries. *Ecology and Society*, 17(1).

Crisp, M. D., S. Laffan, H. P. Linder, and A. Monro
2001. Endemism in the australian flora. *Journal of Biogeography*, 28(2):183–198.

Dansgaard, W., S. J. Johnsen, H. Clausen, D. Dahljensen, and N. S. Gundestrup
1993. Evidence for general instability of past climate from a 250-kyr ice-core record. *Nature*, 364(6434):218–220.

de Fraiture, C., D. Molden, U. Amarasinghe, and I. Makin
2001. Podium: Projecting water supply and demand for food production in 2025. *Physics and Chemistry of the Earth Part B-Hydrology Oceans and Atmosphere*, 26(11-12):869–876.

Dietz, T., E. A. Rosa, and R. York
2007. Driving the human ecological footprint. *Frontiers in Ecology and the Environment*, 5(1):13–18.

Döll, P. and J. Zhang
2010. Impact of climate change on freshwater ecosystems: a global-scale analysis of ecologically relevant river flow alterations. *Hydrology and Earth System Sciences*, 14(5):783–799.

Dudgeon, D., A. H. Arthington, M. O. Gessner, Z. I. Kawabata, D. J. Knowler, C. Leveque, R. J. Naiman, A. H. Prieur-Richard, D. Soto, M. L. J. Stiassny, and C. A. Sullivan
2006. Freshwater biodiversity: importance, threats, status and conservation challenges. *Biological Reviews*, 81(2):163–182.

Dynesius, M. and C. Nilsson
1994. Fragmentation and flow regulation of river systems in the northern 3rd of the world. *Science*, 266(5186):753–762.

Ellis, E. C.
2011. Anthropogenic transformation of the terrestrial biosphere. *Philosophical Transactions of the Royal Society a-Mathematical Physical and Engineering Sciences*, 369(1938):1010–1035.

EU
2015. Ecological flows in the implementation of the water framework directive - guidance document no. 31. Report, European Commission.

Fader, M., S. Rost, C. Muller, A. Bondeau, and D. Gerten
2010. Virtual water content of temperate cereals and maize: Present and potential future patterns. *Journal of Hydrology*, 384(3-4):218–231.

Falkenmark, M.
2013. Growing water scarcity in agriculture: future challenge to global water security. *Philosophical Transactions of the Royal Society a-Mathematical Physical and Engineering Sciences*, 371(2002).

Falkenmark, M. and M. Lannerstad
2005. Consumptive water use to feed humanity - curing a blind spot. *Hydrology and Earth System Sciences*, 9(1-2):15–28.

Falkenmark, M. and J. Rockström
2004. *Balancing water for humans and nature the new approach in ecohydrology*. London: Earthscan.

Falkenmark, M., J. Rockstrom, and L. Karlberg
2009. Present and future water requirements for feeding humanity. *Food Security*, 1(1):59–69.

Famiglietti, J. S.
2014. The global groundwater crisis. *Nature Climate Change*, 4(11):945–948.

FC-GWSP
2005. Framing committee of the global water system project: Science framework and implementation activities. (11.02.2017).

Fekete, B. M., C. J. Vorosmarty, and W. Grabs
2002. High-resolution fields of global runoff combining observed river discharge and simulated water balances. *Global Biogeochemical Cycles*, 16(3).

Ficke, A. D., C. A. Myrick, and L. J. Hansen
2007. Potential impacts of global climate change on freshwater fisheries. *Reviews in Fish Biology and Fisheries*, 17(4):581–613.

Flörke, M., E. Kynast, I. Barlund, S. Eisner, F. Wimmer, and J. Alcamo
2013. Domestic and industrial water uses of the past 60 years as a mirror of socio-economic development: A global simulation study. *Global Environmental Change-Human and Policy Dimensions*, 23(1):144–156.

Foley, J. A., N. Ramankutty, K. A. Brauman, E. S. Cassidy, J. S. Gerber, M. Johnston, N. D. Mueller, C. O'Connell, D. K. Ray, P. C. West, C. Balzer, E. M. Bennett, S. R. Carpenter, J. Hill, C. Monfreda, S. Polasky, J. Rockstrom, J. Sheehan, S. Siebert, D. Tilman, and D. P. M. Zaks
2011. Solutions for a cultivated planet. *Nature*, 478(7369):337–342.

Forum, W. E.
2015. World risk report 2015. Report.

Foster, S. S. D. and P. J. Chilton
2003. Groundwater: the processes and global significance of aquifer degradation. *Philosophical Transactions of the Royal Society of London Series B-Biological Sciences*, 358(1440):1957–1972.

Gaston, K. J.
2000. Global patterns in biodiversity. *Nature*, 405(6783):220–227.

Gaston, K. J., R. M. Quinn, T. M. Blackburn, and B. C. Eversham
1998. Species-range size distributions in britain. *Ecography*, 21(4):361–370.

Gerten, D., J. Heinke, H. Hoff, H. Biemans, M. Fader, and K. Waha
2011. Global water availability and requirements for future food production. *Journal of Hydrometeorology*, 12(5):885–899.

Gerten, D., H. Hoff, J. Rockstrom, J. Jägermeyr, M. Kummu, and A. V. Pastor
2013. Towards a revised planetary boundary for consumptive freshwater use: role of environmental flow requirements. *Current Opinion in Environmental Sustainability*, 5(6):551–558.

Gerten, D., S. Rost, W. von Bloh, and W. Lucht
2008. Causes of change in 20th century global river discharge. *Geophysical Research Letters*, 35(20).

Gerten, D., S. Schaphoff, U. Haberlandt, W. Lucht, and S. Sitch
2004. Terrestrial vegetation and water balance - hydrological evaluation of a dynamic global vegetation model. *Journal of Hydrology*, 286(1-4):249–270.

Gleick, P. H.
2003. Water use. *Annual Review of Environment and Resources*, 28:275–314.

Goldewijk, K. K., A. Beusen, and P. Janssen
2010. Long-term dynamic modeling of global population and built-up area in a spatially explicit way: Hyde 3.1. *The Holocene*, 20(4):565–573.

Gordon, L. J., C. M. Finlayson, and M. Falkenmark
2010. Managing water in agriculture for food production and other ecosystem services. *Agricultural Water Management*, 97(4):512–519.

Griggs, D., M. Stafford-Smith, O. Gaffney, J. Rockstrom, M. C. Ohman, P. Shyamsundar, W. Steffen, G. Glaser, N. Kanie, and I. Noble
2013. Sustainable development goals for people and planet. *Nature*, 495(7441):305–307.

Haberl, H., K. H. Erb, F. Krausmann, V. Gaube, A. Bondeau, C. Plutzar, S. Gingrich, W. Lucht, and M. Fischer-Kowalski
2007. Quantifying and mapping the human appropriation of net primary production in earth's terrestrial ecosystems. *Proceedings of the National Academy of Sciences of the United States of America*, 104(31):12942–12945.

Haddeland, I., D. B. Clark, W. Franssen, F. Ludwig, F. Voss, N. W. Arnell, N. Bertrand, M. Best, S. Folwell, D. Gerten, S. Gomes, S. N. Gosling, S. Hagemann, N. Hanasaki, R. Harding, J. Heinke, P. Kabat, S. Koirala, T. Oki, J. Polcher, T. Stacke, P. Viterbo, G. P. Weedon, and P. Yeh
2011. Multimodel estimate of the global terrestrial water balance: Setup and first results. *Journal of Hydrometeorology*, 12(5):869–884.

Hagemann, S., C. Chen, D. B. Clark, S. Folwell, S. N. Gosling, I. Haddeland, N. Hanasaki, J. Heinke, F. Ludwig, F. Voss, and A. J. Wiltshire
2013. Climate change impact on available water resources obtained using multiple global climate and hydrology models. *Earth System Dynamics*, 4(1):129–144.

Harris, I., P. D. Jones, T. J. Osborn, and D. H. Lister
2014. Updated high-resolution grids of monthly climatic observations - the cru ts3.10 dataset. *International Journal of Climatology*, 34(3):623–642.

Heinke, J., S. Ostberg, S. Schaphoff, K. Frieler, C. Muller, D. Gerten, M. Meinshausen, and W. Lucht
2013. A new climate dataset for systematic assessments of climate change impacts as a function of global warming. *Geoscientific Model Development*, 6(5):1689–1703.

Hoekstra, A. Y.
2011. The global dimension of water governance: Why the river basin approach is no longer sufficient and why cooperative action at global level is needed. *Water*, 3(1):21–46.

Hoekstra, A. Y. and M. M. Mekonnen
2012. The water footprint of humanity. *Proceedings of the National Academy of Sciences of the United States of America*, 109(9):3232–3237.

Hoff, H., M. Falkenmark, D. Gerten, L. Gordon, L. Karlberg, and J. Rockstrom
2010. Greening the global water system. *Journal of Hydrology*, 384(3-4):177–186.

House, J. I., I. C. Prentice, N. Ramankutty, R. A. Houghton, and M. Heimann
2003. Reconciling apparent inconsistencies in estimates of terrestrial co2 sources and sinks. *Tellus Series B-Chemical and Physical Meteorology*, 55(2):345–363.

Hughes, T. P., S. Carpenter, J. Rockstrom, M. Scheffer, and B. Walker
2013. Multiscale regime shifts and planetary boundaries. *Trends in Ecology Evolution*, 28(7):389–395.

IPCC
2014. Climate change 2014: Synthesis report. contribution of working groups i, ii and iii to the fifth assessment report of the intergovernmental panel on climate change. Report, IPCC.

Janse, J. H., J. J. Kuiper, M. J. Weijters, E. P. Westerbeek, M. H. J. L. Jeuken, M. Bakkenes, R. Alkemade, W. M. Mooij, and J. T. A. Verhoeven
2015. Globio-aquatic, a global model of human impact on the biodiversity of inland aquatic ecosystems. *Environmental Science Policy*, 48:99–114.

Jägermeyr, J., D. Gerten, J. Heinke, S. Schaphoff, M. Kummu, and W. Lucht
2015. Water savings potentials of irrigation systems: global simulation of processes and linkages. *Hydrology and Earth System Sciences*, 19(7):3073–3091.

Jägermeyr, J., D. Gerten, S. Schaphoff, J. Heinke, W. Lucht, and J. Rockstrom
2016a. Integrated crop water management might sustainably halve the global food gap. *Environmental Research Letters*, 11(2).

Jägermeyr, J., A. Pastor, H. Biemans, and D. Gerten
2016b. Reconcile irrigated food production with environmental flows in face of sdg implementation.

Junk, W. J., P. Bayley, and R. E. Sparks
1989. The flood pulse concept in river-floodplain systems. *Proceedings of the International Large River Symposium (LARS)*, Pp. 110–127.

King, J. and D. Louw
1998. Instream flow assessments for regulated rivers in south africa using the building block methodology. *Aquatic Ecosystem Health Management*, 1(2):109–124.

Kummu, M., P. J. Ward, H. de Moel, and O. Varis
2010. Is physical water scarcity a new phenomenon? global assessment of water shortage over the last two millennia. *Environmental Research Letters*, 5(3).

Kundzewicz, Z. W., L. J. Mata, N. W. Arnell, P. Döll, B. Jimenez, K. Miller, T. Oki, Z. Sen, and I. Shiklomanov
2008. The implications of projected climate change for freshwater resources and their management. *Hydrological Sciences Journal-Journal Des Sciences Hydrologiques*, 53(1):3–10.

Le Quesne, T., E. Kendy, and D. Weston
2010. The implementation challenge - taking stock of government policies to protect and restore environmental flows. (20.02.2017).

Lehner, B. and P. Döll
2004. Development and validation of a global database of lakes, reservoirs and wetlands. *Journal of Hydrology*, 296(1-4):1–22.

Lehner, B. and G. Grill
2013. Global river hydrography and network routing: baseline data and new approaches to study the world's large river systems. *Hydrological Processes*, 27(15):2171–2186.

Lehner, B., C. R. Liermann, C. Revenga, C. Vörösmarty, B. Fekete, P. Crouzet, P. Döll, M. Endejan, K. Frenken, J. Magome, C. Nilsson, J. C. Robertson, R. Rödel, N. Sindorf,

and D. Wisser
2011. High-resolution mapping of the world's reservoirs and dams for sustainable river-flow management. *Frontiers in Ecology and the Environment*, 9(9):494–502.

Linder, H. P.
2001. Plant diversity and endemism in sub-saharan tropical africa. *Journal of Biogeography*, 28(2):169–182.

Liu, J. G., A. J. B. Zehnder, and H. Yang
2009. Global consumptive water use for crop production: The importance of green water and virtual water. *Water Resources Research*, 45.

L'Vovich, M., G. White, A. Belyaev, J. Kindler, N. Koronkevic, T. Lee, and G. Voropaev
1990. *Use and Transformation of Terrestrial Water Systems*. Cambridge: Cambridge University Press.

Maddison, A.
2001. The world economy: A millenial perspective. Report, OECD.

McNutt, M.
2014. The drought you can't see. *Science*, 345(6204):1543–1543.

Milly, P. C. D., K. A. Dunne, and A. V. Vecchia
2005. Global pattern of trends in streamflow and water availability in a changing climate. *Nature*, 438(7066):347–350.

Minckley, T. A., R. K. Shriver, and B. Shuman
2012. Resilience and regime change in a southern rocky mountain ecosystem during the past 17 000 years. *Ecological Monographs*, 82(1):49–68.

Molden, D.
2007. Comprehensive assessment of water management in agriculture series foreword. *Agricultural Groundwater Revolution: Opportunities and Threats to Development*, Pp. Xi–Xii.

Moore, M.
2004. *Perceptions and interpretations of environmental flows and implications for future water resource management: A survey study.* Thesis.

Naiman, R. J., S. E. Bunn, C. Nilsson, G. E. Petts, G. Pinay, and L. C. Thompson
2002. Legitimizing fluvial ecosystems as users of water: An overview. *Environmental Management*, 30(4):455–467.

Nilsson, C. and B. M. Renofalt
2008. Linking flow regime and water quality in rivers: a challenge to adaptive catchment management. *Ecology and Society*, 13(2).

Nordhaus, T., M. Shellenberger, and L. Blomqvist
2012. The planetary boundaries hypothesis - a review of the evidence. Report, Breakthrough Institute.

Norris, R. H. and M. C. Thoms
1999. What is river health? *Freshwater Biology*, 41(2):197–209.

Orr, J. C., V. J. Fabry, O. Aumont, L. Bopp, S. C. Doney, R. A. Feely, A. Gnanadesikan, N. Gruber, A. Ishida, F. Joos, R. M. Key, K. Lindsay, E. Maier-Reimer, R. Matear, P. Monfray, A. Mouchet, R. G. Najjar, G. K. Plattner, K. B. Rodgers, C. L. Sabine, J. L. Sarmiento, R. Schlitzer, R. D. Slater, I. J. Totterdell, M. F. Weirig, Y. Yamanaka, and A. Yool
2005. Anthropogenic ocean acidification over the twenty-first century and its impact on calcifying organisms. *Nature*, 437(7059):681–686.

Oweis, T. and A. Hachum
2006. Water harvesting and supplemental irrigation for improved water productivity of dry farming systems in west asia and north africa. *Agricultural Water Management*, 80(1-3):57–73.

Pastor, A. V., F. Ludwig, H. Biemans, H. Hoff, and P. Kabat
2014. Accounting for environmental flow requirements in global water assessments. *Hydrology and Earth System Sciences*, 18(12):5041–5059.

Perea, R. G., E. C. Poyato, P. Montesinos, and J. A. R. Diaz
2016. Optimization of irrigation scheduling using soil water balance and genetic algorithms. *Water Resources Management*, 30(8):2815–2830.

Petit, J. R., J. Jouzel, D. Raynaud, N. I. Barkov, J. M. Barnola, I. Basile, M. Bender, J. Chappellaz, M. Davis, G. Delaygue, M. Delmotte, V. M. Kotlyakov, M. Legrand, V. Y. Lipenkov, C. Lorius, L. Pepin, C. Ritz, E. Saltzman, and M. Stievenard
1999. Climate and atmospheric history of the past 420,000 years from the vostok ice core, antarctica. *Nature*, 399(6735):429–436.

Poff, N. L., J. D. Allan, M. B. Bain, J. R. Karr, K. L. Prestegaard, B. D. Richter, R. E. Sparks, and J. C. Stromberg
1997. The natural flow regime. *Bioscience*, 47(11):769–784.

Poff, N. L., B. D. Richter, A. H. Arthington, S. E. Bunn, R. J. Naiman, E. Kendy, M. Acreman, C. Apse, B. P. Bledsoe, M. C. Freeman, J. Henriksen, R. B. Jacobson, J. G. Kennen, D. M. Merritt, J. H. OâKeeffe, J. D. Olden, K. Rogers, R. E. Tharme, and A. Warner
2010. The ecological limits of hydrologic alteration (eloha): a new framework for developing regional environmental flow standards. *Freshwater Biology*, 55(1):147–170.

Portmann, F. T., S. Siebert, and P. Döll
2010. Mirca2000-global monthly irrigated and rainfed crop areas around the year 2000: A new high-resolution data set for agricultural and hydrological modeling. *Global Biogeochemical Cycles*, 24.

Postel, S. L., G. C. Daily, and P. R. Ehrlich
1996. Human appropriation of renewable fresh water. *Science*, 271(5250):785–788.

Power, A. G.
2010. Ecosystem services and agriculture: tradeoffs and synergies. *Philosophical Transactions of the Royal Society - Biological Sciences*, 365(1554):2959–2971.

Richter, B. D., J. V. Baumgartner, R. Wigington, and D. P. Braun
1997. How much water does a river need? *Freshwater Biology*, 37(1):231–249.

Richter, B. D., M. M. Davis, C. Apse, and C. Konrad
2012. A presumptive standard for environmental flow protection. *River Research and Applications*, 28(8):1312–1321.

Rockström, J., M. Falkenmark, T. Allan, C. Folke, L. Gordon, A. Jagerskog, M. Kummu, M. Lannerstad, M. Meybeck, D. Molden, S. Postel, H. H. G. Savenije, U. Svedin, A. Turton, and O. Varis
2014a. The unfolding water drama in the anthropocene: towards a resilience-based perspective on water for global sustainability. *Ecohydrology*, 7(5):1249–1261.

Rockström, J., M. Falkenmark, C. Folke, M. Lannerstad, J. Barron, E. Enfors, L. Gordon, and J. Heinke
2014b. *Water Resilience for Human Prosperty*. Cambridge: Cambridge University Press.

Rockström, J., M. Falkenmark, L. Karlberg, H. Hoff, S. Rost, and D. Gerten
2009a. Future water availability for global food production: The potential of green water for increasing resilience to global change. *Water Resources Research*, 45.

Rockström, J., W. Steffen, K. Noone, A. Persson, F. S. Chapin, E. Lambin, T. M. Lenton, M. Scheffer, C. Folke, H. J. Schellnhuber, B. Nykvist, C. A. de Wit, T. Hughes, S. van der Leeuw, H. Rodhe, S. Sorlin, P. K. Snyder, R. Costanza, U. Svedin, M. Falkenmark, L. Karlberg, R. W. Corell, V. J. Fabry, J. Hansen, B. Walker, D. Liverman, K. Richardson, P. Crutzen, and J. Foley
2009b. Planetary boundaries: Exploring the safe operating space for humanity. *Ecology and Society*, 14(2).

Rockström, J., W. Steffen, K. Noone, A. Persson, F. S. Chapin, E. F. Lambin, T. M. Lenton, M. Scheffer, C. Folke, H. J. Schellnhuber, B. Nykvist, C. A. de Wit, T. Hughes, S. van der Leeuw, H. Rodhe, S. Sorlin, P. K. Snyder, R. Costanza, U. Svedin, M. Falkenmark, L. Karlberg, R. W. Corell, V. J. Fabry, J. Hansen, B. Walker, D. Liverman, K. Richardson, P. Crutzen, and J. A. Foley
2009c. A safe operating space for humanity. *Nature*, 461(7263):472–475.

Rost, S., D. Gerten, A. Bondeau, W. Lucht, J. Rohwer, and S. Schaphoff
2008. Agricultural green and blue water consumption and its influence on the global water system. *Water Resources Research*, 44(9).

Rudolf, B., A. Becker, U. Chneider, A. Meyer-Christoffer, and M. Ziese
2010. Gpcc full data reanalysis version 5. Access Date: 18.10.2016.

Sala, O. E., F. S. Chapin, J. J. Armesto, E. Berlow, J. Bloomfield, R. Dirzo, E. Huber-Sanwald, L. F. Huenneke, R. B. Jackson, A. Kinzig, R. Leemans, D. M. Lodge, H. A. Mooney, M. Oesterheld, N. L. Poff, M. T. Sykes, B. H. Walker, M. Walker, and D. H. Wall
2000. Biodiversity - global biodiversity scenarios for the year 2100. *Science*, 287(5459):1770–1774.

Scheffer, M., S. Carpenter, J. A. Foley, C. Folke, and B. Walker
2001. Catastrophic shifts in ecosystems. *Nature*, 413(6856):591–596.

Schellnhuber, H. J.
2009. Tipping elements in the earth system. *Proceedings of the National Academy of Sciences of the United States of America*, 106(49):20561–20563.

Schneider, U., A. Becker, P. Finger, A. Meyer-Christoffer, M. Ziese, and B. Rudolf
2014. Gpcc's new land surface precipitation climatology based on quality-controlled in situ data and its role in quantifying the global water cycle. *Theoretical and Applied Climatology*, 115(1-2):15–40.

SEI
1997. Stockholm environment institute - comprehensive assessment of the freshwater resources of the world. Report.

Siebert, S. and P. Döll
2010. Quantifying blue and green virtual water contents in global crop production as well as potential production losses without irrigation. *Journal of Hydrology*, 384(3-4):198–217.

Siebert, S., M. Kummu, M. Porkka, P. Döll, N. Ramankutty, and B. R. Scanlon
2015. A global data set of the extent of irrigated land from 1900 to 2005. *Hydrology and Earth System Sciences*, 19(3):1521–1545.

Sitch, S., B. Smith, I. C. Prentice, A. Arneth, A. Bondeau, W. Cramer, J. O. Kaplan, S. Levis, W. Lucht, M. T. Sykes, K. Thonicke, and S. Venevsky
2003. Evaluation of ecosystem dynamics, plant geography and terrestrial carbon cycling in the lpj dynamic global vegetation model. *Global Change Biology*, 9(2):161–185.

Smakhtin, V.
2008. Basin closure and environmental flow requirements. *International Journal of Water Resources Development*, 24(2):227–233.

Smakhtin, V., C. Revenga, and P. Döll
2004a. A pilot global assessment of environmental water requirements and scarcity. *Water International*, 29(3):307–317.

Smakhtin, V., C. Revenga, and P. Döll
2004b. Taking into account environmental water requirements in global-scale water resources assessments. Report, International Water Management Institute IWMI.

Smith, T. M.
1997. *Plant functional types their relevance to ecosystem properties and global change*, International Geosphere Biosphere Programme: a Study of Global Change: International Geosphere Biosphere Programme book series, 1. publ. edition. Cambridge u.a.: Cambridge Univ. Press.

Steffen, W., A. Persson, L. Deutsch, J. Zalasiewicz, M. Williams, K. Richardson, C. Crumley, P. Crutzen, C. Folke, L. Gordon, M. Molina, V. Ramanathan, J. Rockstrom, M. Scheffer, H. J. Schellnhuber, and U. Svedin
2011. The anthropocene: From global change to planetary stewardship. *Ambio*, 40(7):739–761.

Steffen, W., K. Richardson, J. Rockstrom, S. E. Cornell, I. Fetzer, E. M. Bennett, R. Biggs, S. R. Carpenter, W. de Vries, C. A. de Wit, C. Folke, D. Gerten, J. Heinke, G. M. Mace, L. M. Persson, V. Ramanathan, B. Reyers, and S. Sorlin
2015. Planetary boundaries: Guiding human development on a changing planet. *Science*, 347(6223).

Strayer, D. L.
2006. Challenges for freshwater invertebrate conservation. *Journal of the North American Benthological Society*, 25(2):271–287.

Strayer, D. L. and D. Dudgeon
2010. Freshwater biodiversity conservation: recent progress and future challenges. *Journal of the North American Benthological Society*, 29(1):344–358.

Tennant, D.
1976. Instream flow regimens for fish, wildlife, recreation and related environmental resources. *Fisheries*, 1:6–10.

Tessmann, S.
1980. Environmental assessment, technical appendix e. *Reconnaissance Elements of the Western Dakotas Region of South Dakota*.

Tharme, R. E.
2003. A global perspective on environmental flow assessment: Emerging trends in the development and application of environmental flow methodologies for rivers. *River Research and Applications*, 19(5-6):397–441.

Tilman, D., K. G. Cassman, P. A. Matson, R. Naylor, and S. Polasky
2002. Agricultural sustainability and intensive production practices. *Nature*, 418(6898):671–677.

Tisseuil, C., J. F. Cornu, O. Beauchard, S. Brosse, W. Darwall, R. Holland, B. Hugueny, P. A. Tedesco, and T. Oberdorff
2013. Global diversity patterns and cross-taxa convergence in freshwater systems. *Journal of Animal Ecology*, 82(2):365–376.

Trenberth, K. E., L. Smith, T. T. Qian, A. Dai, and J. Fasullo
2007. Estimates of the global water budget and its annual cycle using observational and model data. *Journal of Hydrometeorology*, 8(4):758–769.

UN
2015. Transforming our world: the 2030 agenda for sustainable development. Report, A/70/L1.

UNEP
2008. Vital water graphics - an overview of the state of the world's fresh and marine waters - 2nd edition. Report, United Nations Environment Programme.

UNEP
2016. A snapshot of the world's water quality: Towards a global assessment (wwqa pre-study). Report, Helmholtz Centre for Environmental Research - UFZ United Nations Environment Programme - UNEP.

van Vliet, M. T. H., F. Ludwig, and P. Kabat
2013. Global streamflow and thermal habitats of freshwater fishes under climate change. *Climatic Change*, 121(4):739–754.

van Vliet, M. T. H., F. Ludwig, J. J. G. Zwolsman, G. P. Weedon, and P. Kabat
2011. Global river temperatures and sensitivity to atmospheric warming and changes in river flow. *Water Resources Research*, 47.

Villalobos, F., L. Mateos, and E. Fereres
2016. *Irrigation Scheduling Using the Water Balance*, Pp. 269–279. Springer International Publishing.

von Bloh, W., S. Rost, D. Gerten, and W. Lucht
2010. Efficient parallelization of a dynamic global vegetation model with river routing. *Environmental Modelling Software*, 25(6):685–690.

Vörösmarty, C., C. Lévêque, C. Revenga, R. Bos, C. Caudill, J. Chilton, E. Douglas, M. Meybeck, D. Prager, P. Balvanera, S. Barker, M. Maas, C. Nilsson, O. Taikan, and C. Reydi
2005. *Fresh Water*, Ecosystems and Human Well-being: Current State and Trends. Island Press.

Vörösmarty, C. J., B. M. Fekete, M. Meybeck, and R. B. Lammers
2000a. Geomorphometric attributes of the global system of rivers at 30-minute spatial resolution. *Journal of Hydrology*, 237(1-2):17–39.

Vörösmarty, C. J., P. Green, J. Salisbury, and R. B. Lammers
2000b. Global water resources: Vulnerability from climate change and population growth. *Science*, 289(5477):284–288.

Vörösmarty, C. J., P. B. McIntyre, M. O. Gessner, D. Dudgeon, A. Prusevich, P. Green, S. Glidden, S. E. Bunn, C. A. Sullivan, C. R. Liermann, and P. M. Davies
2010. Global threats to human water security and river biodiversity. *Nature*, 467(7315):555–561.

Vörösmarty, C. J. and D. Sahagian
2000. Anthropogenic disturbance of the terrestrial water cycle. *Bioscience*, 50(9):753–765.

Vörösmarty, C. J., K. P. Sharma, B. M. Fekete, A. H. Copeland, J. Holden, J. Marble, and J. A. Lough
1997. The storage and aging of continental runoff in large reservoir systems of the world. *Ambio*, 26(4):210–219.

Wada, Y., L. P. H. van Beek, C. M. van Kempen, J. W. T. M. Reckman, S. Vasak, and M. F. P. Bierkens
2010. Global depletion of groundwater resources. *Geophysical Research Letters*, 37.

Wallace, J. S. and C. H. Batchelor
1997. Managing water resources for crop production. *Philosophical Transactions of the Royal Society B-Biological Sciences*, 352(1356):937–946.

Ward, J. V., K. Tockner, and F. Schiemer
1999. Biodiversity of floodplain river ecosystems: Ecotones and connectivity. *Regulated Rivers-Research Management*, 15(1-3):125–139.

WHO
2015. Progress on sanitation and drinking water - 2015 update and mdg assessment. Report, UNICEF and World Health Oranization.

Wichelns, D.
2001. The role of 'virtual water' in efforts to achieve food security and other national goals, with an example from egypt. *Agricultural Water Management*, 49(2):131–151.

Wisser, D., S. Frolking, E. M. Douglas, B. M. Fekete, C. J. Vorosmarty, and A. H. Schumann
2008. Global irrigation water demand: Variability and uncertainties arising from agricultural and climate data sets. *Geophysical Research Letters*, 35(24).

Wittekind, C., F. Ewich, and K.-J. Peters
2016. Climate change awareness and smallholder-oriented constraints and opportunities in the upper rift valley in ethiopia. *Tropentag 2016, September 18-21, Vienna, Austria*.

WWAP
2015. United nations world water assessment programme; world water development report 2015: Water for a sustainable world. Report, The United Nations.

WWF
2016. Living planet report 2016 - risk and resilience in a new era. *World Wildlife Fund International Report*.

Supplementary Material

List of supplementary Figures

List of supplementary Tables

S 1 Overview of recent planetary boundary calculations, control values and current values

S 1.1 Overview of the nine planetary boundaries, control variables and current values according to Steffen et al. (2015)

Table ST 1: The updated control variables and their current values, along with the proposed boundaries and zones of uncertainty according to Steffen et al. (2015)

Earth-system process	Control variable(s)	Planetary boundary (zone of uncertainty)	Current value of control variable
Climate Change	Atmospheric CO_2 concentration, ppm	350 ppm CO_2 (350−450 ppm)	398.5 ppm CO_2
	Energy imbalance at top-of-atmosphere, Wm^{-2}	$+1Wm^{-2}$ $(+1.0-1.5Wm^{-2})$	$2.3Wm^{-2}$ (1.1-3.3Wm^{-2})
Change in biosphere integrity	*Genetic diversity*: Extinction rate	<10E/MSY $(10-100E/MSY)$ but with an aspirational goal of ca. 1E/MSY (the background rate of extinction loss). E/MSY =extinctions per million species-years	100−1000E/MSY

Table ST 1 continued

	Functional diversity: Biodiversity Intactness Index (BII)	Maintain BII at 90% (90−30%) or above, assessed geographically by biomes/large regional areas (e.g.southern Africa), major marine ecosystems (e.g. coral reefs) or by large functional groups	∼84%, applied to southern Africa only
Stratospheric ozone depletion	Stratospheric O_3 concentration, DU	<5% reduction from preindustrial level of 290DU (5%−10%), assessed by latitude	Only transgressed over Antarctica in Austral spring (−200DU)
Ocean acidification	Carbonate ion concentration, average global surface ocean saturation state with respect to aragonite (Ω_{arag})	$\geq$ 80% of the pre-industrial aragonite saturation state of mean surface ocean, including natural diel and seasonal variability ($\geq 80\% - 70\%$)	80% of the preindustrial aragonite saturation state
Biogeochemical flows: (P and N cycles)	*P Global*: P flow from freshwater systems into the ocean	11 Tg P yr^{-1}	
	P Regional: P flow from fertilizers to erodible soils	$6.2Tgyr^{-1}$ mined and applied to erodible (agricultural) soils ($6.2 - 11.2Tgyr^{-1}$). Boundary is a global average but regional distribution is critical for impacts.	∼14Tg P yr^{-1}

Table ST 1 continued

	N Global: Industrial and intentional biological fixation of N	$62TgNyr^{-1}$(62-82Tg N yr^{-1}). Boundary acts as a global ‘ valve ’ limiting introduction of new reactive N to Earth System, but regional distribution of fertilizer N is critical for impacts.	∼15Tg N yr^{-1}
Land System Change	*Global*: Area of forested land as % of original forest cover	*Global*: 75% (75-54%) Values are a weighted average of the three individual biome boundaries and their uncertainty zones	∼62%
	Biome: Area of forested land as % of potential forest	*Biome*: Tropical: 85% (85-60%), Temperate: 50% (50-30%), Boreal: 85% (85-60%)	
Freshwater use	*Global*: Maximum amount of consumptive blue water use (km^3/yr)	Global: $4000km^3/yr$ (4000-$6000km^3/yr$)	$\sim 2600km^3/yr$
	Basin: Blue water withdrawal as % of mean monthly river flow	Basin: Maximum monthly withdrawal as percentage of mean monthly river flow. For low-flow months: 25% (25-55%): for intermediate flow months: 30% (30-60%): for high-flow months: 55% (55-85%)	

Table ST 1 continued

Atmospheric aerosol loading	Global: Aerosol Optical Depth (AOD), but much regional variation		
	Regional: AOD as a seasonal average over a region. South Asian Monsoon used in a case study	Regional: (South Asian Monsoon as a case study): anthropogenic total (absorbing and scattering) AOD over Indian subcontinent of 0.25 (0.25-0.50): absorbind (warming) AOD less than 10% of total AOD	0.30AOD, over South Asian Region
Introduction of novel entities	No control variable currently defined	No boundary currently identified, but see boundary for stratospheric ozone for an example of a boundary related to novel entity (CFCs)	

S 1.2 Conceptual overview of the calculations of the planetary boundary of freshwater use

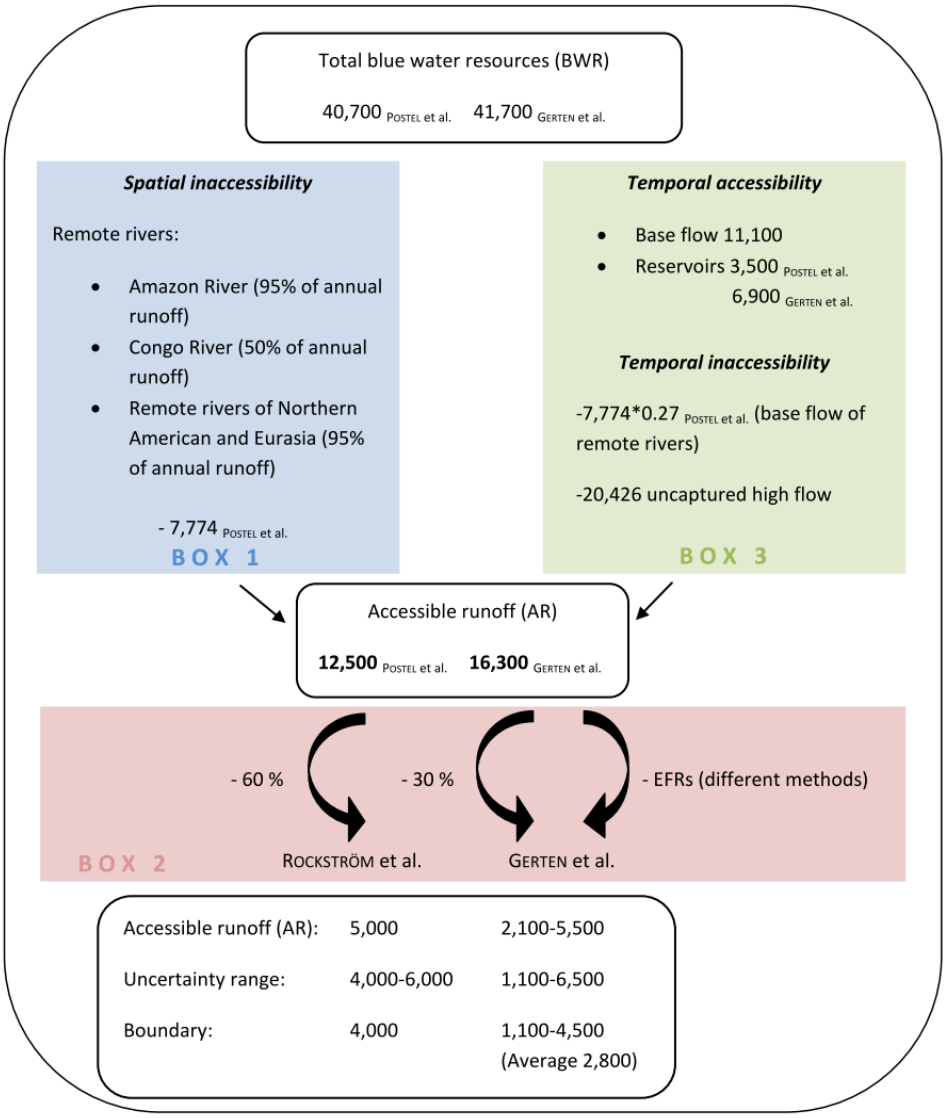

Figure SF 1: Conceptual overview of the calculations of the planetary boundary of freshwater use by Brauns (2016) showing the approaches by Gerten et al. (2013) and Rockström et al. (2009) with basis values by Postel et al. (1996). Estimates in km^3/yr

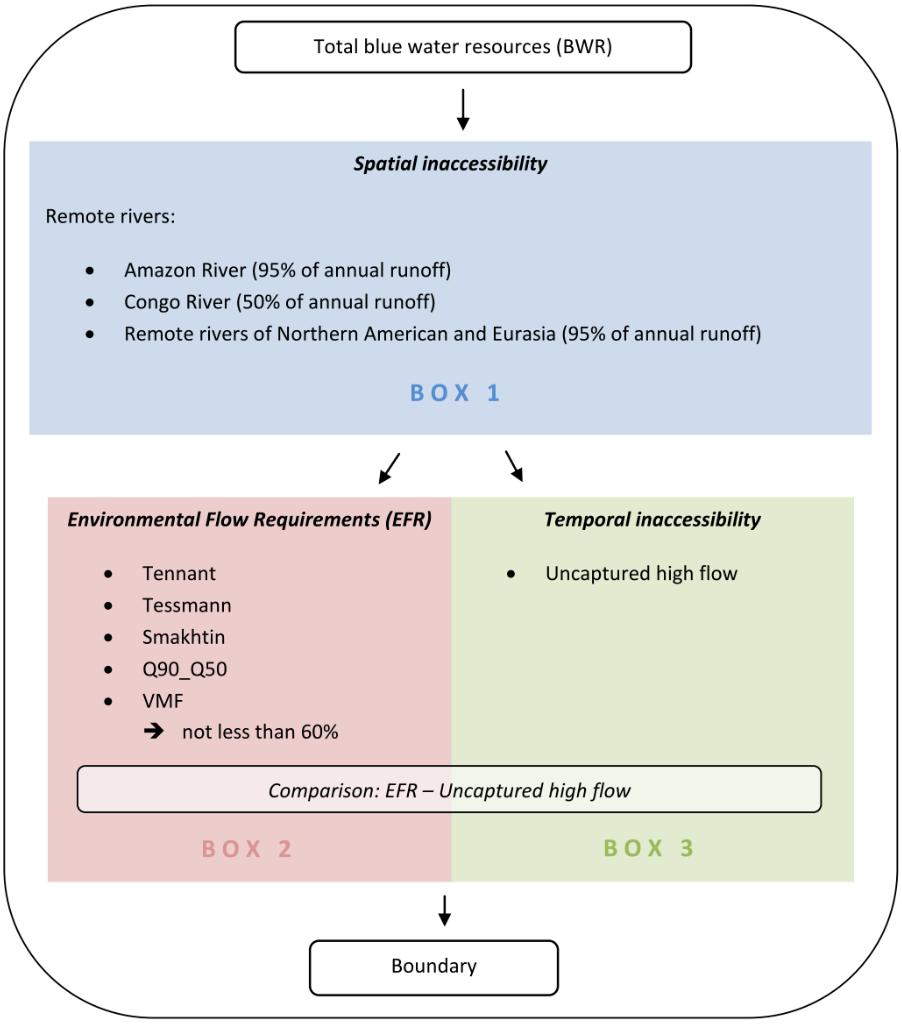

Figure SF 2: Conceptual Overview of the calculation of the boundary for freshwater use by Brauns (2016) Estimates in km^3/yr

S 1.3 Detailed description of the different PB calculations

Total renewable BW resource

The global BW availability serves as a basis for calculating accessible BW volumes. This is done by correcting it with spatially and temporally inaccessible and accessible flows. Three main components have been considered in recent approaches: remote flows that are inaccessible due to their geography, uncaptured high/flood flows and water stored in reservoirs. The estimates by Rockström et al. (2009) and Gerten et al. (2013) are based on Postel et al. (1996) but differ in the adjustments and assumptions. Brauns (2016) as well as Gerten et al. and Steffen et al. used LPJmL for the calculation of total runoff, these approaches are therefore similar in many aspects though Brauns included a refinement of spatial (remote flows) and temporal (high flow and seasonality) inaccessibility. An overview of the different approaches of calculating the accessible runoff is given in Table ST 3 and Table ST 2. Concerning the basis value of BW availability, Rockström et al. assumed the volume of global BW availability to be around 40,700km^3/yrmainly based on the assumptions by Postel et al. who in turn were based on earlier calculations by L'Vovich et al. (1990), while Gerten et al. received 41,700km^3/yr using the LPJmL outputs based on specified climatic data with a time frame of 1980-2009. Global blue water availability can be estimated by considering precipitation over land and subtracting total evapotranspiration on land (Postel et al., 1996). Brauns based her calculations on an LPJmL simulation output of 55,582km^3/yr ,~36% higher than Rockström et al. and 33% higher than Gerten et al.. This difference is mainly due to the use of different land masks in the respective LPJmL simulation runs.

Accessible BW

Rockström et al. assumed the accessible BW resource/river runoff to be between 12.500km^3/yr as estimated by Postel et al. and 15,000km^3/yr as estimated by de Fraiture et al. (2001) and the rest of BW availability to generally being constrained by the remote location or storm flow. Gerten et al. used 16,300km^3/yras basis for their calculations, as they accounted for the significant volumes currently stored by dams and actively used in flow regulation. Brauns, while not considering reservoir storage, included temporal inaccessibility due to storm flows and combined these calculations with the EFR assessment and applied the reassessed spatially inaccessible volumes as calculated by Billing (2016). As the high flows vary depending on EFR calculation method, the resulting estimate of accessible runoff varies between 8,802 and 21,441km^3/yr. These steps are shortly explained in detail. *Remote Flows* As discussed in chapter kl, global freshwater resources are not evenly distributed and there are several regions with high volumes of freshwater supply that are (still) largely untapped by humanity. As a first adjustment, remote rivers in North America as well as in Eurasia that are largely untapped as they are mostly in tundra and taiga biomes have to be subtracted. In the calculations of all three, Gerten et al., Rockstörm et al. and Brauns, 95% of the average annual flow of these rivers is subtracted like Postel et al. suggested. Postel calculated these flows to be 1,725km^3/yr and LPJmL calculated 1,513km^3/yr (Billing, 2016). Moreover, inaccessible remote flows of the Amazon and Congo region have to be excluded from calculations. All approaches considered 90% of the Amazon flow (Postel/Rockström: 5.387 km^3/yr; LPJmL: 6,955km^3/yr) and 50% of the Congo flow (662km^3/yr and 1,094km^3/yr) as inaccessible. The calculations with LPJmL were in total 23% higher (9,562km^3/yr) than the ones by Postel et al. (7,774km^3/yr) (Billing, 2016). Brauns (2016) considered 102 catchments in the northern hemisphere as unaffected like defined by Dynesius and Nilsson (1994) also complying with their requirements for catchment size. The reductions in these northern regions and in the Amazon and Congo basins by 50% or 95% respectively were taken into account for the calculation of EFRs on basin scale by lowering the discharge by the share of it contained in the remote flow.

Flood Water/High Flows

Furthermore, not only geographical inaccessibility but also temporal inaccessibility has to be taken into account and leaves room for further refinement. This applies to flood water, which is often very hard to capture and can therefore largely be subtracted though some of it is captured in dams (Postel et al., 1996). As discussed before and shown in ST 3, though increasing the value by volumes of storage capacity, Gerten et al. fundamentally followed Rockström et al. in the accounting for high flows/uncaptured storm flows by regarding 69% of total global discharge as runoff either in remote regions or as uncaptured high flows. Assuming 11,100km^3/yr of global runoff as renewable ground water and base river flow (L'Vovich et al., 1990) the remaining runoff mainly consisting of high flow and therefore largely inaccessible is 29,600km^3/yr. By subtracting the share of base flow in remote rivers that is 27% of the spatially inaccessible volume (=2,100km^3/yr), the intermediate result of accessible base flow is 9,000km^3/yr (Postel et al., 1996).

Reservoirs

Moreover, the physical alterations that many rivers have undergone have to be considered as they have strong impact on natural flow regimes (Poff et al., 1997). Dams store a significant amount of BW and these volumes have to be added to the amount of accessible BW as a large part would otherwise be inaccessible flood flows (Gerten et al., 2013). While Rockström et al. did not include this adjustment explicitly but instead used the estimate of accessible runoff by Postel et al. that contained an estimated storage capacity of 5,500km^3/yr, but only assumed 3,500km^3/yr to actively be used in the regulation of river runoff, Gerten et al. estimated the storage capacity to be 6,900 km 3 yr-1, so 3,400km^3/yr higher than Postel et al./Rockström et al.. While the latter assumed 31% of total runoff to be accessible, Gerten et al. increased the estimate by 8% (3,400 of 40,700) and therefore defined 39% of total runoff to be accessible which equals 16.300 km^3/yr in their approach (=39% of (41,700km^3/yr). Brauns did not consider dams and reservoirs, as her approach relies on discharge data simulated under naturalized condition (Brauns, 2016).

Environmental Flow Requirements and Water stress

Rockström et al. assumed that physical water scarcity is reached when withdrawals of runoff/blue water exceed 40% (=5,000 – 6.000 km^3/yr) (Vörösmarty et al., 2000, Stockholm Environment Institute, 1997), therefore leaving 60% as a fixed fraction to cover half the potential water stress and observe environmental flow requirements (3,750km^3/yr for each). Gerten et al. applied a water stress buffer of 30% and used a more detailed method to account for EFRs . While Gerten et al. subtracted water stress directly from accessible runoff to then calculate EFRs using five different methods, Brauns connected the calculation of EFRs with calculation of water stress and high flows, receiving five different values for EFRs and physical water stress and seven different values for high flows and consequently seven different boundary values, for further details on Brauns' calculation of EFRs see chapter xy EFR and Figure KÖ. Brauns indirectly applied a water stress buffer of 40% by increasing EFRs to 60% if their share at basin scale did not already represent at least 60%. Therefore, the values for water stress (given in ST 2) in Brauns' approach don't necessarily represent 40% of discharge, but water stress is included in EFRs (Brauns, 2016). In the refinement by Steffen et al. (2015) EFRs are calculated with one method (vmf) only, the aim was to improve the river basin scale boundary, as shown in ST 2, the result was a maximum withdrawal of 25 – 55% of MMF for rivers and the scaling up was not done individually but included in Gerten et al. (2013).

High Flow and correction with EFR

Unlike Rockström et al. and Gerten et al., Brauns combined the calculation of temporally inaccessible flows (high/flood flows) with the calculation of EFRs. The volumes of flood water are calculated by first defining high flow and low flow months. Then the volume of water in low flow months averaged over the year (=base flow) is subtracted from the average volume of water in high flow months for each cell. After some corrections, [1] the resulting difference represents the volume of flood water/high flows. Depending on the calculation method, the received values of high flow range between 24,579 and 37,218km^3/yr (Brauns, 2016). The calculation of EFR is based on the same outputs as the calculation of flood water (high flow, intermediate and low flow months) and as they are designed to mimic the natural flow regime as close as possible they should incorporate flood water. Hence, values for EFRs and for flood volumes partly represent the same and restrict one another (Pastor et al., 2014, Smakhtin et al., 2004). Therefore, an adjustment is needed and only the higher value of the two, either EFR or flood water volume is subtracted from the intermediate result in each of the five methods (Brauns, 2016).

Calculation of PB Values

The boundary of ~4,000km^3/yr calculated by Rockström et al. (2009) represents the lower limit of an uncertainty zone of 4,000-6,000km^3/yr. The received boundary of 2,800km^3/yr by Gerten et al. (2013) is the average of the uncertainty range of 1,100-4.500 km^3/yr and the PB value of Brauns ranges between 6,410 and 12,990km^3/yr depending on the scenario, Tessmann's method being the most permissive and Tennant's the strictest. If the strictest calculation is considered for each catchment, the boundary lies at 5,205km^3/yr.

[1] For areas/cells that don't generate individual base flow (where no low flows can be assigned because there is either no discharge due to model limitations or very uniform monthly flows) the global average of the other base flows is assigned as base flow in the respective cell. This was done for each of the methods that differentiate low and high flows (Tennant, Smakhtin, Q_{90}-Q_{50}) but the other two methods (Tessmann & VMF) require a distinction of two cases because they differentiate low, intermediate and high flows. Therefore, either intermediate flow is part of the high-flow fraction or it is part of the base-flow fraction, see Brauns (2016) for more details.

S 1.4 Overview of the different PB calculations

Table ST 2: Overview of the boundary calculations of Rockström et al. (2009b), Gerten et al. (2013) and Brauns (2016) and the values used in this study (Estimates in km^3/yr)

	Rockström et al. (2009b)	**Gerten et al. (2013)**	**Brauns (2016)**	**This study**
Total Runoff	**40 700**	**41 700**	**55 582**	**54 602**
Remote Flow	7 774	-	9 562	1 589
Not accessed yet/small basins	-	-	-	15 598
High Flow	20 426	-	24 579- 37 218	Not considered explicitly*
Reservoirs	3 500	6 900	Not considered	
Accessible Runoff	**12 500**	**16 300**	**8 802 - 21 441**	**39 400** [2]
Environmental Flow Requirements	3 750 (30%)	5 910 - 9 310	11 458 - 20 772	11 931 - 18 156
Physical Water Stress	3 750 (30%)	4 890	7 341 - 16 126	
Usable Water	5 000	2 100 - 5 500 25 - 50% of MMF (Steffen applied only VMF)	6 410 - 12 990	
Uncertainty Range	4 000 - 6 000	1 100 - 4 500	-	Not calculated
Planetary Boundary	**4 000**	**2 800**	6 410 - 12 990 **5 205** (applying the individually strictest method in each basin)	

[2]corrected for inaccessible high flows and reservoirs indirectly through the model

Table ST 3: Accessible Runoff calculations and spatial and temporal inaccessibility as calculated by Postel et al. (1996) & Rockström et al. (2009b), Gerten et al. (2013) and Brauns (2016) (estimates in km^3/yr)

	Postel et al. (1996)& Rockström et al. (2009b)	**Gerten et al. (2013)**	**Brauns (2016)**	**This study**
Total runoff	40 700	41 700	55 582	54 602
Amazonas (95% inaccessible)	5 387		6 955	
Zaire-Congo (50% inaccessible)	662		1 094	
Northern remote (95%) North America+Eurasia	979+746		1 513	1 589
No irrigation				13 433
Small basins				7 778
Spatial inaccessibility Total	=7 774		=9 562	=15 598 (= corrected for overlapping areas)
Spatial accessible Total	32 900			39 004
Renewable runoff (groundwater and base river flow)	11 100 (∼27% of 40 700)			
Remaining runoff	29 600			
Share of base flow in remote rivers (share of base flow in total runoff)	2 100 (27% of 7 774)			
Accessible Base Flow	=9 000			

Table ST 3: Continued

Dams' storage capacity	5 500 (3 500 in river runoff)	6 900		
Uncaptured High Flow			24 579–37 218	
Gerten Basis	6 900–3 500= 3 400 (8% of 40 700)	31% + 8%		
Accessible Runoff	12 500	16 300	8 802–21 441	
(% of total)	(31%)	(39%)	(16–39%)	

S 1.5 Description of the Tennant and Q_{90}_Q_{50} method

Tennant's method

The approach suggested by Tennant (1976) doesn't define intermediate-flow months, but only distinguishes high- and low-flow months. The allocation of EFRs is based on mean annual flows and all months where the MMF is lower than the MAF are defined as low-flow and all months were it is higher are defined as high-flow months. Tennant allocates 20% of MAF as EFR to low-flow months and 40% of MAF as high flow requirement (Pastor et al., 2014). Tennant's method sometimes allocates EFRs that are higher than the monthly discharge, therefore also requiring a correction where this is the case by assigning MMF as EFR.

Q_{90}_Q_{50}

Both, the VMF method and the Q_{90}_Q_{50} method were developed by Pastor et al. (2014). Like Tennant, this approach only distinguishes low flow and high flow months. During low flow months when MMF $\leq$ MAF, Q_{90} is defined as flow requirement. During high flow months, when MMF $\geq$ MAF, Q_{50} is allocated as flow requirement. Brauns (2016) adapted this approach. A low flow month is only a low flow month if its MMF is not only less than MAF but also higher than Q_{90} and high flow months are only those where MMF is not only higher than MAF but also higher than Q_{50}. For cases when either MMF $\leq$ MAF but MMF $<$ Q_{90} or MMF $\geq$ MAF but MMF $<$ Q_{50} which wouldn't fall in any category, EFRs are defined as MMF. Like Tennant and Smakhtin, the Q_{90}_Q_{50} method in some cases recommends higher EFRs than discharge is available, this is corrected by assigning the MMF as EFR is these months (Brauns, 2016).

See ST 4 for a comparison of Q_{90}_Q_{50} and Tennant method with the methods used in this study.

S 1.6 Comparison of the EFR methods

Table ST 4: Comparison of Environmental Flow Methods, adapted from Pastor et al. (2014)

Hydrological Season	**VMF (2014)**	**Tessmann (1980)**	**Smakhtin et al. (2004b)**	**Tennant (1976)**	**Q_{90}-Q_{50}(2014)**
Determination of low-flow months	MMF $\leq$ 0.4 MAF	MMF $\leq$ 0.4 MAF	MMF $\leq$ MAF (entire year)	MMF $\leq$ MAF	MMF $\leq$ MAF
low flow requirements	0.6 MAF	MMF	Q_{90}	0.2 MAF	Q_{90}
Determination of intermediate-flow months	MMF $>$ 0.4 MAF & MMF $\leq$ 0.8 MAF	MMF $>$ 0.4 MAF & 0.4 MMF $\leq$ 0.4 MAF			
intermediate-flow requirements	0.45 MMF	0.4 MAF			
Determination of high-flow months	MMF $>$ 0.8 MAF	MMF $>$ 0.4 MAF & 0.4 MMF $>$ 0.4 MAF	MMF>MAF (entire year)	MMF>MAF	MMF $>$ MAF
High-flow requirements	0.3 MAF	0.4 MAF	0 to 0.2 MAF	0.4 MAF	Q_{50}

S 2 Detailed description of the adjustments of the considered area

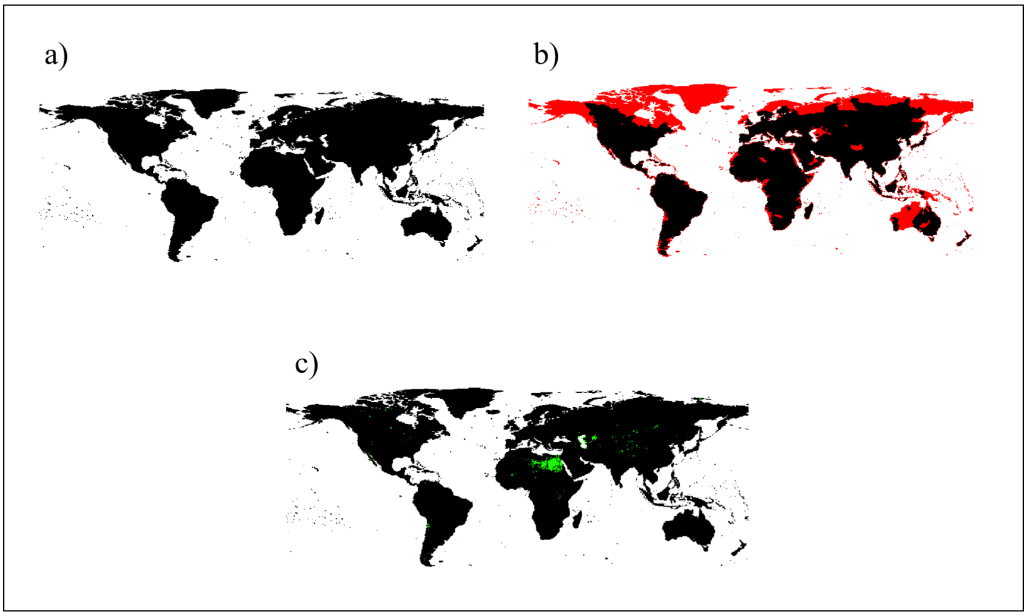

Figure SF 3: The original land mask of LPJmL (a) and the land mask with adjustments for unaffectedness (b) and small discharge (c)

First, based on the mask by Billing (2016), northern remote rivers were excluded, given in red in Figure S 1.2. These rivers are inaccessible due to their geography and accounted for 1,588km^3/yr of discharge in the simulation of the CS. Furthermore, very small basins only consisting of one cell were excluded. Their discharge is considerable small and these cells/basins don't drain into and therefore don't affect other cells, their effect concerning propagation across scales is negligible. These small basins accounted for 7,778km^3/yr of simulated discharge. Furthermore, basins not equipped for irrigation as described by Siebert et al. (2015) and of areas not affected by HIL as computed in LPJmL were excluded to assure that transgressions of EFR were only considered when they were taking place in areas that underlie human influence and are not due to the model. These are given in green in Figure S 1.2. 13,433km^3/yr of discharge were regarded as unaffected by humans as they occurred in basins not equipped for irrigation like in wide parts of Western Australia and 1,893km^3/yr occurred in basins not affected by HIL. These cells without withdrawal for HIL are predefined to lie in areas not equipped for irrigation either, the discharge for these areas is therefore already included in the 13,433km^3/yr (see r̃efVR). In total, 15,597km^3/yr of discharge is regarded as either unaffected by human influence or occurring in basins of only one grid cell, therefore not draining in other cells. Note that cells excluded for more than one reason were only counted once.

The world's total land area is 146,376,945km^2 of which 110,675,112km^2 (= 75.61%) were regarded as affected by humans in the calculations. Furthermore, there were no

Table ST 5: Excluded Areas and respective discharge in HIL

	Affected discharge	Discharge of non-overlapping areas	Affected area	Non-overlapping area
	in km^3/yr		in km^2	
Northern Remote	1 589		7 190 536	
No irrigation	13 434	13 434	32 817 110	32 817 110
No HIL	1 893		5 462 932	
Basins with only 1 cell	7 778	2 164	11 803 254	2 884 723
Total		15 598		35 701 833

EFRs assigned to months where discharge in PNV was less than 1 m^2/s. Therefore, cells where this is the case twelve months a year were not considered when area shares are calculated as is the case when aggregating transgression from cell to basin scale. The annual sum of discharge in these areas is 3.96 km^3/yr. Especially the lower Nile Basin is affected by this as shown in green in subsection S 1.2. See also section 6.

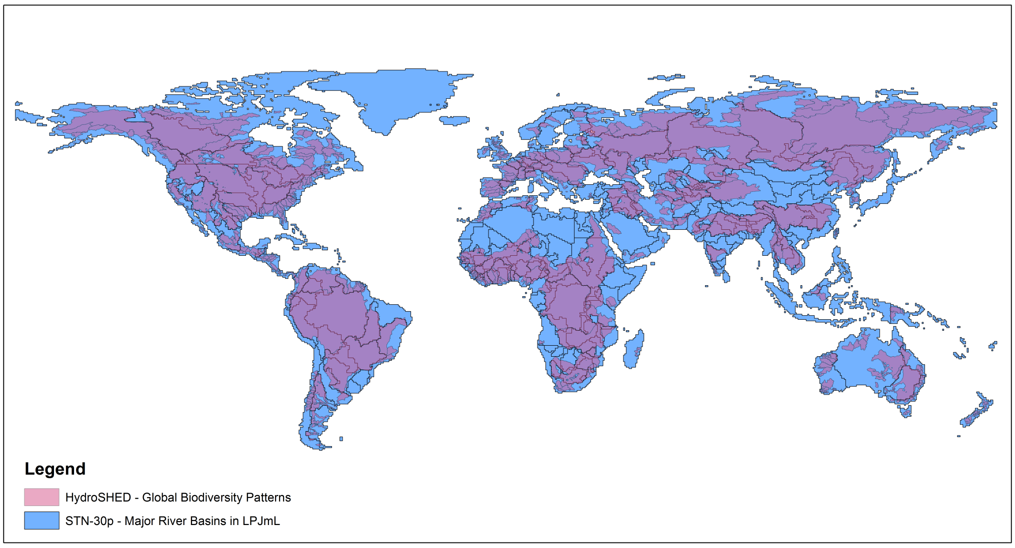

Figure SF 4: Comparison HydroSHED by Lehner and Grill (2013) and STN by Vörösmarty et al. (2000a)

HydroSHED and STN30p (the DDM underlying the simulations by LPJmL) overlap only partly and a further bias in the results (additionally to the information loss inherent in the biodiversity dataset due to its focus on basin grain) is therefore not preventable. Particularly in cases where the assessment by Tisseuil et al. covers large basins and hence assigns only one value for biodiversity for an area that displays considerable variation. For example, if high endemicity is mostly due to only one small lake in the catchment. When the rest of the area is characterized by rather low endemicity as well as species richness and the basin of interest in STN covers only the areas with low endemicity, distorted results are hard to prevent.

S 3 Details for the results on cell scale

S 3.1 Cell scale plots of EFRs for mean, strict, VMF, Tessmann and Smakhtin

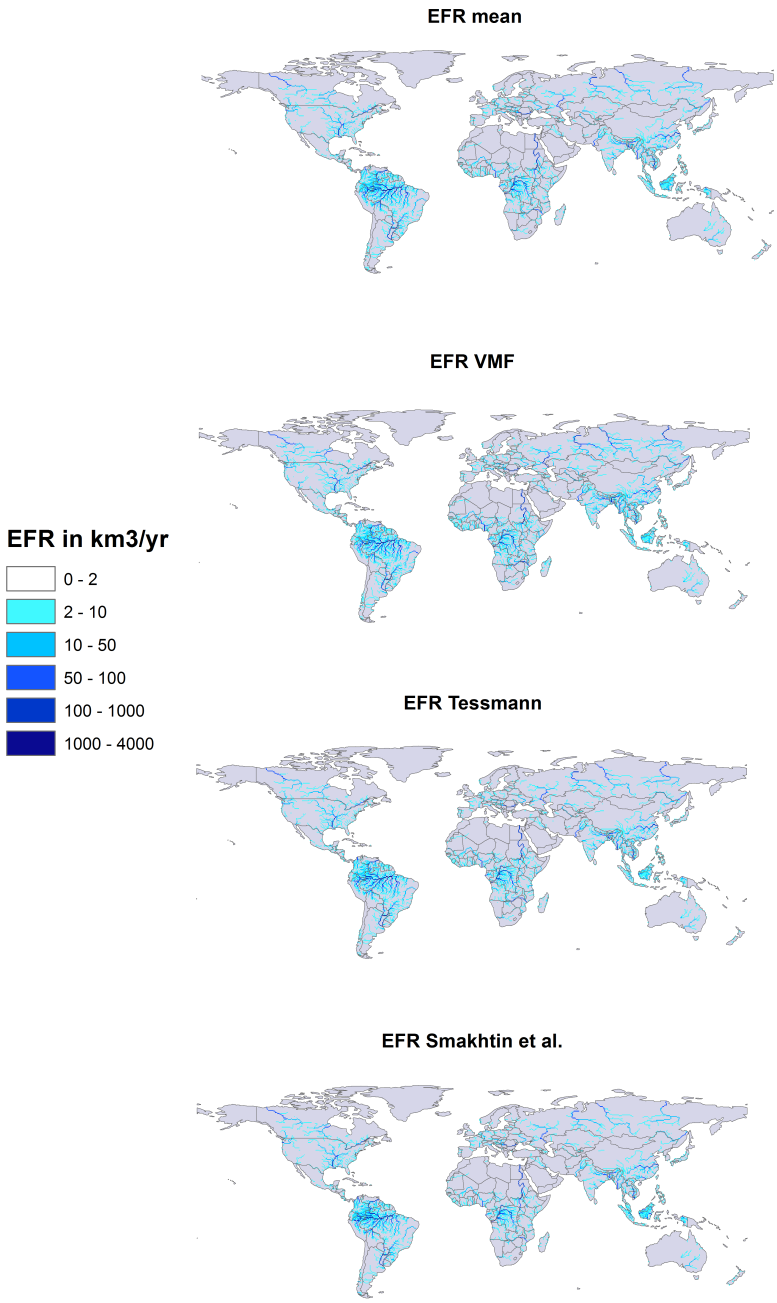

Figure SF 5: Sum of annual EFRs on cell scale (1980-2009, 0.5°resolution) in km^3/yr, major river basins delineated

S 3.2 Cell scale plots for the mean and strict scenarios

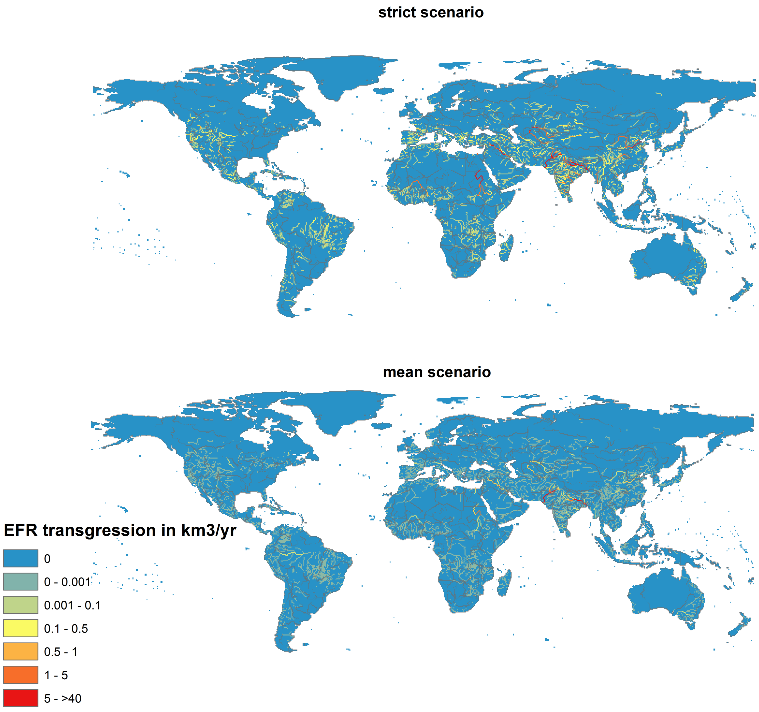

Figure SF 6: Sum of annual transgression of EFRs on cell scale (1980-2009, 0.5°resolution) in km^3/yr, for the mean and strict scenario, major river basins delineated

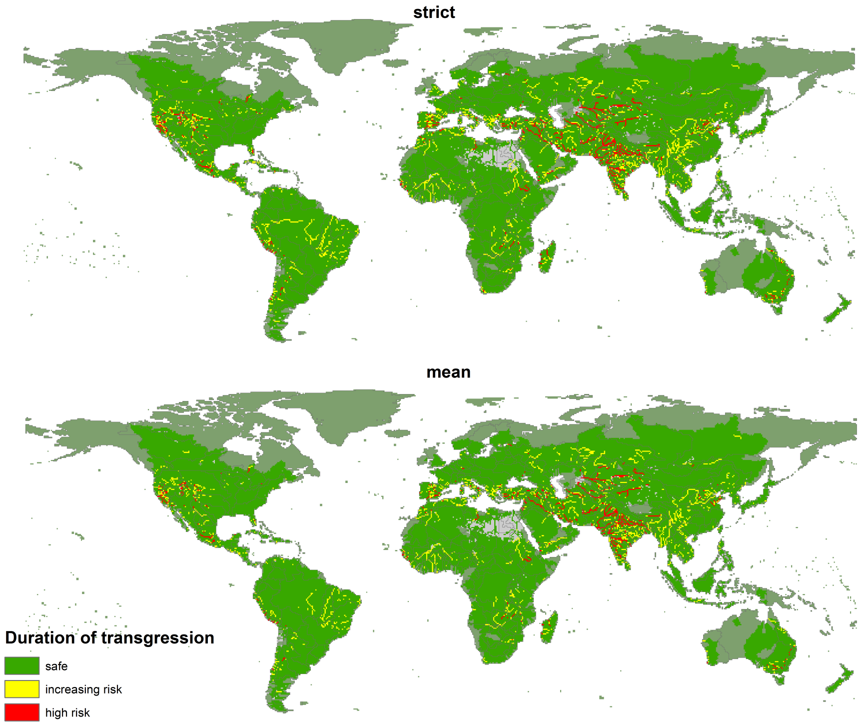

Figure SF 7: Duration of transgression of EFRs on cell scale (1980-2009, 0.5°resolution), in km^3/yr for the mean and strict scenario, major river basins delineated

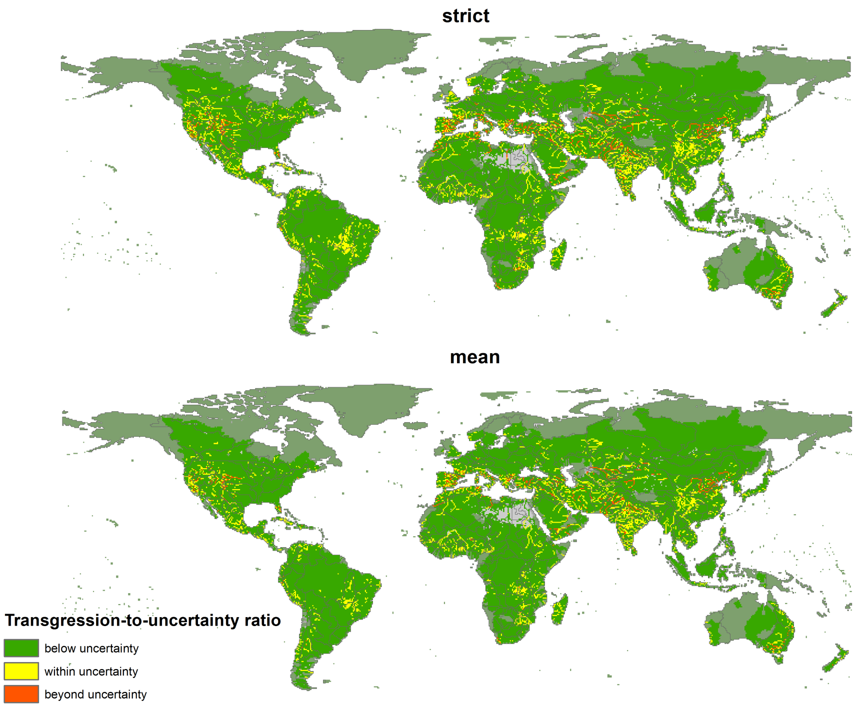

Figure SF 8: Transgression-to-uncertainty ratio on cell scale (1980-2009, 0.5°resolution), in km^3/yr for the mean and strict scenario, major river basins delineated

Table ST 6: Number of affected cells and indirectly affected basins for both criteria

EFR method	EFRstrict	EFRmean	EFRvmf	EFRtess	EFRsmak
All affected cells (showing transgression)	7234	5601	3406	5705	6369
Directly affected area	19 190 025	14 946 643	8 817 455	15 222 549	16 992 852
All affected basins	829	662	476	694	758
Indirectly affected (basin) area	98 262 708	94 069 723	90 228 191	94 914 163	96 197 454
Criteria					
Transgression-to-uncertainty					
No of cells where it exists (!=0)	6795	5342	3325	5449	5905
Ranges					
Below uncertainty Affected cells	1546 (1107*)	1280 (1021*)	437 (356*)	(805)	1604 (1140)
Cellarea	4384876	3603177	1212658	134122419	4568599
Within uncertainty Affected cells	4704	3635	2284	3790	4030
Cellarea	12350211	9636720	5889023	10125742	10606578
Beyond uncertainty					

Table ST 6 continued

Affected cells	984	686	685	854	735
Cellarea	2454939	1706745	1715773	2128784	1817676
Duration of transgression					
Ranges					
1-2 months, safe					
Affected cells	3680	2641	1748	2980	3213
Cellarea	9946944	7260640	4535804	8124131	8798711
3-5 month, increasing risk					
Affected cells	2532	2150	1146	1959	2370
Cellarea	6613084	5603539	2968235	5118333	6179341
At least 6 months, high risk					
Affected cells	1022	810	512	766	786
Cellarea	1588858	1185705	846914.3	1185353	1187473

S 3.3 Details on the distribution of transgression volumes into the categories of uncertainty and duration

Looking at Table ST 7, showing the different EFR scenarios, the share of the total volumes of transgression falling into the respective categories– below, within and beyond uncertainty – it is evident, that regardless of the scenario, less than 4 percent of transgression is assigned below uncertainty. Between 41 and 63% of the total global EFR deficits is classed as transgressed beyond uncertainty. Although the total sum of transgressions for the VMF scenario is the smallest, the share of it occurring in transgressed areas is with 63% the highest value.

The details for the second criterion are shown in Table ST 8. Areas with transgressions during 6 months of the year or longer account for around 60% of total transgression. Further 30% of global EFR deficits occur in areas defined as at risk of transgression.

Table ST 7: Volumes of annual EFR transgression in km^3/yr, classification into categories of uncertainty and share of these categories in global sum

Scenario		strict		mean		vmf		Tessmann		Smakhtin et al.	
Sum of annual transgression		207	[%]	148	[%]	117	[%]	152	[%]	153	[%]
Uncertainty range	Below	5.47	3	2.32	2	0.71	0.6	1.49	1	6.02	4
	Within	97.13	47	73.82	50	43.19	37	73.99	49	84.79	55
	Beyond	104.15	50	71.82	48	73.43	63	76.71	50	62.28	41

Table ST 8: Volumes of annual EFR transgression in km^3/yr, classification according to the length of transgression (1-2 months=safe, 2-5=increasing risk, 6-12=high risk)

Scenario		strict		mean		vmf		Tessmann		Smakhtin et al.	
Sum of annual transgression		207	[%]	148	[%]	117	[%]	152	[%]	153	[%]
Uncertainty range	Safe	16.48	8	11.04	7	12.37	10	7.36	5	9.49	6
	Increasing risk	64.36	31	44.0	30	27.58	24	52.37	34	56.84	37
	High risk	125.91	61	92.91	63	77.38	66	92.46	61	86.77	57

S 3.4 EFR plots for the mean scenario, VMF, Tessmann and Smakhtin et al.

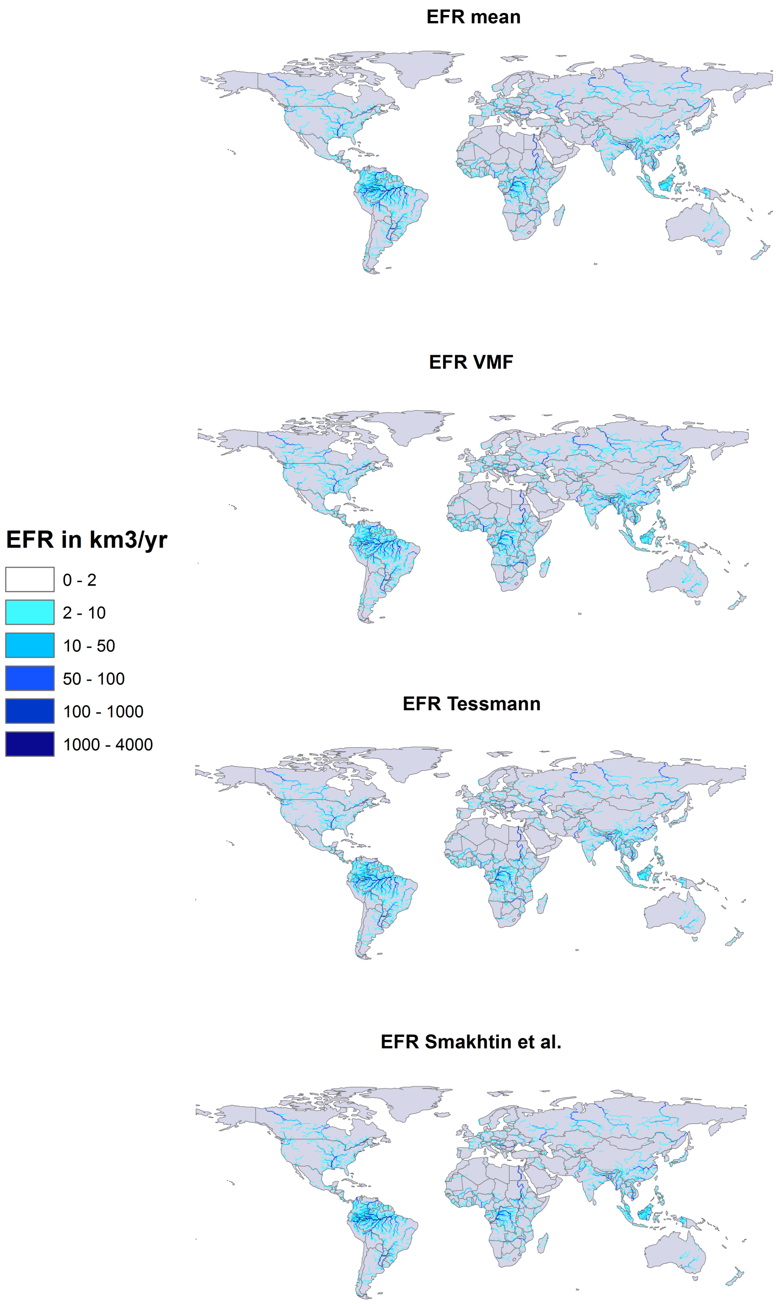

Figure SF 9: Environmental Flow Requirements, in km^3/yr, averaged over the years 1980 to 2009, simulated by LPJmL

S 3.5 Share of transgressed area per basin

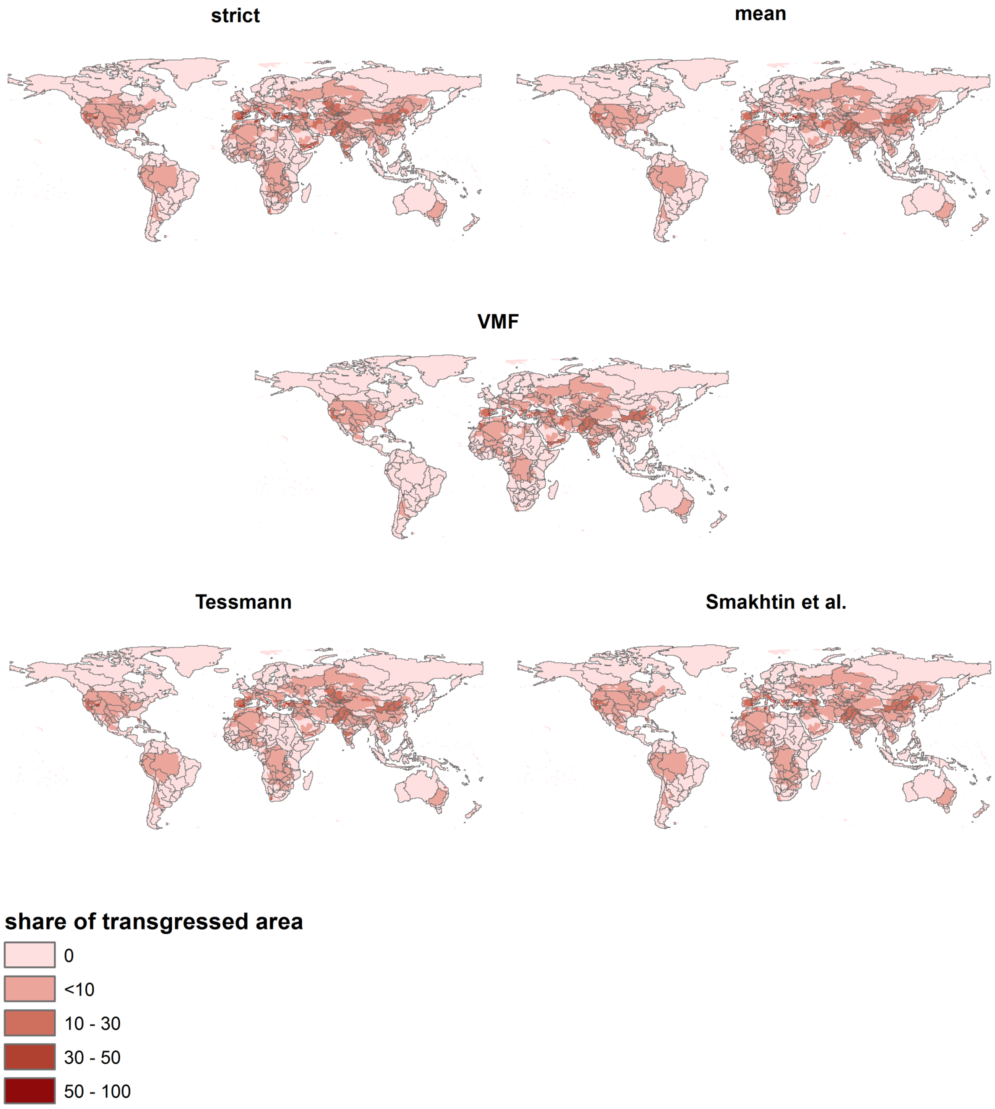

Figure SF 10: Share of transgressed area per basin, according to the 1st criterion - transgression-to-uncertainty ratio

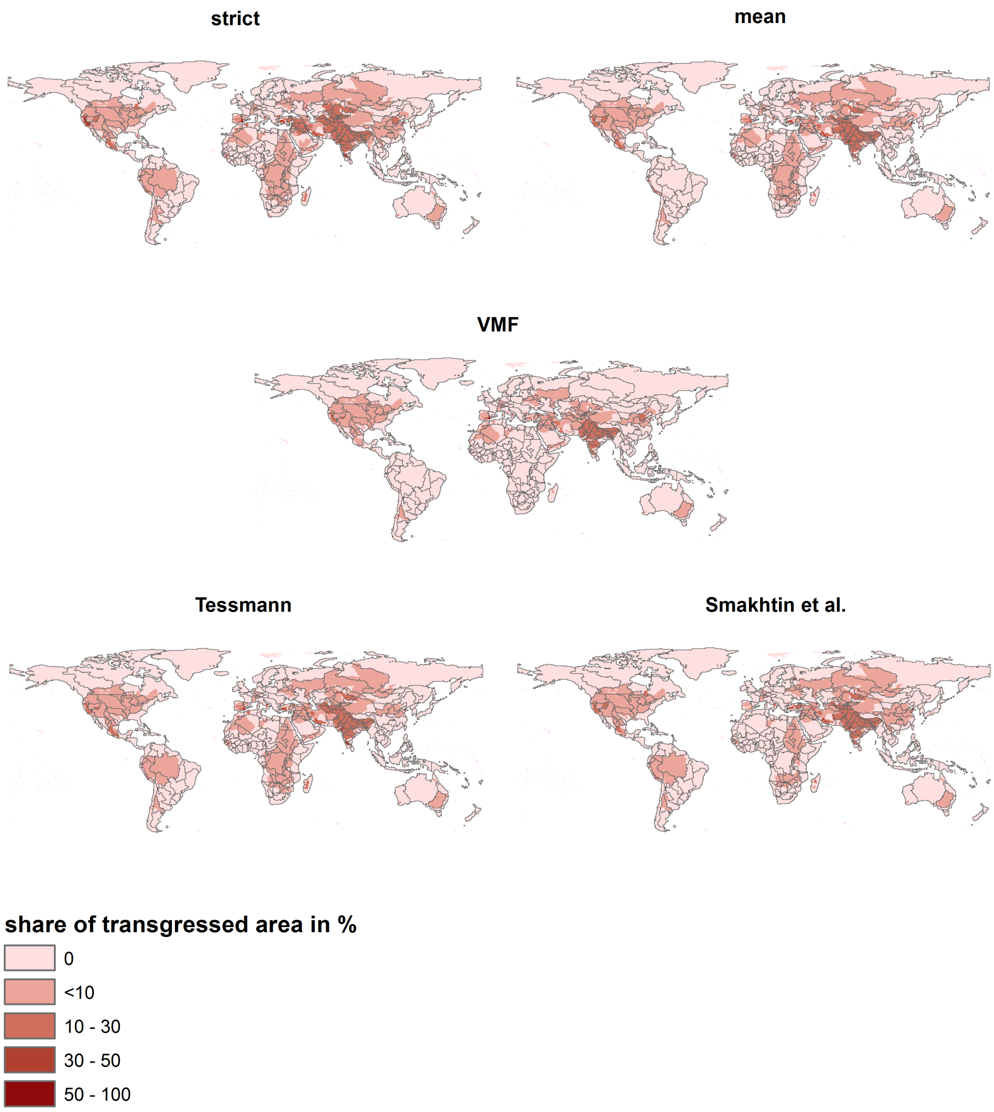

Figure SF 11: Share of transgressed area per basin, according to the 2nd criterion - duration of transgression

S 4 Details for the results on basin scale

S 4.1 Histograms of the basin classes

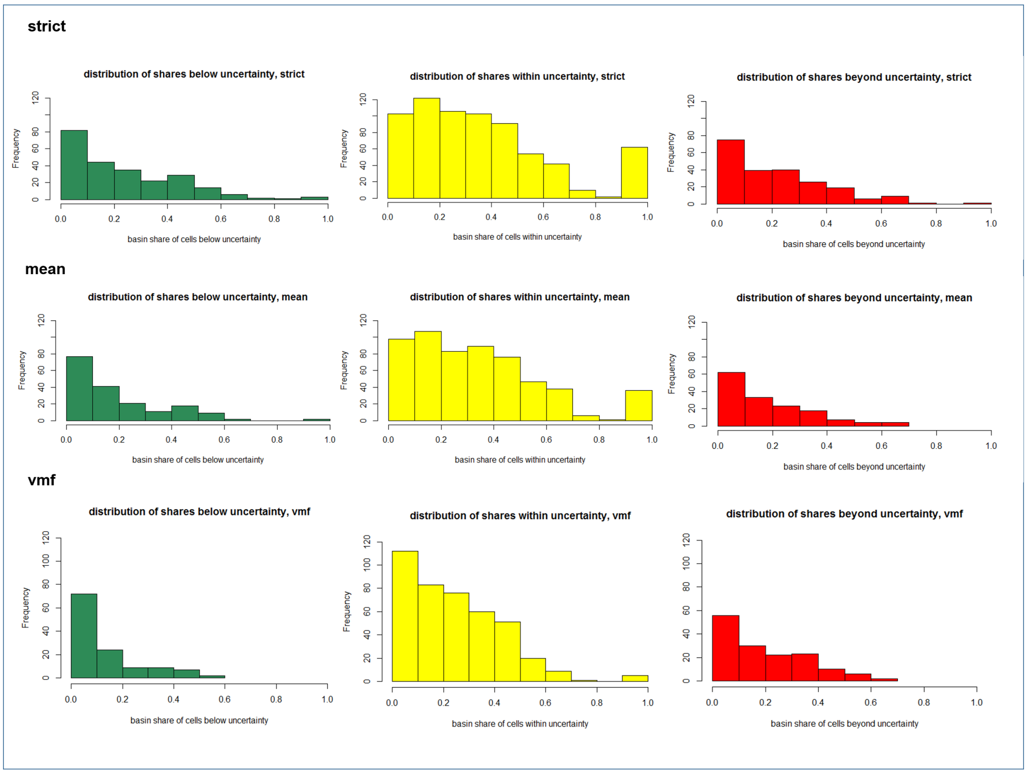

Figure SF 12: Histogram of the of the different basin classes for the strict, mean and vmf scenario, according to the 1st criterion - transgression-to-uncertainty ratio

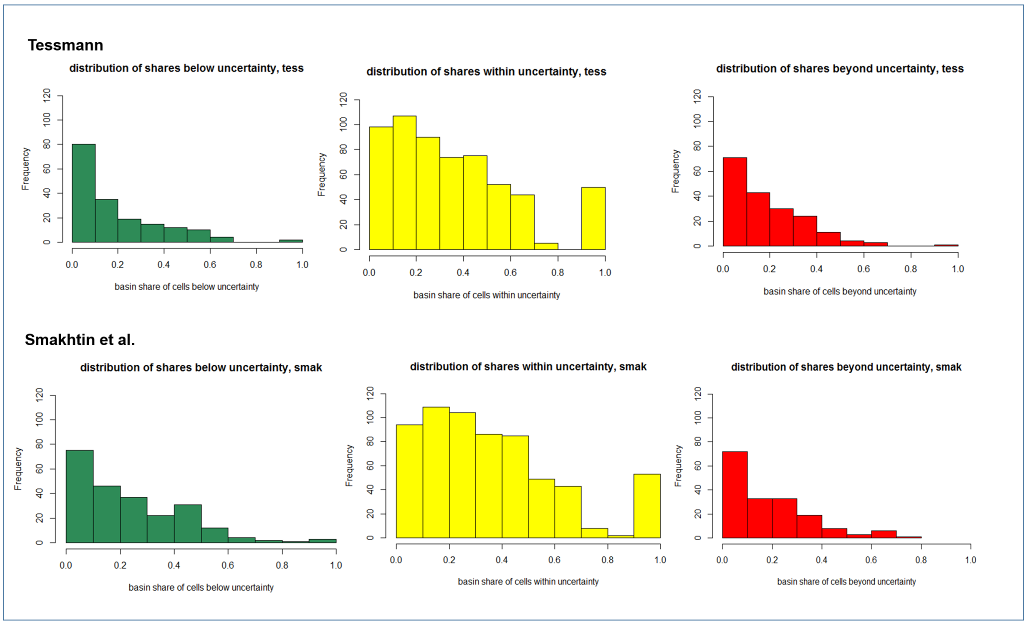

Figure SF 13: Histogram of the of the different basin classes for the Tessmann and Smakhtin method, according to the 1st criterion - transgression-to-uncertainty ratio

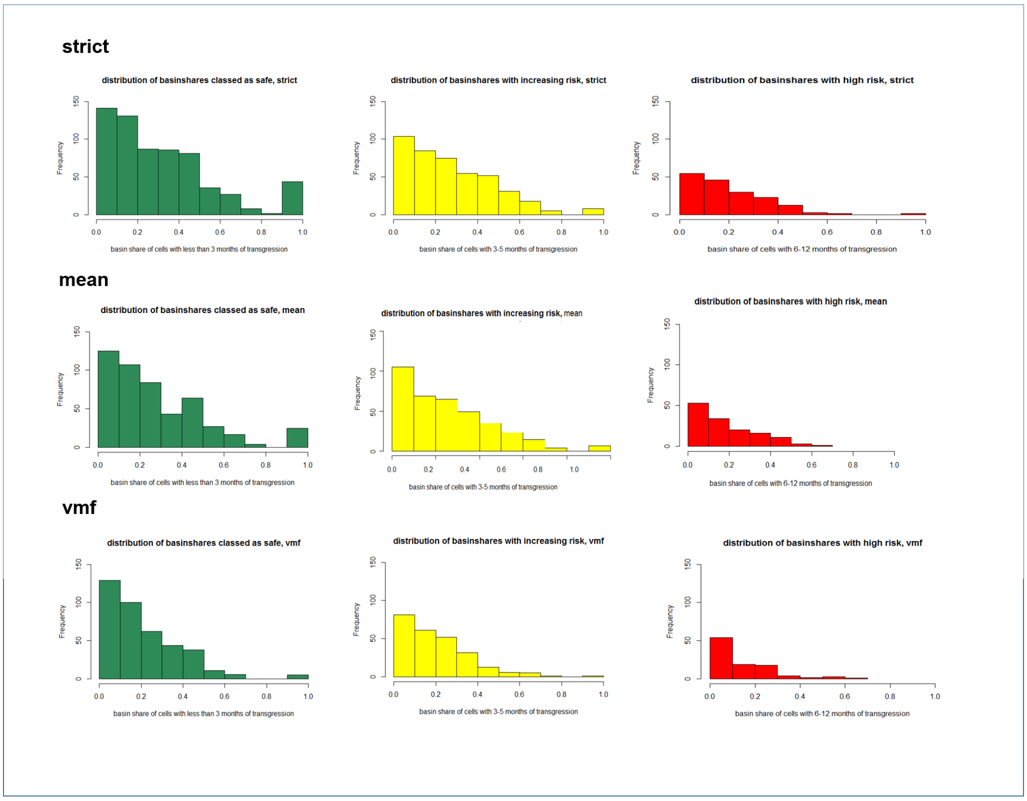

Figure SF 14: Histogram of the of the different basin classes for the strict, mean and vmf scenario, according to the 2nd criterion - duration of transgression

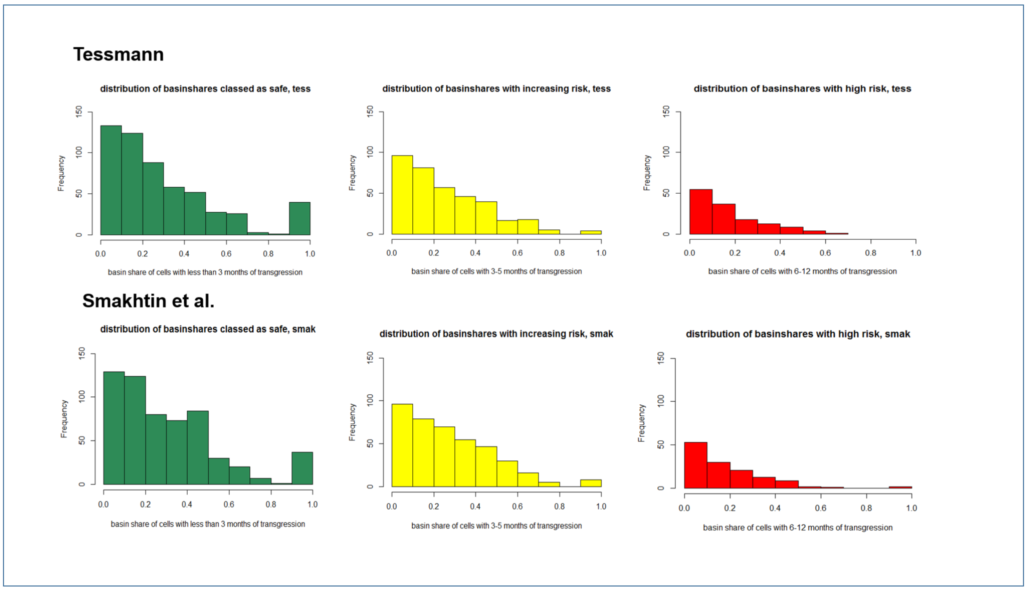

Figure SF 15: Histogram of the of the different basin classes for the Tessmann and Smakhtin method, according to the 2nd criterion - duration of transgression

S 4.2 Alternative threshold for basin classification

The thresholds applied in this thesis are very cautious, a comparison to other less strict approaches is therefore interesting. The alternative thresholds are as follows:

- a basin is classed as transgressed/red if ≥30% of its area is classed as transgressed/red
- a basin is classed as at risk of transgression if ≥50% of its area is classed as at risk of transgression/yellow or transgressed/red (while less than 30% are transgressed)
- a basin is classed as not transgressed/green if >70% of its area show no transgression or their transgression is classed as below uncertainty or safe

The respective maps are given in in Figures SF 16 and SF 17 and a comparison of the different approaches is given in Table ST 9

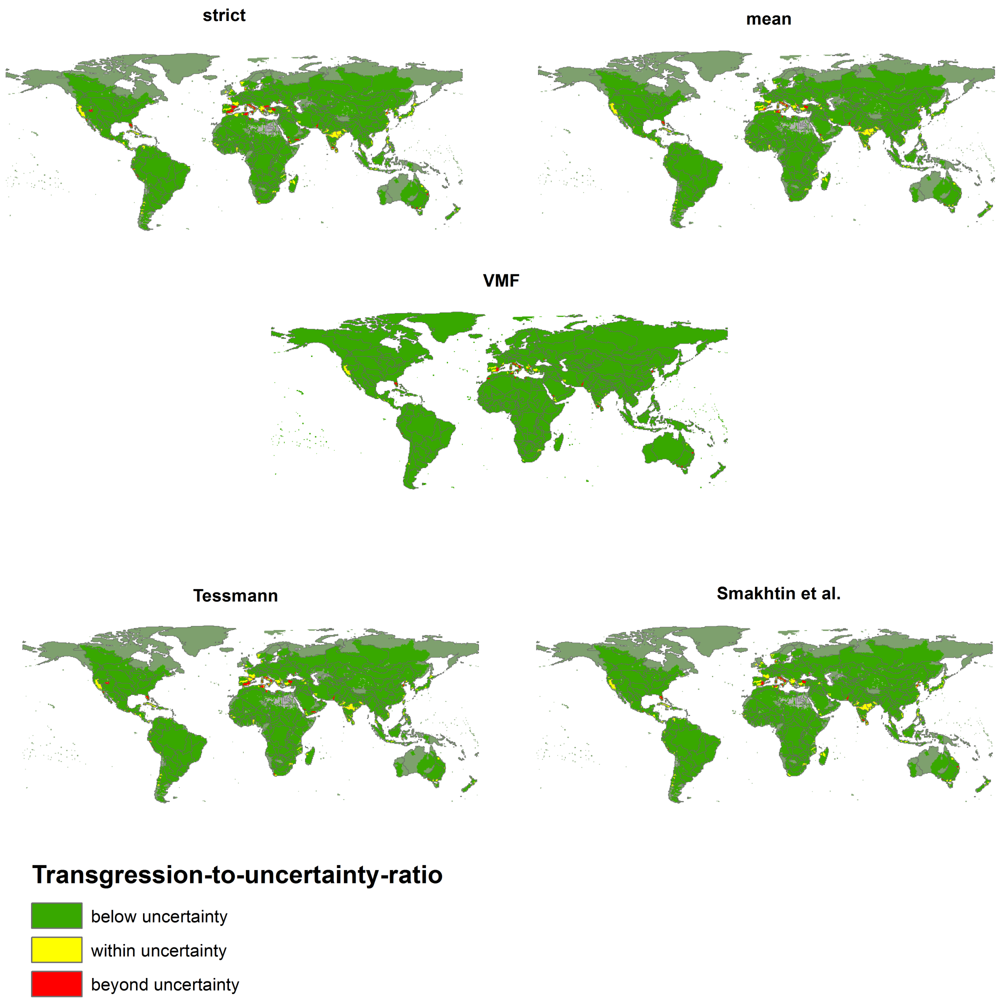

Figure SF 16: Transgression – to – uncertainty ratio, aggregated to basin scale, thresholds: >30% red = red-transgressed, >50% yellow = yellow-risk of transgression

Figure SF 17: Duration of transgression, aggregated to basin scale, thresholds: $>30\%$ red = red-transgressed, $>50\%$ yellow = yellow-risk of transgression

Table ST 9: Comparison between different thresholds for aggregation to basin scale, number of basins and respective share in total area

	Threshold		strict	mean	vmf	Tessmann	Smakhtin et al.
Transgression-to-uncertainty ratio							
Red Basins	≥10% beyond	Number	141	89	93	116	103
		share	0.6	0.4	0.4	0.5	0.4
	≥30% beyond	Number	62	33	41	43	37
		share	0.6	0.3	0.3	0.4	0.3
Yellow Basins	≥30% within	Number	334	274	125	273	307
		share	7.8	4.4	1.8	4.2	4.3
	≥50% within	Number	212	163	56	185	194
		share	2.1	1.8	0.6	1.8	1.9
Green Basins	≥70% below	Number	10846 (6)	10958 (2)	11103 (0)	10932 (2)	10911 (6)
		share	86.6	91.8	94.2	91.1	91.9
	≥50% below	Number	11047 (41)	11125 (21)	11224 (6)	11093 (21)	11090 (39)
		share	97.2	97.9	99.1	97.8	97.8
Duration of Transgression							
Red Basins	≥10% beyond	Number	119	85	47	82	78
		share	7.7	5.2	3.4	5.1	5.0
	≥30% beyond	Number	43	31	10	27	27
		share	0.6	0.3	0.1	0.4	0.2
Yellow Basins	≥30% within	Number	155	129	60	124	160
		share	1.6	1.5	0.9	1.4	1.9

Table ST 9 continued

	≥50% within	Number	95	68	22	66	84
		share	0.9	0.8	0.1	0.5	0.7
Green Basins	≥70% below	Number	11047 (54)	11107 (10)	11214 (2)	11115 (9)	11083 (13)
		share	87.7	91.1	94.2	91.4	90.7
	≥50% below	Number	11183 (150)	11122 (98)	11289 (36)	11228 (114)	11210 (127)
		share	98.4	98.8	99.8	99.1	98.9

S 4.3 Alternative threshold for biodiversity data to be considered

Looking at a comparison of the thresholds for biodiversity data to be considered, one at 30% and one at 50% (given in Figure SF 18 in blue and green respectively), it becomes evident only few basins would additionally be included if a lower threshold would have been chosen. In the case of the Central Asian Amu Darya/Sry Darya basins, a seperate analysis might be interesting as these basins are severely transgressed and home to a considerable amount of endemic species. See also Table 5. Unfortunately, the HydroSHED global biodiversity set's coverage is limited this region of Asia.

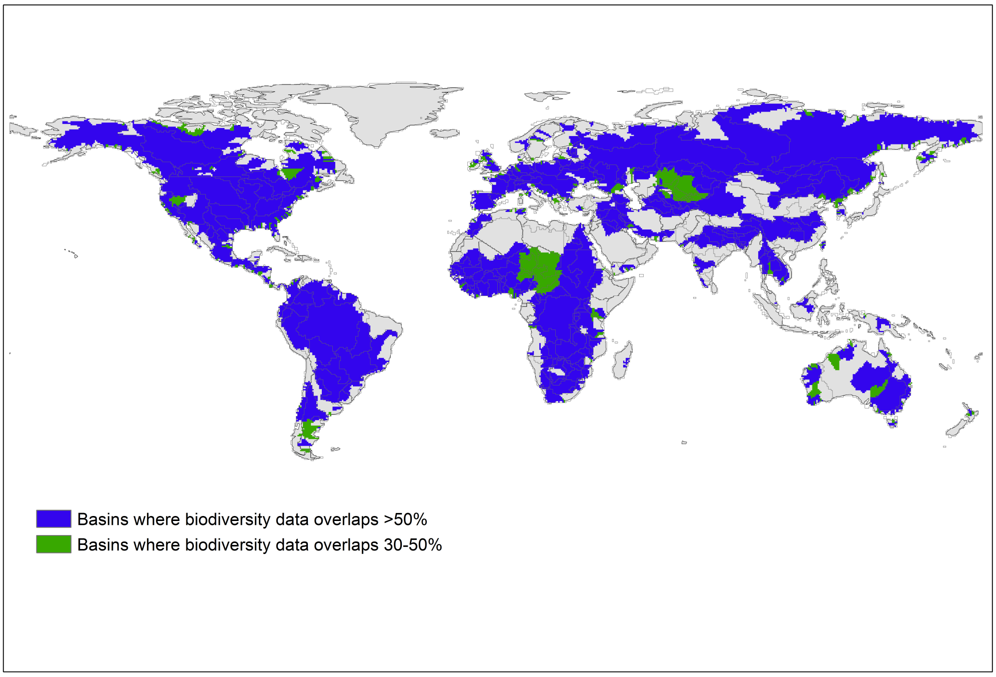

Figure SF 18

S 4.4 Alternative threshold for biodiversity to be considered high

It is not easy to find suitable measures to compare and assess global biodiversity levels (Gaston, 2000). The here chosen threshold of biodiversity are based on a single value – the median - and therefore systematically underestimate biodiversity levels in certain world regions such as at high latitudes. To receive a picture of the effect of this approach another lower threshold is given in Figure SF 19. The 30th percentile for species richness is 8 and the CWEI is 0.030615. Especially in Eurasia additional basins would have been included, particularly due to species richness.

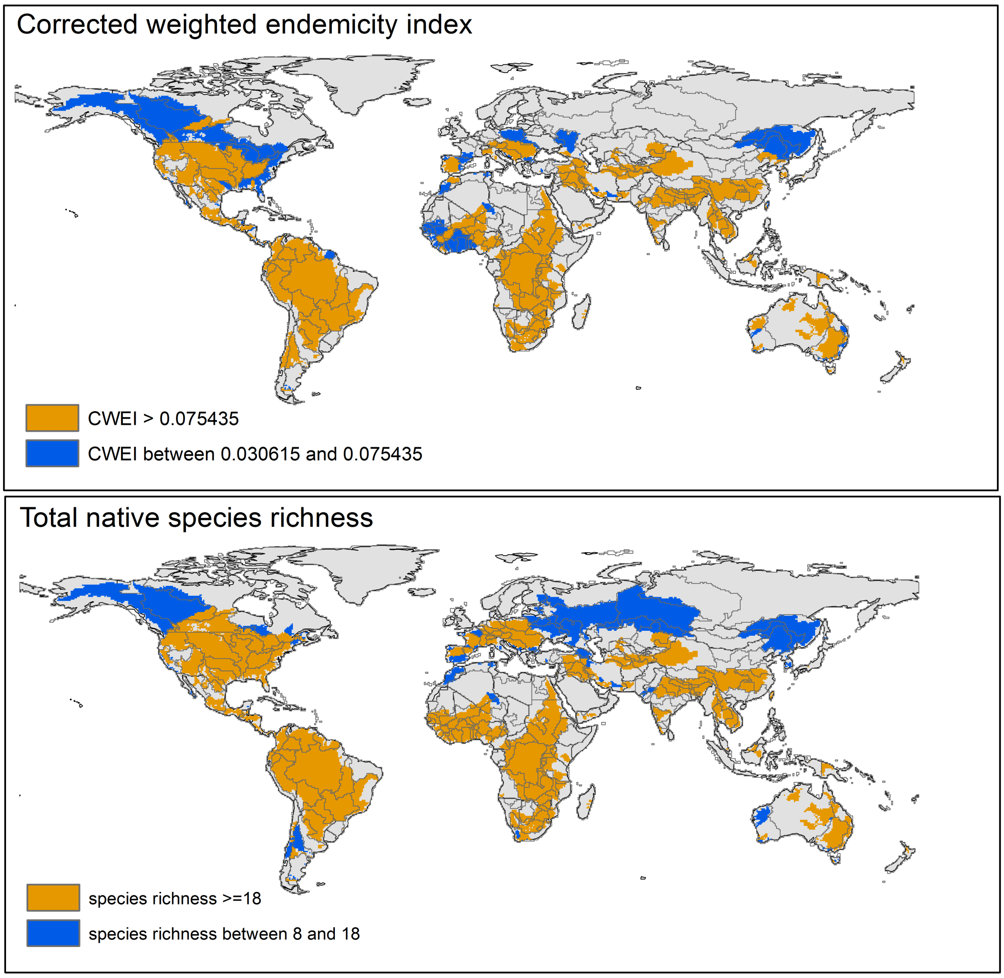

Figure SF 19: Comparison of a median threshold (orange) with a 30th percentile threshold (blue& orange)

S 4.5 Basins' share in global annual transgression

Table ST 10: Major river basins' share in global annual EFR transgression, in %

River Basin	Countries	strict	mean	vmf	Tessmann	Smakhtin et al.
Indus River	Pakistan	26	27	42	28	22
Ganges River	India	11	13	5	14	15
Yellow River	China	4	5	7	5	4
Chu-Talas	Kazakhstan/ Kyrgyzstan	3	4	4	4	4
Amu Darya River	Uzbekistan	4	4	7	4	3
Euphrates-Tigris	Tukey/Syria/ Iraq/Iran	4	3	6	3	2
Nile River	Sudan/Egypt	3	2	0	4	1

S 4.6 EFR transgressions share in mean annual discharge

Table ST 11: EFR transgressions' share in mean annual discharge for major river basins, in %

River Basin	Countries	strict	mean	vmf	Tessmann	Smakhtin et al.
Indus River	Pakistan	309	232	285	234	192
North-Tarim Basin	China	47	33	21	29	43
Yellow River	China	24	19	22	19	16
Chu-Talas	Kazakhstan/ Kyrgyzstan	12	11	9	12	11
Amu Darya River	Uzbekistan	63	38	55	38	29
Euphrates-Tigris	Turkey/Syria/ Iraq/Iran	23	11	20	13	8

S 4.7 Details on the subclasses in transgressed Basins

Table ST 12: Details on transgressed basins and respective biodiversity and water descriptors in subclasses

	strict	**mean**	**vmf**	**Tessmann**	**Smakhtin et al.**
total Number	202	145	111	162	149
Subclasses					
both biodiversity descriptors high	17	13	10	13	13
high endemicity	21	17	12	19	15
high species richness	10	7	4	9	8
no high biodiversity	154	108	85	121	113
Details on Subclasses/Water criteria and associated Biodiversity					
uncertainty ratio & high endemicity	23	18	15	18	17
uncertainty ratio & high species richness	15	11	11	13	14
duration & high endemicity	29	20	16	24	17
duration & high species richness	19	14	8	15	10

S 4.8 Details on the share in land surface area

Table ST 13: Number of basins, affected area and share in total and influenced/accessed area of the two water descriptors combined

		strict	mean	vmf	Tessmann	Smakhtin et al.
Both arguments combined (duration and uncertainty/strictest each)						
Red Basins	Number	202	145	111	162	149
	Area in km^2	15185208	11167800	8380036	12006852	10738704
	Share in total	0.1037	0.0762	0.0572	0.0820	0.0734
	Share in influenced area	0.1372	0.1009	0.0757	0.1085	0.0970
Yellow Basins	Number	294	242	118	245	282
	Area in km^2	7473561	4529154	2031998	4027000	4658746
	Share in total	0.0511	0.0309	0.0139	0.0275	0.0318
	Share in influenced area	0.0675	0.0409	0.0184	0.0364	0.0421
Green Basins	Number	1273	1382	1540	1360	1338
	Area in km^2	88002977	94964793	100249712	94627895	95264297
	Share in total	0.6012	0.6488	0.6849	0.6465	0.6508
	Share in influenced area	0.7951	0.8581	0.9058	0.8550	0.8608

S 5 Details for the results on global scale

S 5.1 Results with consideration of extent of anthropogenic influence

Table ST 14: Area shares with and without adjustments for anthropogenic influence

	strict	**mean**	**vmf**	**Tessmann**	**Smakhtin et al.**
Transgressed basins					
Total number	120	145	111	162	149
Total area	15185208	11167800	8380036	12006852	10738704
Share in total land area in%	10.4	7.6	5.7	8.2	7.3
Share in total area under anthropogenic influence in%	13.7	10.1	7.6	10.9	9.7
Basins at risk of transgression					
Total number	294	242	118	245	282
Total area	7473561	4529154	2031998	4027000	4658746
Share in total land area in%	5.1	3.1	1.4	2.8	3.2
Share in total area under anthropogenic influence in%	6.7	4.1	1.8	3.6	4.2
Basins classed as not transgressed					
Total number	1273	1382	1540	1360	1338
Total area	88002977	94964793	100249712	94627895	95264297
Share in total land area in%	60.1	64.8	68.5	64.6	65.1
Share in total area under anthropogenic influence in%	79.5	85.8	90.6	85.5	86.1

S 6 Datasets on aquatic biodiversity by Tisseuil et al. (2013)

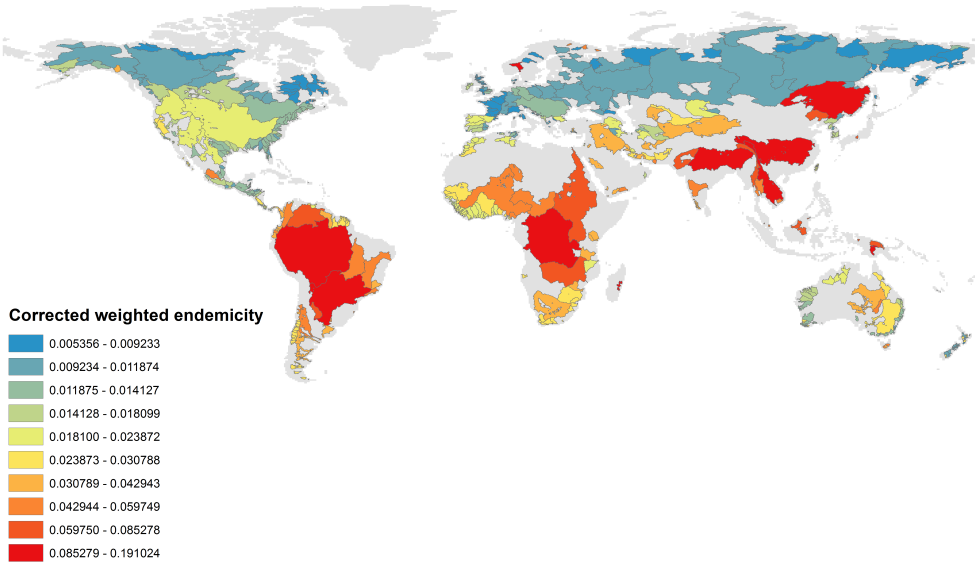

Figure SF 20: Global distribution of aquatic birds, corrected weighted endemicity index (Tisseuil et al., 2013)

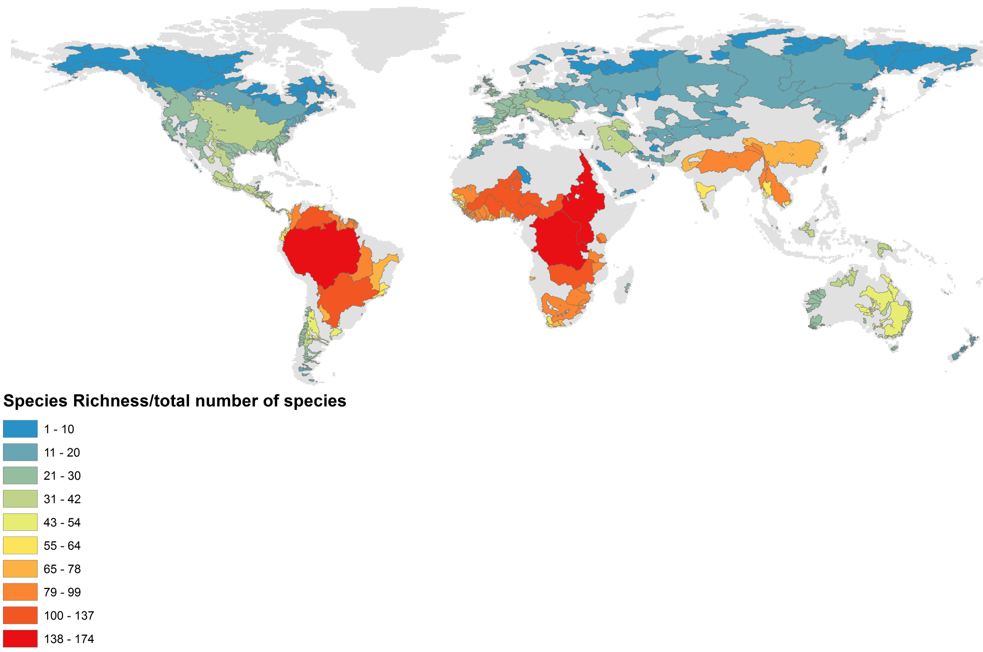

Figure SF 21: Global distribution of aquatic birds, total native species richness (Tisseuil et al., 2013)

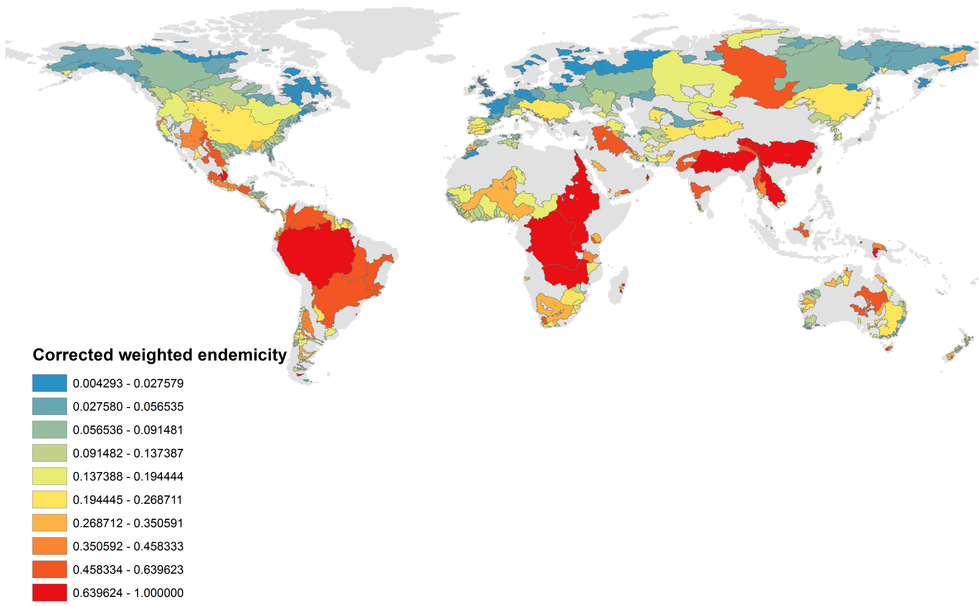

Figure SF 22: Global distribution of fishes, corrected weighted endemicity index (Tisseuil et al., 2013)

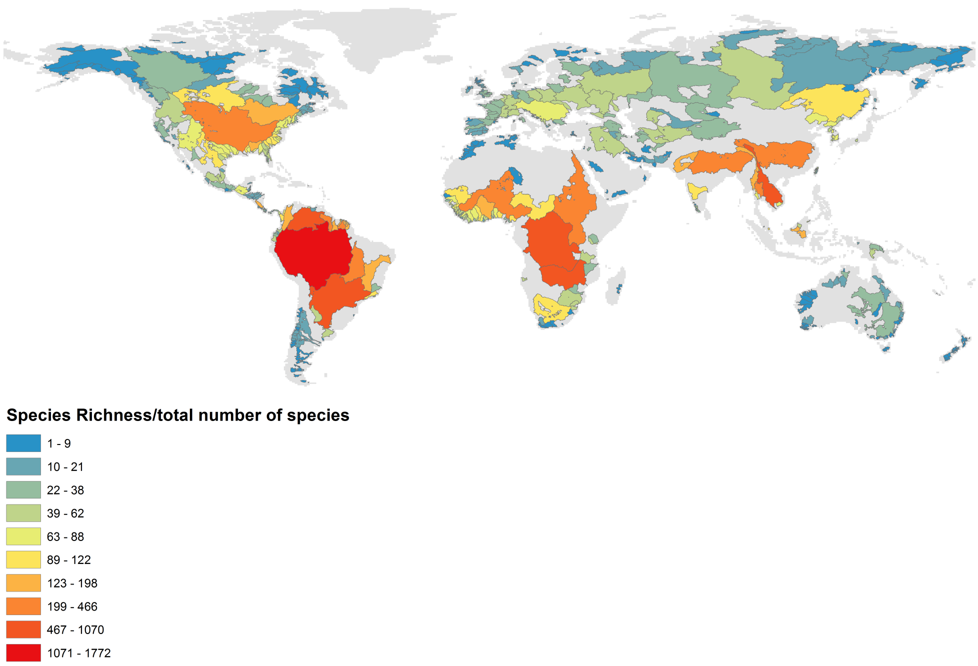

Figure SF 23: Global distribution of fishes, total native species richness (Tisseuil et al., 2013)

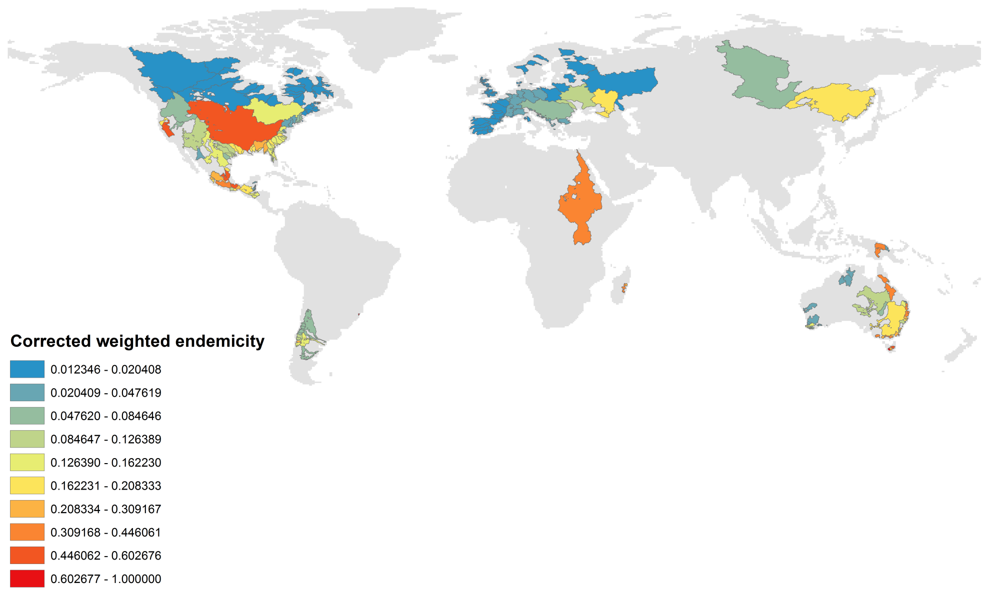

Figure SF 24: Global distribution of crayfish, corrected weighted endemicity index (Tisseuil et al., 2013)

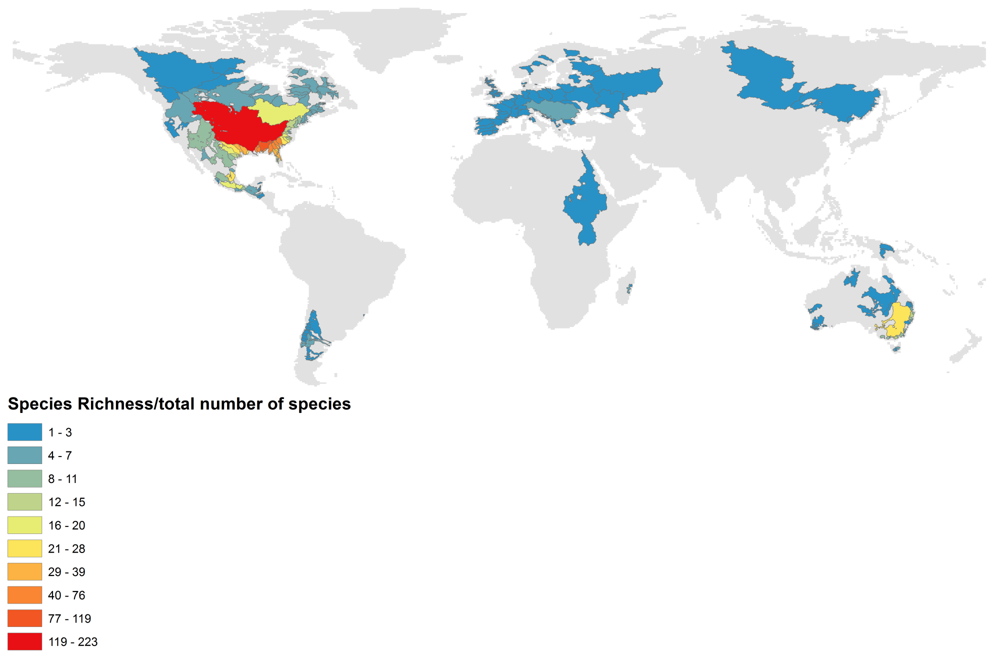

Figure SF 25: Global distribution of crayfish, total native species richness (Tisseuil et al., 2013)

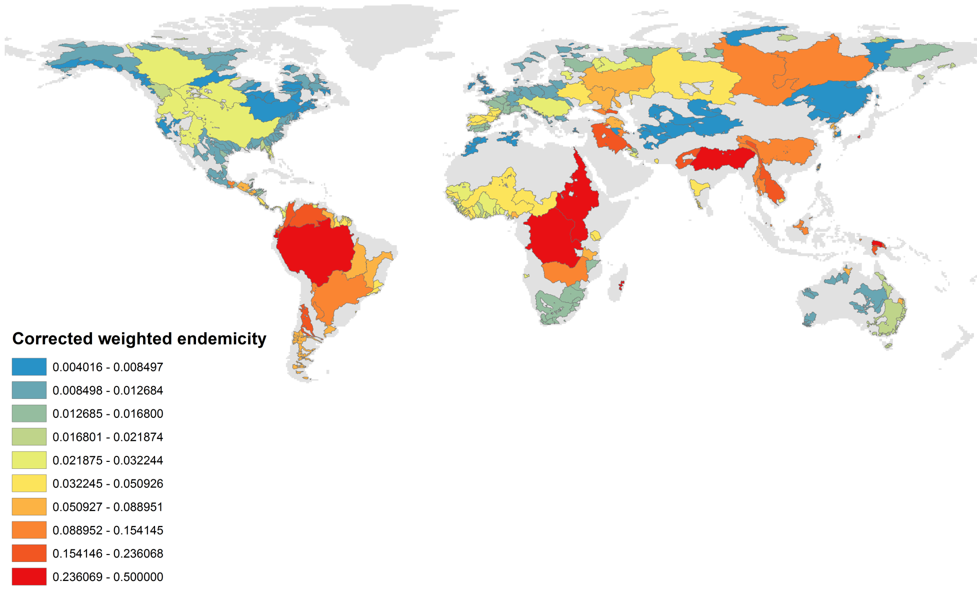

Figure SF 26: Global distribution of aquatic mammals, corrected weighted endemicity index (Tisseuil et al., 2013)

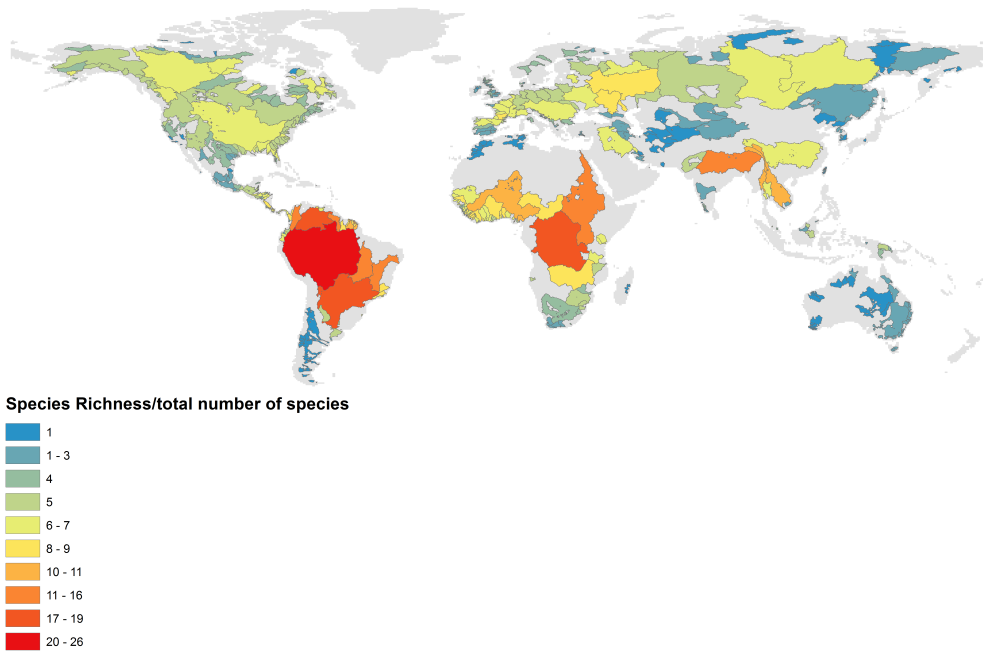

Figure SF 27: Global distribution of aquatic mammals, total native species richness (Tisseuil et al., 2013)

S 7 R Scripts

S 7.1 Basis script to read LPJmL Outputs and calculate EFRs and EFR deficits

```
rm(list=ls(all=TRUE))
gc()
open="G:/open/Cordula"
library(raster)
library(fields)
library(rgeos)
ncell=67420
ndaymonth <- c(31,28,31,30,31,30,31,31,30,31,30,31)
size = 4

source(paste(open,"/functions_to_read_lpjml_outputs.R",sep=""))
source(paste(open,"/LPJmLplots.R",sep=""))
source(paste(open,"/fpu_and_basin_aggregation.R",sep=""))

### Find Basis Drain Cells ###
drainage <- file("G:/open/Cordula/Endzellen/drainagestn.bin","rb")
nbands <- 2
hsize  <- 43
seek(drainage, where= hsize, origin="start")

drain    <- readBin(drainage, what=integer(), n=ncell*nbands*size, size=4)
dim(drain) <- c(nbands,ncell)
close(drainage)
drain_cells <- which(drain[1,]==(-1)| drain[1,]==(-9))
grid <- t(array(readBin(paste(open,"/1950_2009_baseline_noefr/grid.bin",sep=""),
what=integer(),size=2,n=ncell*2),dim=c(2,ncell))/100)
cellwidth <- 6371000.785*pi/180 # earthradius [m] times Pi
cellarea<- (cellwidth*0.5)*(cellwidth*0.5)*cos(grid[,2]/180*pi)   # in m^2
cellarea <- cellarea/1000000 # in km^2
total_area <-sum(cellarea)  # [1] 146.376.945 km^2

########## Cells to take out ##########################
#---------------------# dismiss basins without irrigation
readdir=paste("G:/open/Cordula/water_boundary_paper/1950_2009_baseline_noefr/",sep="")
#noefr --> discharge doesn't contain efr
air = readbin_lpjml(readdir,"airrig",1950,1980,2009,ncell,1,4)
zz<- file("G:/open/Cordula/Endzellzuordnung_bzw_Basins/endcell_drainagestn.bin","rb")
endcell <- readBin(zz,integer(),size=4,n=67420)
close(zz)
basin.ids <- sort(unique(endcell))
irrmask_basin=array(0,ncell)
for(i in 1:length(basin.ids))
{
  basincells <- which(endcell==basin.ids[i])
  if(sum(air[basincells])>0) {
    irrmask_basin[basincells]=1
  }
}
irrmask=array(0,ncell)
irrmask[which(air>0)] = 1
irrmask[47000]<-1
#dismiss basins without water use in HIL
readdir=paste("G:/open/Cordula/water_boundary_paper/1950_2009_baseline_noefr/",sep="")
#noefr --> discharge doesn't contain efr
hil = readbin_lpjml(readdir,"awateruse_hil",1950,1980,2009,ncell,1,4)

hilmask_basin=array(0,ncell)
for(i in 1:length(basin.ids))
{
  basincells <- which(endcell==basin.ids[i])
  if(sum(hil[basincells])>0) {
    hilmask_basin[basincells]=1
  }
}                                 #  var[hilmask_basin==0]<-0  # 5692
hilmask=array(0,ncell)
hilmask[which(hil>0)] =1

### Dismiss basins of northern remote ###
load("G:/open/Cordula/remote_cell.RData") #remote_cell #5540
remote_basin= array(1,ncell)
remote_basin[remote_cell] <-0   # 5540
```

```
### Dismiss basins with one cell ###
size_basins <- ave(endcell,endcell, FUN=length)
small_basins <- ifelse(size_basins==1,0,1)      #7595 cells/basins

### All out ###
out <- c(irrmask_basin,hilmask_basin,remote_basin,small_basins)
out_tog <- array(out,c(1,ncell,4))
cell_out <- apply(out_tog,c(1,2),min)
Cell_out <- array(1,ncell)
Cell_out[cell_out==0] <-0
accessed_area <- sum(cellarea[Cell_out==1])
#Cells_out <-toraster(cell_out)
#writeRaster(Cells_out,filename="G:/open/Cordula/Outputs/161024/Maske_wegfall.tif",
format="GTiff",overwrite=TRUE, bandorder= BSQ)
## share in area
# sum(cellarea[cell_out==0]) # 35701833/total_area = 0.2439034, on regard que 75,60966%
#sum(cellarea[cell_out!= 0]) #110675112 total considered areaa

###PNV Discharge for corrections
readdir=paste("G:/open/Cordula/1950_2009_pnv/",sep="")
dis_pnv = readbin_lpjml(readdir,"mdischarge",1950,1980,2009,ncell,12,4)
# 30-year mean # [m3/s]
#for(m in 1:12) dis_pnv[,m]<- dis_pnv[,m]*ndaymonth[m] *10^-3     #UNIT CHANGE

an_dis_pnv<-apply(dis_pnv,1,sum)
#sum(an_dis_pnv[drain_cells]) #[1] 55514.73

### EFR vmf, smak, tess in LPJmL ###
EFRs=c("VMF","SMAK","TESS")
thres=array(0,c(ncell,12,length(EFRs)))
for(efr in 1:length(EFRs)) {
  readdir=paste("G:/open/Cordula/water_boundary_paper/1950_2009_respect_water_"
        ,EFRs[efr],"/",sep="")
  thres[,,efr] = readbin_lpjml(readdir,"mefr_threshold",1950,1980,2009,ncell,12,4)}

#for(m in 1:12) thres[,m,]<- thres[,m,]*ndaymonth[m] *10^-3     #UNIT CHANGE

### EFR ###
# strict
tar_up=apply(thres,c(1,2),max)
tar_lo=apply(thres,c(1,2),min)

# mean
thres[thres==0]<-NA
tar_mean=apply(thres,c(1,2),mean,na.rm=T) #average efr per cell
tar_mean[is.na(tar_mean)]<-0

thres[is.na(thres)] <-0
# VMF
tar_vmf = thres[,,1]
# SMAK
tar_smak = thres[,,2]
# Tess
tar_tess = thres[,,3]

span=tar_up-tar_lo
span[dis_pnv<0.0864]<-0      #0 for tiny rivers with less than 1m3/s

###Correction for strictness efr###
# strict
def_pnv_up=tar_up-dis_pnv
def_pnv_up[def_pnv_up<0]<-0
def_pnv_up[dis_pnv<0.0864]<-0
# corr liberal
def_pnv_lo=tar_lo-dis_pnv
def_pnv_lo[def_pnv_lo<0]<-0
def_pnv_lo[dis_pnv<0.0864]<-0
# Corr mean
def_pnv_mean=tar_mean -dis_pnv
def_pnv_mean[def_pnv_mean<0] <-0
def_pnv_mean[dis_pnv<0.0864] <-0
# corr vmf
def_pnv_vmf=tar_vmf-dis_pnv
def_pnv_vmf[def_pnv_vmf<0] <-0
def_pnv_vmf[dis_pnv< 0.0864] <-0
# corr smak
def_pnv_smak=tar_smak-dis_pnv
def_pnv_smak[def_pnv_smak<0] <-0
def_pnv_smak[dis_pnv<0.0864] <-0
# corr tess
def_pnv_tess=tar_tess-dis_pnv
def_pnv_tess[def_pnv_tess<0] <-0
```

```
def_pnv_tess[dis_pnv<0.0864] <-0

  # Discharge HIL #
  #Scenarios how discharge is calculated are to be put in here
  scens=c("baseline_noefr_HIL")
  for(scen in 1:length(scens)) {
  print(scens[scen])

  readdir=paste("G:/open/Cordula/water_boundary_paper/1950_2009_",scens[scen],"/",sep="")
  dis = readbin_lpjml(readdir,"mdischarge",1950,1980,2009,ncell,12,4) #
   # for(m in 1:12) dis[,m]<- dis[,m]*ndaymonth[m] *10^-3      #UNIT CHANGE

  sum_an_dischHIL <- apply(dis,1,sum)
  # sum_an_dischHIL[cell_out==0] <-0      # sum(sum_an_dischHIL[drain_cells]) #39004.19
  # sum(sum_an_dischHIL[drain_cells])     #[1] 54601.9 km^3/yr
  # dis_hil <- toraster(sum_an_dischHIL)
  # writeRaster(dis_hil,filename="G:/open/Cordula/Outputs/161231/dis_hil.tif",
        format="GTiff",overwrite=TRUE, bandorder= BSQ)

  ### Transgression
  # strict
  def_up=tar_up-dis
  def_up=def_up-def_pnv_up
  def_up[def_up<0.0864]<-0
  def_up[dis_pnv<0.0864]<-0
  def_up[cell_out==0] <-0

  # liberal
  def_lo=tar_lo-dis
  def_lo=def_lo-def_pnv_lo
  def_lo[def_lo<0.0864] <-0
  def_lo[dis_pnv<0.0864]<-0
  def_lo[cell_out==0] <-0

  # mean
  def_mean =tar_mean-dis
  def_mean= def_mean-def_pnv_mean
  def_mean[def_mean  <0.0864]<-0
  def_mean[dis_pnv<0.0864] <-0
  def_mean[cell_out==0] <-0

  # vmf
  def_vmf =tar_vmf-dis
  def_vmf = def_vmf-def_pnv_vmf
  def_vmf[def_vmf<0.0864] <-0
  def_vmf[dis_pnv<0.0864]<-0
  def_vmf[cell_out==0] <-0

  # smak
  def_smak =tar_smak-dis
  def_smak= def_smak-def_pnv_smak
  def_smak[def_smak<0.0864]<-0
  def_smak[dis_pnv<0.0864]<-0
  def_smak[cell_out==0] <-0

  # tess
  def_tess =tar_tess-dis
  def_tess= def_tess-def_pnv_tess
  def_tess[def_tess <0.0864]<-0
  def_tess[dis_pnv<0.0864]<-0
  def_tess[cell_out==0] <-0
  }

### Correction for small dis_pnv
small_dis <- ifelse(an_dis_pnv>0.0864,1,0)
Small_dis <- toraster(small_dis)

#writeRaster(Small_dis,filename="G:/open/Cordula/Outputs/161221/Maske_kldis.tif",
format="GTiff",overwrite=TRUE, bandorder= BSQ)

#affected discharge, mit km laufen lassen
#klok <- ifelse(small_dis==0,sum_an_dischHIL,0)
#sum(klok[drain_cells]) # [1] 3.963506

### Global sum EFR ###
# corrections from above have to be subtracted and their unit changed separately

### strict sum
efr_strict_o <- tar_up
corr_strict <- def_pnv_up

for(m in 1:12) efr_strict_o[,m]<- efr_strict_o[,m]*ndaymonth[m] *10^-3
```

```
for(m in 1:12) corr_strict[,m]<- corr_strict[,m]*ndaymonth[m] *10^-3
efr_strict <- efr_strict_o - corr_strict
efr_strict[cell_out==0] <-0
efr_strict_an <- apply(efr_strict,1,sum)
sum(efr_strict_an[drain_cells])    #18156.18

# efr_up <- toraster(efr_strict_an)
# writeRaster(efr_up,filename="G:/open/Cordula/Outputs/EFR/efr_up.tif", format="GTiff",overwrite=TRUE, bandorder= BSQ)

### mean sum
efr_mean_o <- tar_mean
corr_mean <- def_pnv_up

for(m in 1:12) efr_mean_o[,m]<- efr_mean_o[,m]*ndaymonth[m] *10^-3
for(m in 1:12) corr_mean[,m]<- corr_mean[,m]*ndaymonth[m] *10^-3
efr_mean <- efr_mean_o - corr_mean
efr_mean[cell_out==0] <-0
efr_mean_an <- apply(efr_mean,1,sum)
sum(efr_mean_an[drain_cells])    #12407.86

# efr_mean <- toraster(efr_mean_an)
# writeRaster(efr_mean,filename="G:/open/Cordula/Outputs/EFR/efr_mean.tif", format="GTiff",overwrite=TRUE, bandorder= BSQ)

### VMF
efr_vmf_o <- tar_vmf
corr_vmf <- def_pnv_vmf

for(m in 1:12) efr_vmf_o[,m]<- efr_vmf_o[,m]*ndaymonth[m] *10^-3
for(m in 1:12) corr_vmf[,m]<- corr_vmf[,m]*ndaymonth[m] *10^-3
efr_vmf <- efr_vmf_o - corr_vmf
efr_vmf[cell_out==0] <-0
efr_vmf_an <- apply(efr_vmf,1,sum)
sum(efr_vmf_an[drain_cells])    #13538.17

# efr_vmf <- toraster(efr_vmf_an)
# writeRaster(efr_vmf,filename="G:/open/Cordula/Outputs/EFR/efr_vmf.tif", format="GTiff",overwrite=TRUE, bandorder= BSQ)

### smak
efr_smak_o <- tar_smak
corr_smak <- def_pnv_smak

for(m in 1:12) efr_smak_o[,m]<- efr_smak_o[,m]*ndaymonth[m] *10^-3
for(m in 1:12) corr_smak[,m]<- corr_smak[,m]*ndaymonth[m] *10^-3
efr_smak <- efr_smak_o - corr_smak
efr_smak[cell_out==0] <-0
efr_smak_an <- apply(efr_smak,1,sum)
sum(efr_smak_an[drain_cells])    #14419.41

# efr_smak <- toraster(efr_smak_an)
# writeRaster(efr_smak,filename="G:/open/Cordula/Outputs/EFR/efr_smak.tif", format="GTiff",overwrite=TRUE, bandorder= BSQ)

### Tess
efr_tess_o <- tar_tess
corr_tess <- def_pnv_tess

for(m in 1:12) efr_tess_o[,m]<- efr_tess_o[,m]*ndaymonth[m] *10^-3
for(m in 1:12) corr_tess[,m]<- corr_tess[,m]*ndaymonth[m] *10^-3
efr_tess <- efr_tess_o - corr_tess
efr_tess[cell_out==0] <-0
efr_tess_an <- apply(efr_tess,1,sum)
sum(efr_tess_an[drain_cells])    #11931.83

# efr_tess <- toraster(efr_tess_an)
# writeRaster(efr_tess,filename="G:/open/Cordula/Outputs/EFR/efr_tess.tif", format="GTiff",overwrite=TRUE, bandorder= BSQ)
```

Declaration

I hereby declare that the present thesis has not been submitted as a part of any other examination procedure and has been independently written. All passages, including those from the internet, which were used directly or in modified form, especially those sources using text, graphs, charts or pictures, are indicated as such. I realize that an infringement of these principles which would amount to either an attempt of deception or deceit will lead to the institution of proceedings against myself.

Berlin, 21.04.2017 Signature